UNIVERSITY OF WARWICK
WMG

Fibre Reinforced Composites via Coaxial Electrospinning

PhD Thesis

Andrew Wooldridge
2016

Supervisors: Dr. Stuart R. Coles

Prof. Kerry Kirwan

Table of Contents

List of Tables iv

List of Figures v

List of Abbreviations ix

Abstract x

Acknowledgements xi

Declaration xii

Thesis Structure xiii

1 Introduction 1
1.1 Fibres 1
1.2 Fibre Spinning 2
1.3 Electrospinning Procedure 4
1.4 Aims and Objectives 5
1.4.1 Hypotheses 7

2 Literature Review 9
2.1 The History of Electrospinning 9
2.2 Literature Analysis 12
2.3 Parameter Control 15
2.3.1 Polymer Concentration, Molecular Weight, and Surface Tension 17
2.3.2 Polymer Delivery 20
2.3.3 Controlled Humidity 23
2.4 Improved Alignment and Control 25
2.5 Coaxial 29
2.5.1 Emulsion 32
2.5.2 Nanosprings 33
2.5.3 Multi-axial 34
2.5.4 Triaxial 36
2.6 High Throughput 40
2.6.1 Single polymer 40
2.6.2 Coaxial 42
2.7 Composites 43
2.7.1 Self-reinforced composites 48

3 Experimental 51
3.1 General Methodology 51
3.1.1 Polymer solutions 51
3.1.2 Single Polymer Electrospinning 52
3.1.3 Coaxial electrospinning 53
3.1.4 Discussion of Parameters 55
3.1.5 Analytical Techniques 58
3.1.6 Confirmation of core-shell coaxial structure 61
3.2 Fibre volume fraction 61
3.2.1 Preparation 62
3.2.2 Electrospinning 62
3.2.3 Composite forming 64
3.2.4 Materials characterisation 66
3.2.5 Rule of Mixtures 69
3.3 Composite forming variation 71
3.3.1 Preparation 72
3.3.2 Electrospinning 73
3.3.3 Hot Pressing 73
3.3.4 Analysis 75
3.4 Coaxial and layering 76
3.4.1 Preparation 76
3.4.2 Electrospinning 78
3.4.3 Composite forming 79
3.4.4 Tensile testing 80

4 Fibre volume fraction 83
4.1 Introduction 83
4.2 Electrospinning Polymer Fibres 87
4.2.1 Fibre Alignment of Electrospun Mats 92
4.3 Characterisation of Electrospun Fibre Mats 95
4.3.1 Thermogravimetric Analysis 95
4.3.2 ^{1}H NMR Analysis of Electrospun Mats 96
4.4 Tensile Testing 100
4.4.1 Rule of Mixtures 108
4.5 Conclusions 114

5 Composite forming variation 117
5.1 Introduction 117
5.2 Crystallinity 118
5.3 Tensile Properties 126
5.4 Fibre Deformation 129
5.5 Conclusions 132

6 Coaxial and layering 134
6.1 Introduction 134
6.2 Electrospinning 134
6.3 Composite Forming 137
6.4 Tensile Properties 139
6.5 Conclusions 142

7 Conclusions 144
7.1 Fibre volume ratio 145
7.2 Composite forming variation 146
7.3 Coaxial and layering 148
7.4 Recommendations for Future Work 149

8 References 152

9 Appendix 161

List of Tables

Table 1.1: Examples of some natural and synthetic fibres. 2
Table 2.1: Parameters affecting the electrospinning process. Adapted from Coles et al.[51] 15
Table 2.2: : Concentration required to electrospin polystyrene fibres using THF.[53] ..18
Table 3.1: Motor input voltage and corresponding collection velocity 57
Table 3.2: Solution flow rates for electrospinning 64
Table 3.3: Taguchi matrix of experiments required for test the composite forming process 72
Table 4.1: Alignment of coaxial electrospun fibres by standard deviation from the average angle of the fibres 93
Table 4.2: Fibre volume fractions of composite samples analysed by NMR 99
Table 4.3: Actual composite test results compared to the theoretical maximum calculated by the rule of mixtures 110
Table 5.1: Raw crystallinity results for the hot pressed samples 123
Table 5.2: Experimental variables with crystallinity and average tensile testing results 127
Table 5.3: Cross-section ratio of fibres compared to UTS of the composite 131
Table 6.1: PLA fibre diameters from different methods of electrospinning 135
Table 6.2: Mass and thickness of polymer sheets used in creating composite material from single polymer electrospun PLA fibres 139

List of Figures

Figure 1.1: Polymer dry spinning diagram 3
Figure 1.2: Electrospinning diagram[11] 5
Figure 2.1: Taylor cone visible from electrospinning polyvinyl alcohol in aqueous solution.[41] A triangle exhibting a semi vertical angle of 49.3 degrees has been superimposed on top of the image. 12
Figure 2.2: The number of electrospinning papers published each year since 1995 (data adapted from Web of Knowledge) 13
Figure 2.3: Electrospinning research topics (data adapted from Web of Knowledge) 14
Figure 2.4: Samples from electrospun polystyrene, Mw = 393,400, at various concentrations in THF.[53] 18
Figure 2.5: A graph showing examples of three modes of distribution. Narrow, wide, and bimodal 22
Figure 2.6: A graph showing how SD (%) varies with relative humidity (RH) (%) for the polymers PSU and PAN. Data adapted from Huang et al.[58] 24
Figure 2.7: SEM images of electrospun PSU fibres spun at different relative humidity. (a) 0 % RH; (b) 10 % RH; (c) 30 % RH; (d) 50 % RH.[58] 25
Figure 2.8: Near-field electrospinning diagram[59] 27
Figure 2.9: Typical electrospinning instability (left), instability observed by Xin & Reneker[60] (right) 28
Figure 2.10: Aligned electrospun fibres produced by melt electrospinning[61] 29
Figure 2.11: Schematic diagram of a coaxial electrospinning spinneret (left) and pictures of a compound Taylor cone forming from a droplet (right)[62] 30
Figure 2.12: Emulsion electrospinning. A) Nozzle setup. B) Emulsion of PMMA in PAN.[64] 33
Figure 2.13: Arrangements of different multi-material electrospun fibres and how they are refered to in this thesis 35
Figure 2.14: A multi-channel electrospinning diagram and SEM images of the resultant fibres. Scale bars are 100 nm[67] 36
Figure 2.15: Images of a triaxial electrospun fibre with a gelatine core and sheath, and a layer of PCL in-between. CFM image with dyed gelatine (left), FIB-FESEM cross-section (right) 38
Figure 2.16: A diagram showing a triaxial electrospinning set-up and cross-section of a triaxial fibre for controlled, sustained drug release.[71] 39

Figure 2.17: Tensile strength of glass fibres with changes in diameter. Data adapted from Griffith.[78] 44
Figure 3.1: Single polymer electrospinning set-up. In this set-up the high voltage power supply is situated outside of the fume hood and is not pictured. 52
Figure 3.2: Coaxial electrospinning apparatus 54
Figure 3.3: Drawing of the coaxial spinneret (left) and the finished part (right) 55
Figure 3.4: Rondol bench top 10 tonne heated hydraulic press 65
Figure 3.5: Cooling profile of the hot press 66
Figure 3.6: TGA heating rate 67
Figure 3.7: Mini injection moulding system, Thermo Scientific HAAKE™ MiniJet Pro (left), PLA dog bone samples produced (right) 70
Figure 3.8: Automated hydraulic press, Collins Platen Press P 200 P/M 74
Figure 3.9: Heating and cooling profile used during DSC analysis of the hot pressed composites 76
Figure 4.1: Hexagonal packing of unidirectional fibres 85
Figure 4.2: Schematic overview of composite forming processes for thermoplastic and thermoset matrices. Adapted from Hull[2] 86
Figure 4.3: PLA electrospun from a solution of 15 wt% PLA in THF (left), and from 25 wt% PLA in THF (right) 88
Figure 4.4: Coaxial fibres showing separation of core and shell from intentional damage. 90
Figure 4.5: A cross-section of coaxial fibres embedded in a matrix of PVOH. 91
Figure 4.6: Coaxial electrospun fibres collected at a linear drum speed of 4.87 ms^{-1}. Yellow lines drawn on using ImageJ to calculate fibre alignment. 94
Figure 4.7: Coaxial electrospun fibres collected at a linear drum speed of 6.86 ms^{-1} 94
Figure 4.8: Coaxial electrospun fibres collected at a linear drum speed of 10.6 ms^{-1} 95
Figure 4.9: ^{1}H NMR spectra for PLA dissolved in d-chloroform 97
Figure 4.10: ^{1}H NMR spectra for PCL dissolved in d-chloroform 97
Figure 4.11: Repeating units for polymers, PLA (left), and PCL (right) 98
Figure 4.12: ^{1}H NMR spectra for 0.75 fibre volume ratio composite dissolved in d-chloroform 98
Figure 4.13: Consolidated coaxial electrospun composites cut into 15 mm strips and labelled for tensile testing. Each square on the mat is 10 x 10 mm. 100
Figure 4.14: Results of tensile breakage on the composite (left) and its constituent parts, the PLA fibres (middle) and the PCL matrix (right). Each sample is 15 mm wide. 101

Figure 4.15: Typical stress-strain curves for the composites from a selection of fibre volume fractions, and compared with the bulk polymers. The bulk PCL curve extends to 22% strain, but it has been truncated in this graph for clarity. 102
Figure 4.16: Young's modulus compared to volume fraction of PLA in the composite with standard deviation error. 103
Figure 4.17: Tensile strength compared to volume fraction of PLA in the composite with standard deviation error. 103
Figure 4.18: Elongation at break compared to volume fraction of PLA in the composite with standard deviation error. 106
Figure 4.19: A sample of tensile test results for composite samples of 0.73 volume fraction of PLA 107
Figure 4.20: A sample of tensile test results for composite samples of 0.92 volume fraction of PLA 108
Figure 4.21: Measured Young's modulus of the electrospun composites compared to the upper and lower bound calculated by the rule of mixtures.....111
Figure 4.22: Measured tensile strength of the electrospun composites compared to the upper and lower bound calculated by the rule of mixtures.....111
Figure 4.23: Cross section of a 0.56 fibre volume fraction composite showing uneven distribution of PLA fibres in the PCL matrix 112
Figure 4.24: Cross section of a 0.73 fibre volume fraction composite showing even distribution of PLA fibres in the PCL matrix 113
Figure 5.1: DSC curve of PLA as received, showing two cycles of heating 119
Figure 5.2: DSC curve of PCL as received, showing two heating cycles and the first cooling cycle. 120
Figure 5.3: DSC curve for a sample of coaxial PCL/PLA as spun, before hot pressing. 121
Figure 5.4: DSC curve for experiment 3, a composite pressed at 10 bar and 110 °C and cooled at 10 K/min, resulting in 27.64 % crystalline PLA. 125
Figure 5.5: Effect of PLA fibre crystallinity on the tensile strength of the composites 127
Figure 5.6: Effect of PLA fibre crystallinity on the Young's modulus of the composites 128
Figure 5.7: Effect of composite forming temperature on the tensile strength 129
Figure 5.8: Cross-section of a composite pressed at 70 °C and 1 bar 130
Figure 5.9: Cross-section of a composite pressed at 110 °C and 1 bar 130
Figure 6.1: Assuming coaxial fibre geometry to calculate the diameter of the core fibre 136

Figure 6.2: Aligned PLA fibres.....137
Figure 6.3: Samples tabbed with different grades of masking tape. Each square on the mat is 10 x 10 mm. 140
Figure 6.4: Comparison of tensile properties between the composite produced from coaxial electrospun fibres and a composite produced from electrospun PLA fibres and PCL sheet material 141
Figure 9.1: TGA results for known volume fractions of PLA in a mixture of PLA and PCL.....161
Figure 9.2: Temperature at 80% mass loss for known volume fractions of PLA in a mixture of PLA and PCL compared with results from electrospun samples. 161

List of Abbreviations

AFM – Atomic force microscopy

CNC - Computer numeric control

CRP – Carbon fibre reinforced polymer

DMF – Dimethylformamide

DoE – Design of experiments

FPR – Fibre reinforced polymer

GRP – Glass fibre reinforced polymer

HVDC – High voltage direct current

PAN - Poly(acrylonitrile)

PCL – Polycaprolactone

PLA – Poly(lactic acid)

PP – Polypropylene

PSU – Polysulfone

PTFE – Polytetrafluoroethylene

PVOH – Polyvinyl alcohol

RH – Relative humidity

SEM – Scanning electron microscope

TEM – Transmission electron microscope

THF – Tetrahydrofuran

wt% - Weight percentage (concentration)

UTS – Ultimate tensile strength

Abstract

This study shows that an all-thermoplastic (nano- or micro-fibre) polymer can be created using coaxial electrospinning to create fibre mats akin to pre-impregnated fabric, which can be formed into a composite without the addition of other materials. This has not yet been accomplished by using the coaxial electrospinning production process. Experimentation to investigate the maximum fibre volume ratio found that these composites were successfully formed at 0.73 fibre volume fraction, which is higher than the maximum found in traditionally formed composites (0.60 – 0.70). The formation of the composite from the fibre mats was investigated, and found that the composites formed at the lowest temperature and pressure (70 °C and 1 bar) exhibited the higher tensile strength, up to 84 % higher than at other temperatures and pressures. Higher pressure and temperature caused deformation in the reinforcing fibres, resulting in lower tensile strength. The composites were shown to have more consistent Young's modulus and higher tensile strength compared to a composite made from the same materials, but with the fibres and matrix materials produced separately, and combined during the composite forming procedure.

The finalised composite produced in this research exhibited an average Young's Modulus of 2.5 GPa, ultimate tensile strength of 33.2 MPa, and elongation at break of 3.8 %.

Acknowledgements

Firstly, I would like to thank my supervisors, Dr. Stuart Coles and Professor Kerry Kirwan, for guiding and supporting me through the PhD process.

Thank you to the University of Warwick, WMG, and all the technical staff who put up with me and my project, and for training me and letting me use their equipment. I am especially grateful to the EPSRC who have made this research possible through their generous funding. Thank you to my friends and co-workers who helped to create an enjoyable and friendly office environment.

I would also like to thank my friends and family for their support, not just during my PhD, but everything they have done for me leading up to it. I am especially thankful to my girlfriend, Louise, for her unconditional love and support.

Lastly, and most importantly, I would like to thank anyone reading my thesis, as this gives my work meaning and purpose.

Declaration

This thesis is submitted to the University of Warwick in support of my application for the degree of Doctor of Philosophy. I hereby declare that this thesis is my own work and effort, and that it has not been submitted anywhere for any other award. Where other sources of information have been used, they have been acknowledged.

Thesis Structure

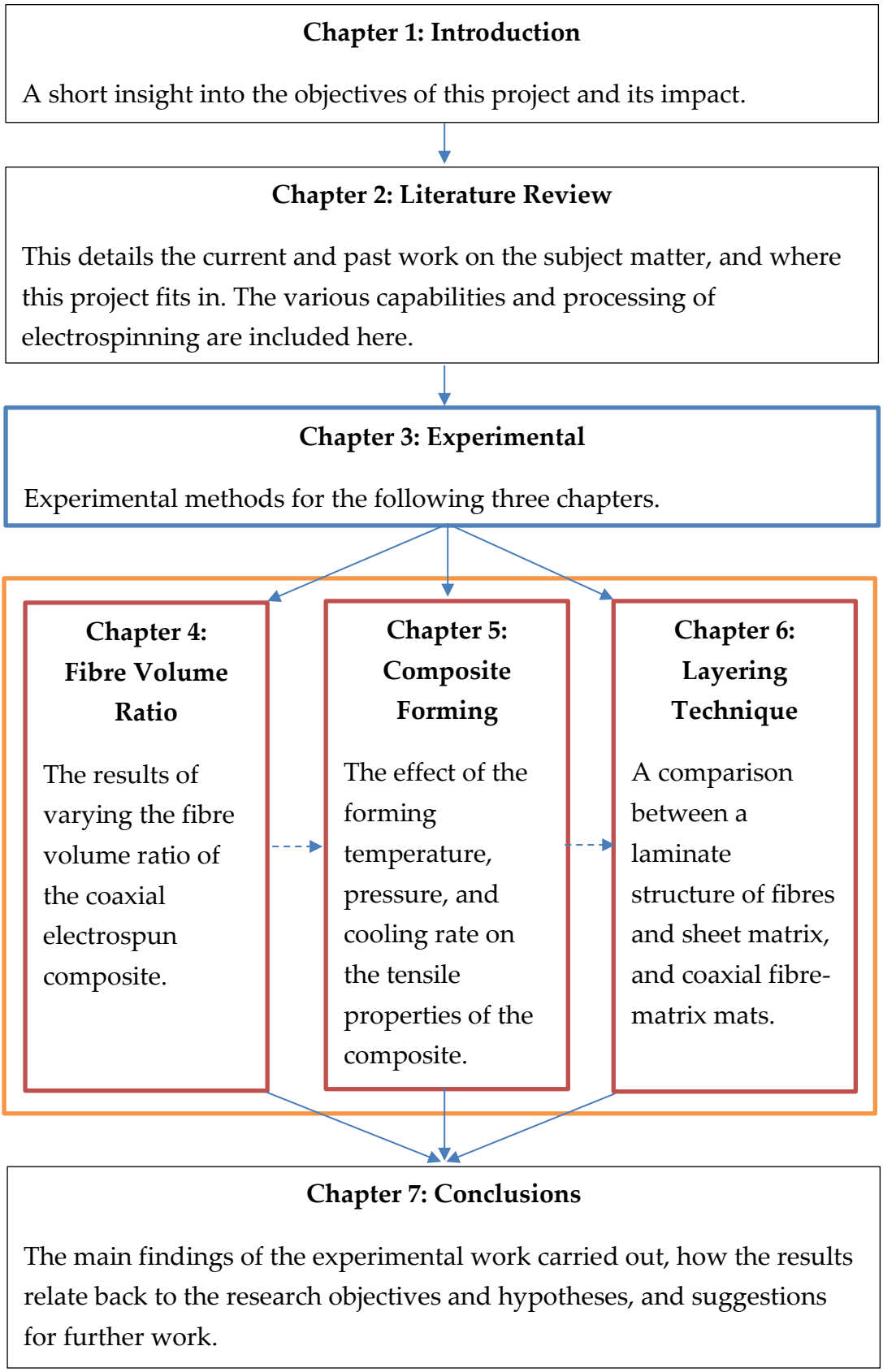

1 Introduction

1.1 Fibres

It is difficult to find a universal definition for a fibre. ISO 8672 is a standard detailing air quality, and defines a fibre as *"any object having a maximum width less than 3 μm, an overall length greater than 5 μm and a length to width ratio greater than 3:1"*.[1] This, however only concerns fibres hazardous to health via inhalation. In reality, the definition of a fibre appears open to interpretation. Within composite materials fibres can be classed as continuous (long) or discontinuous (short).[2] This thesis is concerned with the production of continuous fibre composites.

Fibres are used in everyday life in applications such as textiles, paper, and rope. They are used in place of bulk material due to their inherent high tensile strength. All materials have a theoretical strength calculated from the atomic forces within them, but in reality the strength is much lower than this due to defects and dislocations within the structure creating weak points at which the material can break. Fibres possess a small cross sectional area, so there is little room for defects, resulting in higher strength than bulk material.[3]

The strength of fibres is used throughout nature in plants, animals, and minerals. Table 1.1 shows some examples of some natural and synthetic fibres.

Table 1.1: Examples of some natural and synthetic fibres.

Natural			Synthetic	
Plant	**Animal**	**Mineral**	**Polymer**	**Other**
Cellulose	Silk	Asbestos	Nylon	Glass
Cotton	Wool	Glass*	Rayon	Carbon
Jute			Acrylic	Metallic
Hemp			Polyester	
Flax			Aramids	

*Glass fibres can (rarely) be found naturally as form of lava known as "Pele's Hair"

Since the first synthetic polymer fibre, nylon, was produced in 1935, interest in synthetic fibres has continued to increase due to their low cost and availability. More recently, research has turned back to natural fibres due to the increasing cost of oil, and the drive towards reducing carbon emissions.[4]

1.2 Fibre Spinning

Synthetic polymer fibres are usually produced from an extrusion process called spinning. This involves pushing a viscous liquid through tiny holes of a spinneret and solidifying the liquid into a fibre on the other side. The different processes that can be used are: wet spinning, dry spinning, melt spinning, and electrospinning.[5,6]

Wet and dry spinning both use a polymer dissolved in a solvent to form a solution. In wet spinning the solution is pushed through the spinneret into a chemical bath where the polymer is precipitated out to form a fibre; whereas in dry spinning, air flow is used to evaporate the solvent to solidify the polymer. Melt spinning can be used for thermoplastic polymers. The process is similar, but the molten polymer is

cooled after being pushed through a spinneret. In gel spinning the polymer use is of high molecular weight resulting in a highly viscous solution. This draws out and aligns the polymer chains, increasing the strength of the fibres. Typically, after each of these types of extrusion, post processing of the fibres is carried out to wash and dry the fibres. They are then drawn out to increase strength and orientation of molecular structure.

Figure 1.1 shows a diagram of a basic spinning process. It could be modified to include a chemical bath for wet spinning; or an air flow for dry or melt spinning.

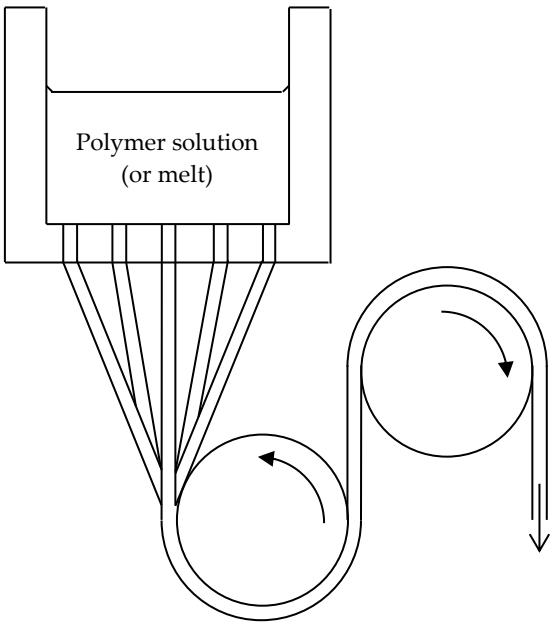

Figure 1.1: Polymer dry spinning diagram

Compared to these more conventional techniques, electrospinning is a differs in that the polymer fibre is drawn out of a solution, or melt, using electrostatic force.

Compared to other spinning techniques, electrospinning can manufacture thinner fibres, ranging from 10 μm to 10 nm.[7]

1.3 Electrospinning Procedure

In a typical modern electrospinning set-up,[8] a droplet of viscous polymer solution, or melt, held on the tip of a needle or nozzle is charged by using a high voltage direct current (HVDC) power supply, typically between 5–20 kV. The polymer can be fed to the needle either using a gravity feed or a syringe pump to ensure a constant droplet is formed. The electric charge causes the droplet to deform, creating a Taylor cone. This is a perfect cone with a semi-vertical angle on 49.3 ° just before it reaches a critical voltage where the electrostatic force overcomes the surface tension of the polymer, ejecting a thin jet from the tip. The jet stretches out and enters an unstable region where it whips about due to the repulsion of charge, which stretches the jet and evaporating the solvent, or cooling the melt. The solid fibre can then be collected onto a grounded or oppositely charged collector. This process is represented in the labelled diagram in Figure 1.2. The collector can either be a stationary plate, in which case the fibres collected will be randomly aligned, or onto a rotating collector, which, if it is rotating at the same speed as the jet is being collected, the fibres will all be aligned in one uniform direction. This rotation speed can vary between a large range of values; for example, Sundaray *et al*.[9] observed that while electrospinning poly(methyl methacrylate) (PMMA) and polystyrene (PS) collection speeds of between 2.5 and 3.0 ms^{-1} produced continuous aligned fibres,

whereas Fennessey and Farris[10] reported optimal fibre alignment when using collection speeds of 8.1 to 9.8 ms^{-1}.

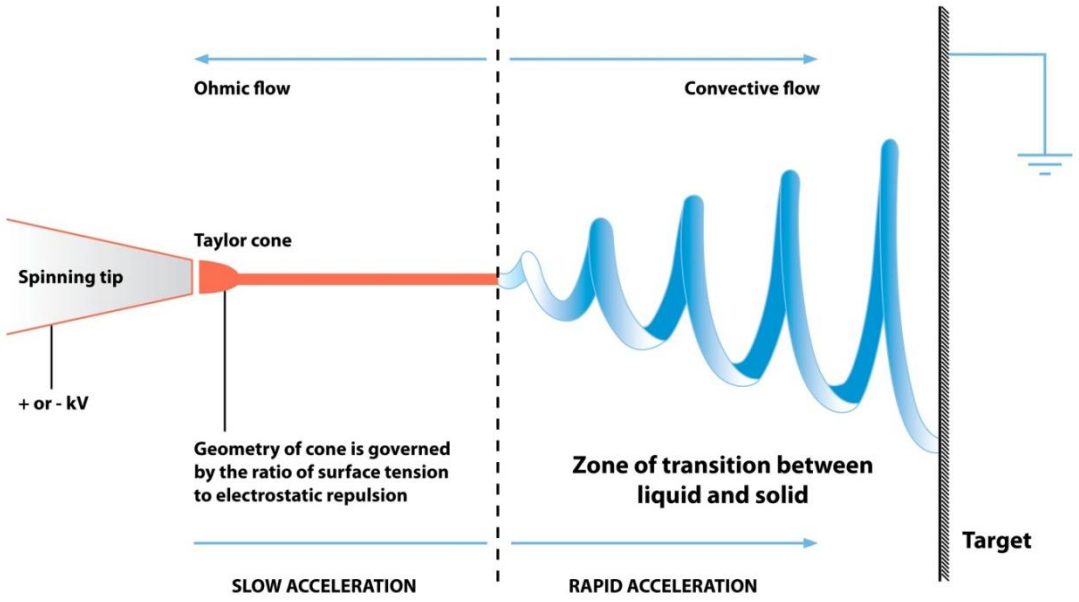

Figure 1.2: Electrospinning diagram[11]

1.4 Aims and Objectives

This thesis looks into a novel methodology for creating fibre-reinforced composites using a coaxial electrospinning technique. The literature review has shown that there is a wealth of electrospinning papers, with the numbers increasing every year. There is currently limited research which looks into the use of electrospun polymer fibres in composite materials, and no research on using coaxial techniques to produce a fibre mat suitable to form a fibre reinforced composite in a one step process of applying heat and pressure. The aim of this thesis is to address that gap.

In order to achieve this, the following objectives have been set:

- Use coaxial electrospinning to produce fibre reinforced polymer composites

- Optimise the technique to improve the tensile properties of the composite
- Investigate and compare the performance of the coaxial electrospun composite

The polymers being used are poly(lactic acid) and polycaprolactone; both of these are biodegradable and biocompatible. These polymers have been chosen due to both these qualities and also their thermal and mechanical properties. The biodegradable and biocompatible nature of the polymers allows the finished composite to be used within the body for soft tissue reinforcement, and the thermal and mechanical properties ensure that the composite can be successfully formed.

Soft tissues within the body can be damaged through everyday wear and tear, and also from accidental injury; particularly when doing sports. Torn tendons and ligaments can be stitched together during surgery, but the result is a weak connection which can easily be subject to further injury before healing has completed.

Various materials can be used to reinforce where the soft tissues have been joined to both take some stress off the stitches, and to cover the soft tissue to prevent abrasive damage. Commercial products currently include reinforcement constructed from human tissue,[12] animal tissue,[13] and synthetic polymers.[14]

Muscle tendons are long fibrous structures,[15] similar, in a fashion, to an aligned, continuous fibre composite material. Research on the tensile properties of muscle

tendons have shown that, depending on the location within the body, and age of the person, they can have a Young's modulus from 0.6 – 2 GPa, ultimate tensile strength from 4 - 100 MPa, and 3 – 10 % elongation at break.[15–18] If the composites produced in this work are to be used as a tendon reinforcement, these values will need to be exceeded, or at least matched.

1.4.1 Hypotheses

It is expected that the composites formed from the coaxial electrospun fibres will be heavily affected by small changes in the production process. In order to improve the tensile properties of the composite, both the electrospinning process and the moulding process will be varied. By varying the electrospinning process, the fibre volume ratio of the composite can be altered. Literature suggests that for this type of composite, fractions between 0.6 and 0.7 are usually considered to be the maximum due to uneven distribution of fibres and imperfect wetting of the fibres by the matrix.[2] This is further discussed in section 2.7. It is expected that the coaxial electrospun fibre composites will be able to challenge this, and produce successful composites with similar or higher fibre volume fractions.

Composite forming is commonly conducted under compression and vacuum moulding. The pressure exerted from vacuum moulding is restricted to one bar (atmospheric pressure), whereas the pressures from compression moulding are much higher, but can be more expensive to run. It is expected that the higher pressure will favour the consolidation of the composite and produce composite with

higher tensile properties by reducing voids and facilitating better fibre to matrix adhesion. Although higher moulding temperatures will reduce the viscosity of the molten PCL matrix, the PLA fibres have a low glass transition temperature and the heat combined with the pressure could deform the fibres. There is also the possibility that the crystallinity of the PLA fibres could be increased by pressing at a higher temperature, as it can undergo cold crystallisation from 90 -100 °C.[19] A change in crystallinity can affect the tensile strength and Young's modulus of the fibres, and therefore, the composite.[20] Composites with different tensile properties could be produced from either a lower temperature forming process just above the melting point of PCL, and a higher temperature process to encourage the crystallisation of PLA.

The coaxial fibres are structured so that low penetration of the matrix material through the fibres is needed, as the material is already dispersed throughout them. This counteracts the main disadvantage of the high viscosity of a thermoplastic compared to a thermoset, as the matrix material is already in place. It is expected that this placement of the matrix will result in a better performing composite, compared to one formed using the same conditions as the coaxial fibres, but with the PLA reinforcing fibres electrospun alone, and the matrix applied during pressing.

2 Literature Review

2.1 The History of Electrospinning

The effect of electricity on fluids was realised before electricity was even fully understood. This began in 1600, when William Gilbert observed that a droplet of liquid could be deformed into a cone shape (now known as a Taylor cone) using a piece of charged amber. However, a stream or jet of ejected particles was not noted until 1750 by Jean-Antoine Nollet, who realised a charged droplet would eject a spray if near an electrical ground. This is thought to be the first reference to electrospraying, the precursor to electrospinning, where the conditions are not suitable for electrospinning (such as the viscosity of the liquid being too low), and the jet breaks up into droplets due to the Rayleigh instability.

Electrospinning was first documented in 1887 by C. V. Boys.[21] He refers to it as *"the old, but now apparently little-known experiment of electrical spinning"*, and made the observation that when the solution was viscous and expelled at high voltage it became a fibre, but as the liquid was heated and became less viscous, the jets broke up into droplets, as in electrospraying.

The first British patent for electrospinning was issued in May 1900 to J.F. Cooley,[22] and the first US patents issued in February 1902 to J.F. Cooley[23] and in July 1902 to W.J. Morton.[24] In these patents, Cooley specified a number of different nozzle designs, including a coaxial nozzle intended to pump a solvent or a neutral fluid

around the polymer, slowing down the evaporation of the solvent and the solidification of the polymer.

The first attempt to mathematically model the electrostatic deformation of liquids was by John Zeleny who published a number of papers from 1907 to 1920.[25–29] He investigated how the liquids behaved under various voltages from different electrodes, determining that the diameter rather than the shape of the electrode affected the discharge. His experiments with different voltages also showed the change in shape of the droplet as the voltage increased, the stability of the current flow over these voltages, and how it varied from being steady to unstable and steady again as the voltage increased.[26]

Electrospinning patents continued to be filed, with Anton Formhals being issued 10 electrospinning patents in the United States of America, and 22 worldwide[30] from 1931 to 1944. In his patents, Formhals mainly focused on variations of the electrospinning set-up and using them to produces textiles and yarns. His inventions included different collection methods; such as, on rotating belts[31–35] and between charged wires,[36] and different charging methods; charging the nozzle and the collector,[31–35,37–39] and only charging the collector.[36]

In 1938 in Russia, Igor Vasil'evich Petryanov-Sokolov and Natalya D. Rosenblum produced fibres from cellulose acetate from which they developed a filter, known as a "Petryanov filter". A factory producing these filters was established, producing them for use in gas masks to filter smoke. The filters proved useful, and in the 1950s

were used in the "Lepestok" particulate filter mask in the nuclear industry. Five billion units were produced by 2003 and they are still commercially available today.[30] These filters have been claimed by the source to be the first commercial usage of electrospun fibres.

In 1964, Sir Geoffrey Ingram Taylor started to look at the deformation of liquid droplets in more detail. He built on Zeleny's work from earlier in the century; applying corrections to the work and implementing his own theories. Taylor theorised that when a droplet was extended to 1.9 times its equatorial diameter it would become unstable, developing a conical point which would project jets of the fluid. He derived that the cone would exist in equilibrium with a semi-vertical angle of 49.3°, and showed experimentally that the cone would expel jets of liquid as it neared this value.[40] This cone, formed from a fluid droplet under the influence of an electric field, is now known as a Taylor cone. Figure 2.1 shows a Taylor cone formed from electrospinning a solution of polyvinyl alcohol. A triangle with a semi vertical angle of 49.3 degrees has been drawn on top of the image to visualise Taylor's theory.

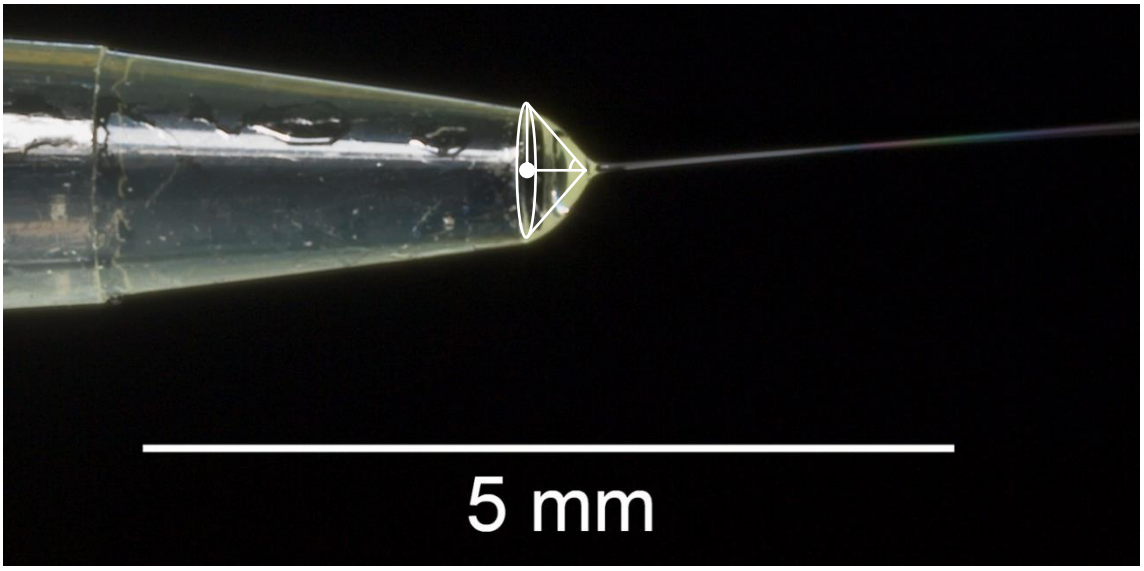

Figure 2.1: Taylor cone visible from electrospinning polyvinyl alcohol in aqueous solution.[41] A triangle exhibting a semi vertical angle of 49.3 degrees has been superimposed on top of the image.

Interest in electrospinning halted for a time, as few applications could be identified. However, advances in nanomaterials in the 1980s and 1990s once again sparked interest into the potential uses for electrospun fibres. The modern age of electrospinning began in 1995, with the publication of the Doshi & Reneker paper[42] which popularised the term "electrospinning" for the process; previously known as either electrical or electrostatic spinning.

2.2 Literature Analysis

Since the dawn of modern electrospinning research in 1995, studies into this field have gathered more interest every year. This is evidenced by the increasing number of papers published in the field, shown in Figure 2.2.

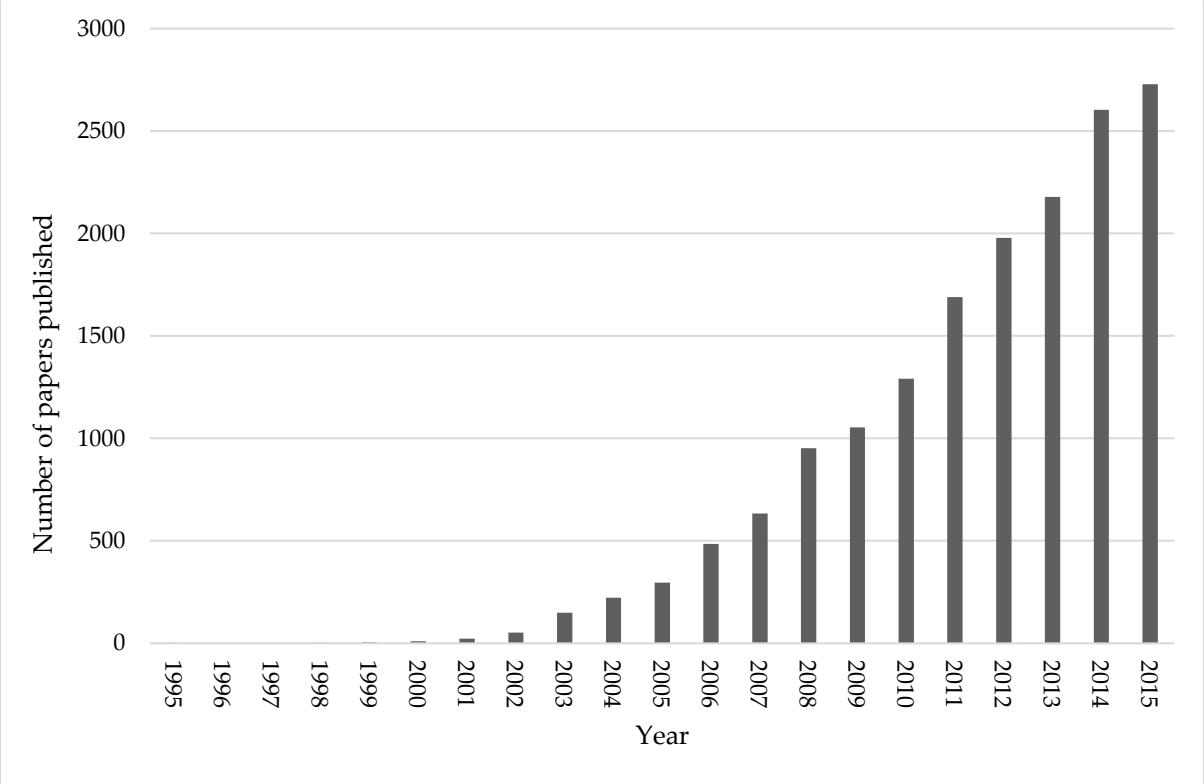

Figure 2.2: The number of electrospinning papers published each year since 1995 (data adapted from Web of Knowledge)

Electrospinning is a versatile process with a lot of scope. Although more demanding to replicate on an industrial scale, a basic laboratory set-up for research can be relatively cheap and simple. The process of electrospinning is quite sensitive and can be difficult to control, as minor changes in the parameters can affect the resulting fibres. As a result of this, and the inexpensive cost, many papers are published merely detailing the successful electrospinning parameters and investigating the subsequent morphology of the resulting fibres. A 2005 study[20] showed that 60 % of electrospinning research was on processing and characterisation of electrospun fibres. A Web of Knowledge search shows that more recently this number has dropped to 30 % as shown in Figure 2.3. This could be due to a shift from the

exploration of the fundamental principles to the consideration of material properties and applications.

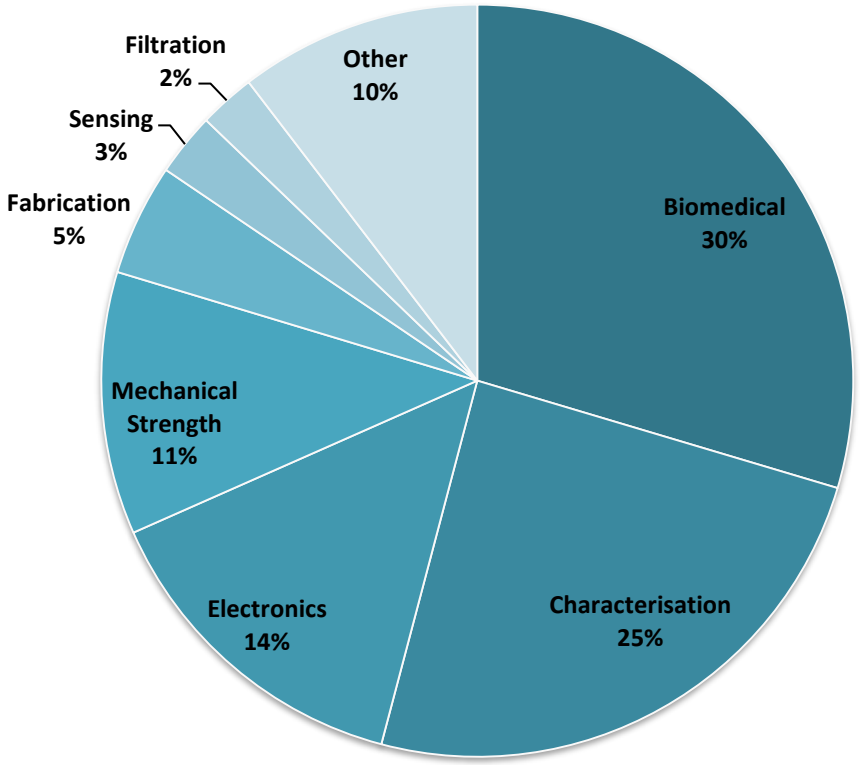

Figure 2.3: Electrospinning research topics (data adapted from Web of Knowledge)

The largest area studied appears to be in the biomedical field, where many uses have been found due to the ease of fabricating biocompatible polymers with large surface areas. The small batch, customisable production of electrospinning also fits well within this niche area due to requirements for bespoke applications within the body. Research is on-going using electrospun fibres for drug delivery,[43] wound dressing,[44–46] and bone scaffolds.[47,48]

The second largest area with regards to applications is within electronics as recently there has been a surge of interest in alternative energy; as electrospun fibres have

been shown to be of use as membranes in fuel cells,[49] and as electrodes in lithium ion batteries.[50]

2.3 Parameter Control

Although the research into characterisation and fabrication is slowing down, it remains relevant as it provides an understanding of the fundamentals of the process. At the forefront of this is the control of the parameters, which can be grouped into solution, process, or environmental, as shown in Table 2.1. Some of the environmental parameters involved affect the process by modifying the others. For example, an increase in temperature can decrease the viscosity of the solution, and a decrease in pressure will cause the solvent to become more volatile.

Table 2.1: Parameters affecting the electrospinning process. Adapted from Coles *et al*.[51]

Solution parameters	**Process parameters**	**Environmental parameters**
Concentration	Electrostatic potential	Temperature
Viscosity	Electric field strength	Humidity
Surface tension	Electrostatic field shape	Local atmosphere flow
Conductivity	Working distance	Atmospheric composition
Dielectric constant	Feed rate	Pressure
Solvent volatility	Orifice diameter	

The successful production of fibres from electrospinning requires a careful balance of the parameters involved.[52] For example, if the spinning voltage is increased the polymer will be ejected more rapidly from the spinneret, therefore the polymer feed rate should be increased to compensate. Likewise, if the distance from the spinneret

to the collector is increased, the voltage would also have to be amplified to maintain the electric field strength, in order for the polymer strands to be ejected. These limiting conditions were realised in the first documented electrospinning experiment:

> *"The conditions for the success of this beautiful experiment are not very easily obtained"*
>
> -C.V. Boys, 1887[21]

This encourages researchers to investigate additional control measures to stabilise the process, and offers a way to alter the properties and morphology of the resulting fibres whilst keeping the input material constant. The production of smooth, consistent electrospun fibres is important in a wide range of applications. A homogenous mat ensures even pore size, important for use as a filter; mechanical strength, for general use and especially as reinforcement in composites; and an even surface area across the mat, for biomedical uses such as drug delivery and cell scaffolds.

Coles *et al.*[51] conducted a design of experiments (DoE) to investigate the effect of variables on the fibre output of polymers polylactic acid and poly(vinyl alcohol). The variables examined were: conductivity with the addition of salt, concentration, electrostatic potential, and the collection distance. It was concluded that the interactions between the variables had a great effect on the output fibres and material properties, which were able to vary diameters from 0.16 to 5.29 μm, and the deposition rate from 7.6 to 298.0 mg h^{-1}.

This was a simple experiment demonstrating the ease at which a single variation in the experimental setup can have a profound effect on the fibres produced.

The following sections details some of the parameters which have the greatest effect on the outcome and success of the electrospinning process. Firstly, the parameters of the polymer solution will be discussed, which can determine whether a fibre can be produced. This will be followed by variations in which the polymer can be delivered, and finally how variation in humidity can affect the surface of the electrospun fibres, introducing roughness and pores.

2.3.1 Polymer Concentration, Molecular Weight, and Surface Tension

As the concentration and molecular weight of a polymer in solution increases, the viscosity of the solution increases. This is because of the nature of the polymer chains; as the longer chains, or higher concentration of chains increases, the interactions between then increase in the form of the Van de Waals forces and chain entanglement.[20] This is an important parameter in forming the fibres during electrospinning.

Eda & Shivkumar[53] experimented with varying the concentration of polystyrene dissolved in tetrahydrofuran and dimethylformamide, for a variety of different molecular weights. Using polystyrene at M_w = 393,400 g mol^{-1} it was observed that for low concentrations, 5.1 wt%, only beads were formed. At both 7.5 and 13.9 wt% thin

fibres are visible connecting the beads, and at 18.9 wt% the polymer transitions to a bead on a string structure. At 21.2 wt% smooth fibres are formed with no beading. SEM images of these results are shown in Figure 2.4.

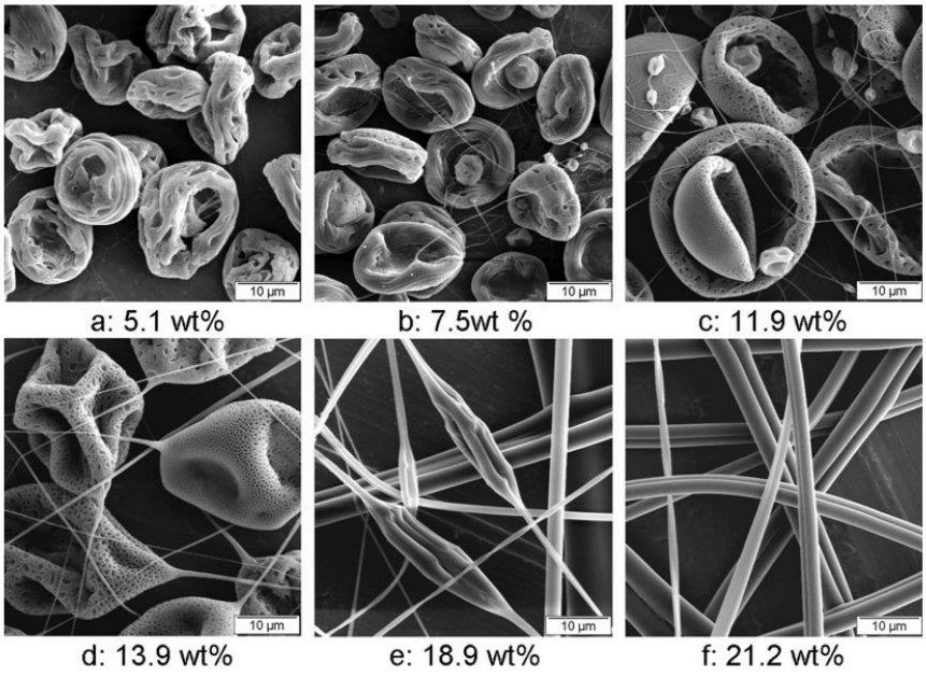

Figure 2.4: Samples from electrospun polystyrene, Mw = 393,400, at various concentrations in THF.[53]

The same pattern was observed for all molecular weights tested, however the critical concentration at which the smooth fibres were formed decreased as molecular weight increased and vice versa. Table 2.2 shows the finding for the critical concentration for each molecular weight tested.

Table 2.2: : Concentration required to electrospin polystyrene fibres using THF.[53]

Molecular Weight (g mol^{-1})	19,300	44,100	111,400	393,400	1,045,000	1,877,000
Critical Concentration (wt%)	48.9	39.7	34.1	21.2	11.9	7.8

These results imply that the effect of both the molecular weight and concentration have on the viscosity are the main factors in forming the fibres, rather than the variables themselves, and as expected critical concentration decreases as viscosity increases. Further work could be done to investigate the viscosity of the solutions at the critical concentrations for each molecular weight.

Yang *et al.*[54] performed similar work investigating the influence of solvent on electrospinning poly(vinyl pyrrolidine). They reported the same findings as Eda & Shivkumar[53] for low concentrations of polymer in solution producing the bead on a string morphology. In addition, they found that a further increase of concentration caused the average fibre diameter to increase from 120 nm to 1.5 μm for concentrations of 2 wt% to 10 wt%. At 20 wt% it was observed that the fibres formed a helical pattern on the collector resulting from the bending instability of the process. The process was unsuccessful from 25 wt% as the viscosity of the solution was too high.

Yang *et al.*[54] also investigated the effect of surface tension on the electrospinning process by dissolving the polymer in different solvents, and by using a mix of solvents. The solvents used were: dimethylformamide (DMF), dichloromethane (DCM), and ethanol. It was found for the solutions with low surface tension, using ethanol, smooth fibres were produced, but with high surface tension, using DMF, significant beading was apparent in the fibres.

These beading effects are due to fluid thread breakup which causes the jet to divide up into droplets. In electrospraying, this effect is taken advantage of, but in electrospinning everything is done to prevent this from happening. The rate at which a viscous fluid thread is broken up into droplets is governed by equation (2.1), derived by Rayleigh in 1892:[55]

$$in = \frac{\boldsymbol{\sigma}}{6a\boldsymbol{\mu}} \tag{2.1}$$

In this equation **σ** is the surface tension of the fluid, **μ** is the viscosity of the fluid, *a* is the initial radius of the fluid jet, and *in* is the growth rate of the instability. The equation shows that increased viscosity and decreased surface tension will each slow the rate at which the thread is broken up into droplets. This results in less beading and smoother fibres being produced from electrospinning.

2.3.2 Polymer Delivery

A challenge which may be faced when electrospinning is to keep the polymer droplet a constant size and shape, in order to protect the stability of the jet. This ensures that the fibres deposited on the collector are of a consistent diameter, an advantage in almost all applications. This is usually done by using a syringe pump set to a constant flow rate to match the rate at which the polymer is ejected. Some researchers have attempted to ensure a stable droplet by using feedback control, creating a closed loop system. Research in this area is lacking, but there is evidence

of using cameras to measure the volume of the droplet, and measuring the current across the jet to keep it constant.[56]

Druesedow *et al*.[56] used an elaborate setup of pneumatics and pressure control devices to achieve a constant droplet. The syringe pump pumps air into a bottle containing polymer solution, which is ejected out of the bottom through a needle. The pressure control system employs sensors to measure the air pressure inside the bottle, and the height of the polymer solution. Two methods for measuring the level of the solution were tested: infrared, and ultrasonic. Both of these methods appear to have their advantages and disadvantages. The infrared method is a cheaper solution, but is intrusive, as a float has to be employed on the surface of the polymer solution to get an accurate measurement. A number of drips were also observed with this method. The ultrasonic transducer, however, was non-intrusive, but more expensive and more sensitive to disturbances. However, no drips were observed. Despite the poorer performance of the infrared sensor, both methods appeared to produce fibre mats similar in fibre density and morphology (500 - 850 nm), and the diameter of the fibres was easily controlled by adjusting the pressure of the system.

This report, however, does not comment on a comparison with a fibre mat spun without any feedback control, and no detailed information is given about the spread data. Although a rough range of data is presented, the standard deviation of the fibre diameters calculated from a representative sample would provide better evidence for producing consistent fibres. Figure 2.5 shows some examples of how a

distribution of fibre diameters might appear. The narrow distribution is preferable when trying to create the most consistent fibres in the mat as the range of fibres is contained. The wide distribution represents a sample without consistent fibre diameters, and the bimodal distribution characterises a sample in which the fibres diameters converge upon two points. This shows that there may be few fibres measuring around the mean values, and without more information it is impossible to know the reliability of the data presented.

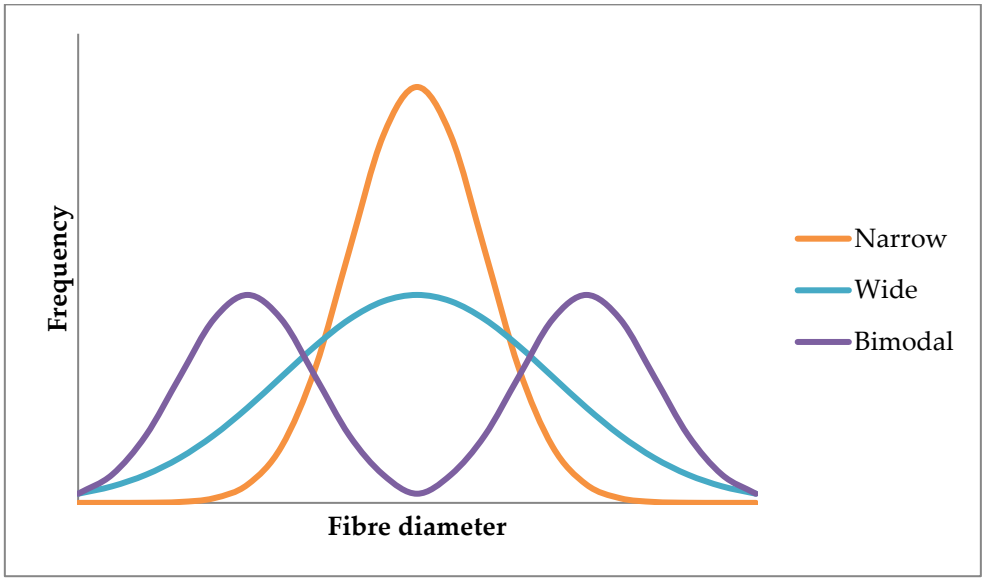

Figure 2.5: A graph showing examples of three modes of distribution. Narrow, wide, and bimodal

The quality of electrospinning results can vary widely, so without a proper comparison with the more traditional method of using a constant flow rate the experiment has not proven that its more elaborate set-up is necessarily advantageous. It does, however, successfully offer a different approach to delivering the polymer solution which may be valuable if traditional methods are unsuccessful.

2.3.3 Controlled Humidity

Varying the humidity during electrospinning can introduce pores onto the surface of the fibres. In dry conditions smooth fibres can be produced, but as humidity increases, as does pore frequency and size (diameter and depth).[57] Controlling the humidity is one of the simplest ways to control the surface of electrospun fibres as it remains a one-step process as no post processing is required.

Huang *et al*.[58] performed humidity control while electrospinning poly(acrylonitrile) (PAN) and polysulfone (PSU), each dissolved in DMF. The morphology and mechanical strength was investigated as the relative humidity (RH) was increased in 10 % increments from 0 %. The PSU fibres appeared to be affected by a greater degree than the PAN fibres by the changes in RH, as pores were formed on the PSU fibres, but the PAN fibre only exhibited increased surface roughness. This is attributed to PSU being hydrophobic, and PAN being hydrophilic, so the moisture on the PSU will form droplets on the surface, leaving indentations (pores). Figure 2.7 shows detailed SEM images of some of the PSU fibres produced with visible pores. Electrospinning at high humidity was unsuccessful as no fibres could be produced after 50 % for PSU and 60 % for PAN.

As the RH increased a steady increase in the average diameter of the fibres was observed, from 1.15 μm to 3.58 μm for PSU and from 150 nm to 630 nm for PAN, with the standard deviation (SD) peaking at the low and high humidity values, as shown in Figure 2.6.

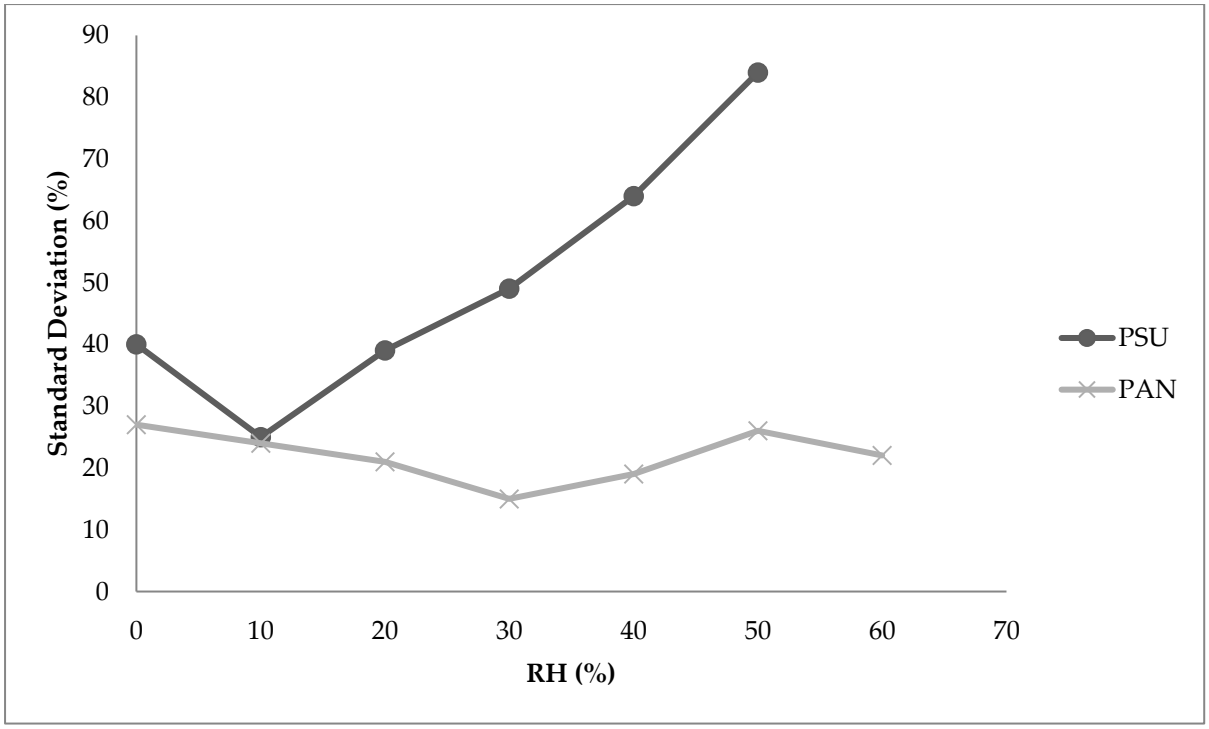

Figure 2.6: A graph showing how SD (%) varies with relative humidity (RH) (%) for the polymers PSU and PAN. Data adapted from Huang et al.[58]

Both polymers appear to have a point where mechanical strength increases with humidity, but quickly drops as humidity further increases. For the PAN this appears at 20 % RH and for the PSU at 10 % RH. The electrospun fibres were only being collected at 70 RPM, which appears to be slower than the deposition rate of the fibre, as the mats produced are not aligned. As a result, the adhesion between the fibres will be a main contributor to the tensile properties of the mat. It is theorised in the paper that the high humidity results in phase separation causing a skin to form on the surface of the jet, and resulting in weaker fibre to fibre adhesion in the mat, causing the decrease in strength at high RH.

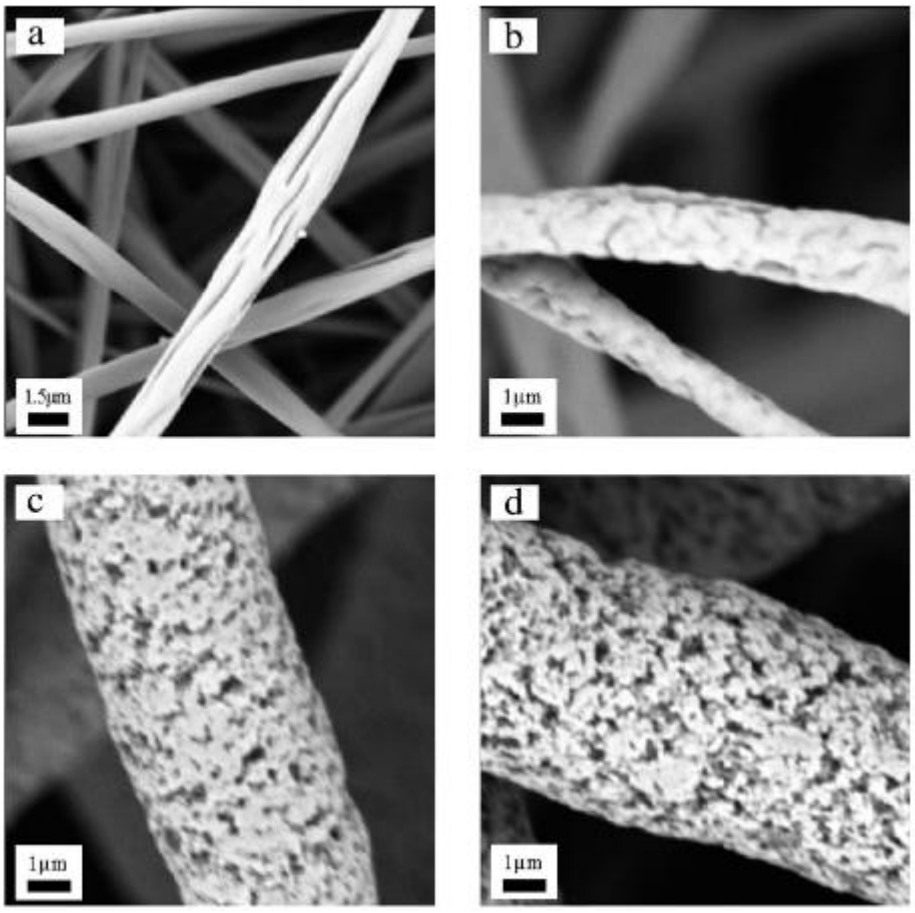

Figure 2.7: SEM images of electrospun PSU fibres spun at different relative humidity. (a) 0 % RH; (b) 10 % RH; (c) 30 % RH; (d) 50 % RH.[58]

Controlling atmospheric conditions is difficult without the correct equipment, but it is clear that it can affect the results of the electrospinning process enormously. Further experimentation could be conducted to investigate the effects of humidity on the mechanical strength of aligned fibres.

2.4 Improved Alignment and Control

In some applications, such as composites, the alignment of the fibres plays an important role in the performance of the product. Using a rotating mandrel to collect the fibres allows for a varying degree in alignment of the collected fibres, depending

on the speed of the mandrel. While this method is satisfactory for most applications, it is possible to produce accurately aligned fibres by removing the instability portion of the electrospinning process; either by reducing the collection distance so that the fibre does not have a chance to enter this instability,[59] or by adjusting the voltage to a point where there is an instability at the beginning of the jet, but the coils shrink, and the jet becomes straight again.[60] This manipulation of the jet can allow for the controlled deposition of the polymer fibre making it possible for it to be used in a similar fashion to a printer. Reducing the bending instability, however, means that the fibre may not stretch as much, and will be thicker.

Sun *et al*.[59] used a short collection distance, with a tungsten electrode with a 25 μm tip to construct fibres 50-500 nm in diameter. Unlike a conventional electrospinning set-up, the polymer solution is applied to the tip of the electrode by dipping it in the solution prior to the spinning. This, however, presents the disadvantage of not being able to produce a continuous jet. Concentrations of solution from 3 - 5 wt% of poly(ethylene oxide) were used. The experiment was successful with the minimum spinning voltage at 600 V, and the minimum collection distance 0.5 mm. Figure 2.8 shows a diagram for this process, with *h* denoting the collection distance.

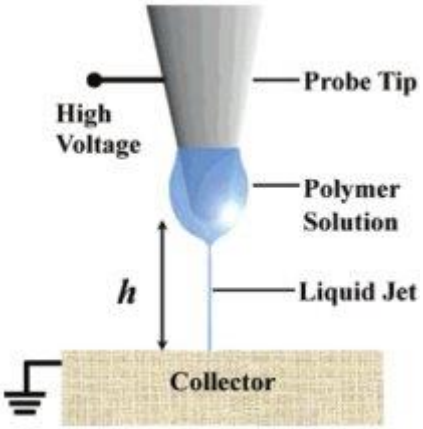

Figure 2.8: Near-field electrospinning diagram[59]

Using such small collection distances reduces the time the solvent has to evaporate, solidifying the polymer. As a result, a highly volatile solvent would need to be used for this procedure to ensure that solid fibres are collected, however, the paper does not mention the solvent used, or comment on the dryness of the collected fibres.

A different method was used by Xin & Reneker,[60] who found that, when using a 25 wt% solution of polystyrene dissolved in dimethylformamide (DMF), the whipping instability settled at low voltages producing a straight jet again, shown in Figure 2.9. This effect was less stable at lower concentrations, and was not detected for concentrations from below 15 wt%. It was observed that at 2.8 kV the instability settled and the jet became straight again. The size of the instability region decreased with the voltage, when finally, at 2.5 kV the region disappeared, and only a straight jet from the nozzle to the collector was observed. This was demonstrated for collection distances from 2 cm to up to 16 cm. It is stated in the paper that there could be many reasons for the appearance and disappearance of the instability, but it is not discussed any further. The diameter of the fibres produced is not explicitly

stated in the paper, but from the SEM images provided they appear to be in the region of 10 μm. Straight fibres were successfully deposited by matching speed of deposition to the movement speed. When the deposition speed was faster, uniform buckling patterns were created as the fibre was deposited, with the size and shape varying with the collection distance.

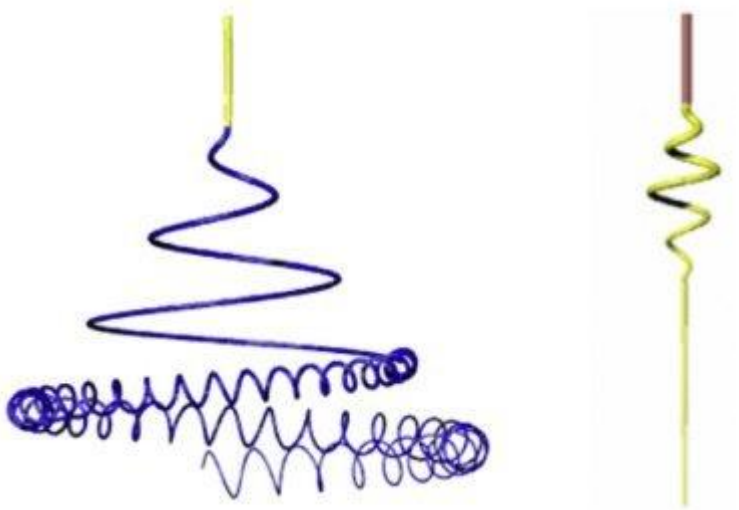

Figure 2.9: Typical electrospinning instability (left), instability observed by Xin & Reneker[60] (right)

The slight difference in techniques here is the collection distance. As in the first, the fibre is collected at short distances before it can enter the whipping instability. In the other the voltage is reduced, such that a fibre jet is still ejected, but is low enough that the whipping instability occurs only briefly or not at all.

Recently it has been found that melt electrospinning, using hot polymer melt to electrospin rather than a solution, can produce these straight jets with ease.[61] This may be due to the lower conductivities and higher viscosities of melts compared to solutions. Research into this is increasing as the potential to use this phenomenon in three dimensional (3D) printing is being realised. The highly aligned fibres produced

by this method can be seen in Figure 2.10. The precision at which the fibre can be deposited can even allow stacking of the fibres up to approximately 1 mm in height.

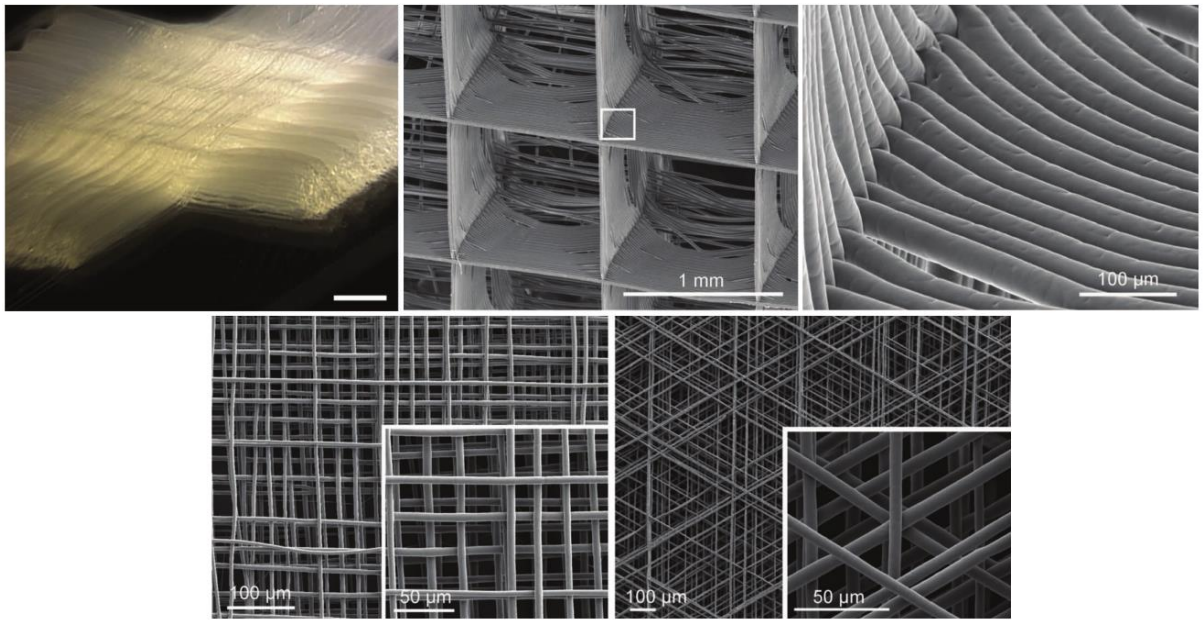

Figure 2.10: Aligned electrospun fibres produced by melt electrospinning[61]

2.5 Coaxial

Establishing control over the basic monolithic electrospinning is important before moving on to more complex coaxial electrospinning. Coaxial indicates a fibre or a cable with two concentric (about a common axis) materials. These can be produced by extrusion processes. “Overjacketing extrusion” is where a polymer is extruded while coating another material, such as a wire. “Coextrusion” is where two (or more) polymers are extruded simultaneously to form multiple layers. This method is used to create synthetic fencing using the core material for strength and the sheath to protect it from weathering effects and for colour. Coaxial electrospinning has the potential to create much thinner fibres with similar properties and applications.

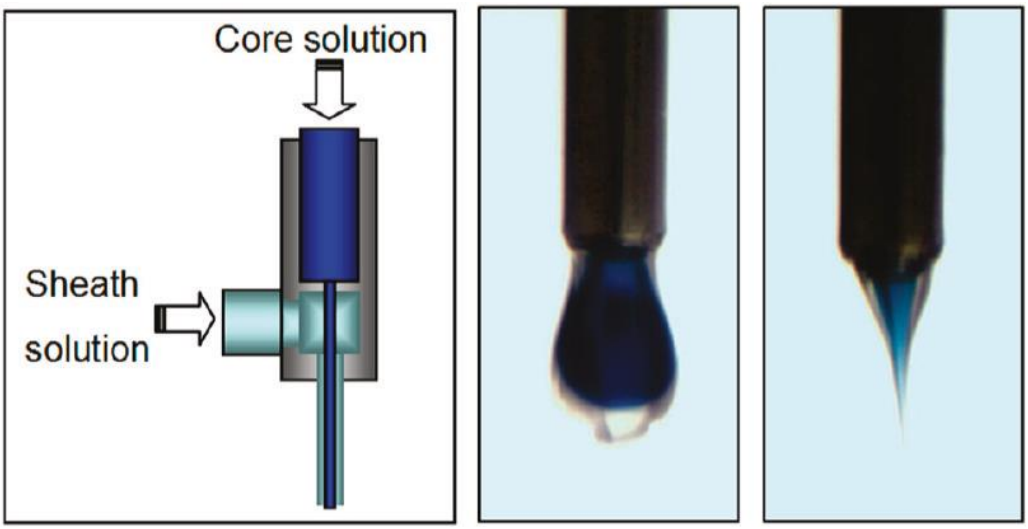

Figure 2.11: Schematic diagram of a coaxial electrospinning spinneret (left) and pictures of a compound Taylor cone forming from a droplet (right)[62]

To produce a coaxial fibre, a sheath solution must surround the core solution to produce a droplet within a droplet. The electrostatic charge applied to the needle is distributed within the sheath solution which is drawn out as usual, but the viscous force draws the core solution out with it as it forms the Taylor cone, as shown in Figure 2.11. By using this viscous force, solutions which cannot usually be used in electrospinning can be spun as a core, providing that the sheath solution is suitable.

Coaxial electrospinning is a fairly recent development, first appearing in the literature in 2003.[63] Sun *et al.* investigated coaxially electrospinning: poly(ethylene oxide) (PEO), PSU, poly(dodecylthiophene) (PDT), and palladium (II) acetate ($Pd(OAc)_2$), in the following shell-core configurations: PEO-PEO, PEO-PSU, PEO-PDT, and PLA-$Pd(OAc)_2$. The structure of the PEO-PEO fibres were viewed optically as the core and the shell had different amounts of bromphenol dye in them; the diameters for the shell and the core measured 3 μm and 2 μm. The structure of the

PEO-PSU and PEO-PDT fibres were clearly visible under a TEM, with shell and core diameters measuring 60 nm and 40 nm, and 1 μm and 200 nm respectively. This large difference in diameter despite the same shell polymer can be explained by the varying experimental technique. The PEO-PEO fibres were spun using 3 to 5 kV, whereas the for PEO-PSU, 9 kV was used, and for the PEO-PDT fibres, a lower molecular weight PEO was used. The PLA-$Pd(OAc)_2$ fibres were annealed to produce a core of solid palladium. Transmission electron microscope (TEM) imaging also clearly showed the structure of the fibres here revealing diameters of 500 nm and 60 nm for the shell and core. Both the PSU and $Pd(OAc)_2$ did not form fibres independently, as the molecular weight of the PSU used was too low, resulting in a solution with too low viscosity for electrospinning; and as $Pd(OAc)_2$ is not a polymer it cannot be electrospun by itself in a one-step process. This shows the shell solution can provide a template for the core to be drawn out, and opens up the opportunity to electrospin many more substances than previously thought, by using a coaxial system.

The following sub-sections delve deeper into coaxial electrospinning, including: an alternative method of production, an instability unique to coaxial electrospinning, and the addition of more axes within the fibre in both multi-axial and triaxial methods. The literature discussed all present improvements which can be made to the process, enabling increased control, and to further understand the process.

2.5.1 Emulsion

It is possible to produce coaxial fibres without specialized equipment. This is, however, limited to producing fibres in which the core solution can form an emulsion in the sheath solution. The core solution which is dispersed as droplets in the sheath solution is then drawn out with the sheath solution during spinning.

Bazilevsky *et al*.[64] suspended an emulsion of poly(methyl methacrylate) (PMMA) in a matrix of polyacrylonitrile (PAN); both solutions were 6 wt% dissolved in dimethylformamide (DMF). When the solutions were mixed they formed a metastable solution, but after one day the mixture decomposed into an emulsion containing droplets of PMMA 100–200 μm wide (Figure 2.12B). After two days, the mixture separated into layers with the PAN solution on top. The emulsion was pumped into a single-axial nozzle using a syringe pump and electrospun onto a grounded collector wheel, as shown in Figure 2.12A. The resulting fibres were in the range of 0.5–5.0 μm and were similar to fibres spun from a coaxial nozzle. This method makes it difficult to control the relative sizes of the sheath and core fibres, as it depends on the surface tensions of the two solutions and cannot be varied as easily as with a syringe pump control.

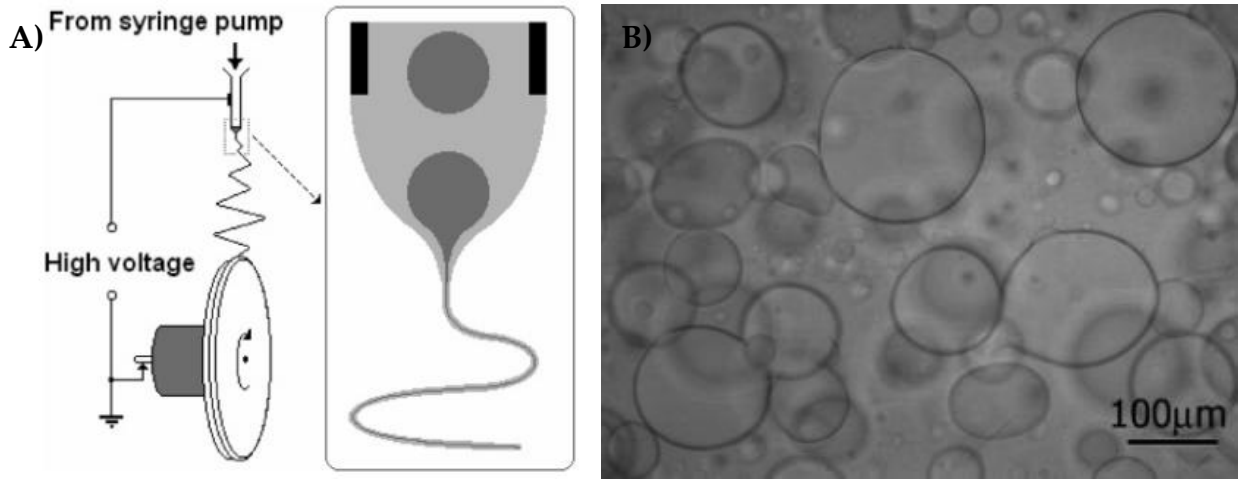

Figure 2.12: Emulsion electrospinning. A) Nozzle setup. B) Emulsion of PMMA in PAN.[64]

A variation of this method can use particles suspended in a matrix solution to produce fibres containing the particles. Experiments show that this can produce fibres with a uniform spacing of particles, even with particles that can typically be difficult to disperse evenly, such as silver nanoparticles.[65]

2.5.2 Nanosprings

The addition of a second material allows new properties to be incorporated, but new instabilities can arise as well. Although this could be useful in some applications to create a ductile mat, this could also be seen as an instability in the process. It is important to understand possible instabilities when electrospinning in order to prevent them and to optimise the process and therefore the results.

Chen *et al.*[66] details how when spinning two materials with different shrinkage, it can cause the fibres to coil, resulting in the formation of nanosprings. Nomex and thermoplastic polyurethane fibres were spun and nanocoils were successfully produced using off-centred coaxial and side-by-side setups. The coiling fibres were

collected on a rotating collector at two speeds, 2 m s^{-1} and 16 m s^{-1}. At 2 m s^{-1} about 50 % of the fibres were aligned and at 16 m s^{-1} all the fibres were aligned, but in doing so, the nanocoils were stretched straight, resulting in a straight fibre mat.

Mechanical testing was conducted on the fibre mats spun at 2 and 16 m s^{-1} to compare the aligned fibres with the nanosprings. The tensile strength in the nanospring mats was lower than the aligned fibres (151 MPa compared to 202 MPa). This was due to the poor connections between fibres and a lack of alignment in the nanospring sample, which also displayed just under three times the elongation of the aligned sample (97 % compared to 33 %).

2.5.3 Multi-axial

By definition, co-axial indicates multiple materials arranged concentrically around a single axis. The next two sections deal with variations of the traditional two material co-axial electrospinning. Figure 2.13 shows how these arrangements will be referred to in this thesis. Although the arrangement labelled "tri-axial" also adheres to the co-axial definition, it will be labelled as such to differentiate it from the traditional setup.

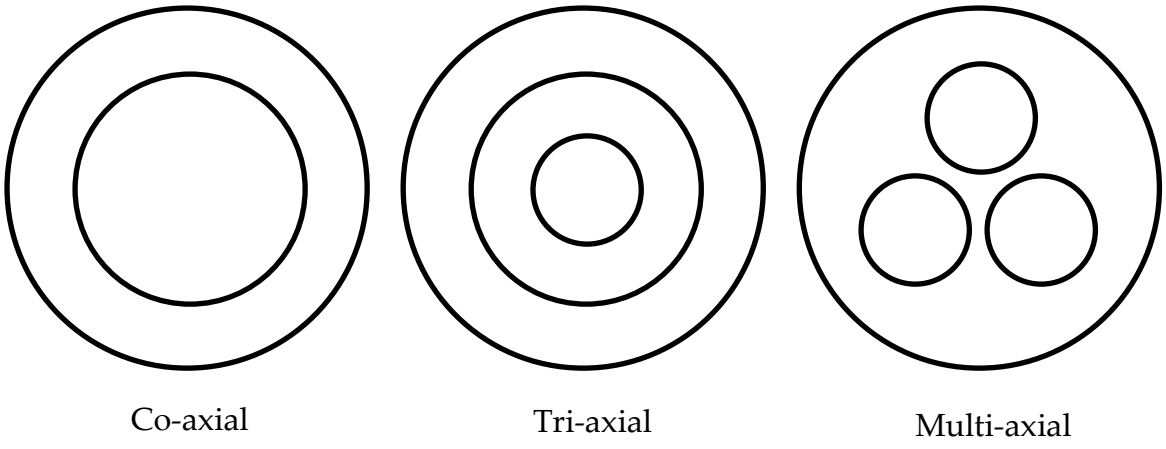

Figure 2.13: Arrangements of different multi-material electrospun fibres and how they are refered to in this thesis

Multi-axial electrospinning can be considered a development from coaxial spinning. In using this technique, more than two different materials can be spun within the same fibre, and in a variety of arrangements.

In an attempt to mimic nature, Zhao *et al.*[67] produced multi-channel fibres using a mixture of polyvinylpyrrolidone (PVP) and Ti(O*i*Pr)$_4$ in ethanol solvent for the shell, and paraffin oil for the channels. By removing the organic compounds from the resulting fibres, multi-channel fibres of TiO_2 were formed. Similar structures can be found in nature and for a variety of uses; for example, the insulating hair on a polar bear,[68] the light-weighting of feathers in birds, and materials delivery in the lotus root. Successful results from this study are shown in Figure 2.14. In this figure, multiple axes are present. In each, the sheath or the cores does not share their axes with any others, so in each, the number of axes is one, plus the number of cores. In (a) there are 3 axes, in (b) 4 axes, in (c) 5 axes, and in (d) there are 6 axes.

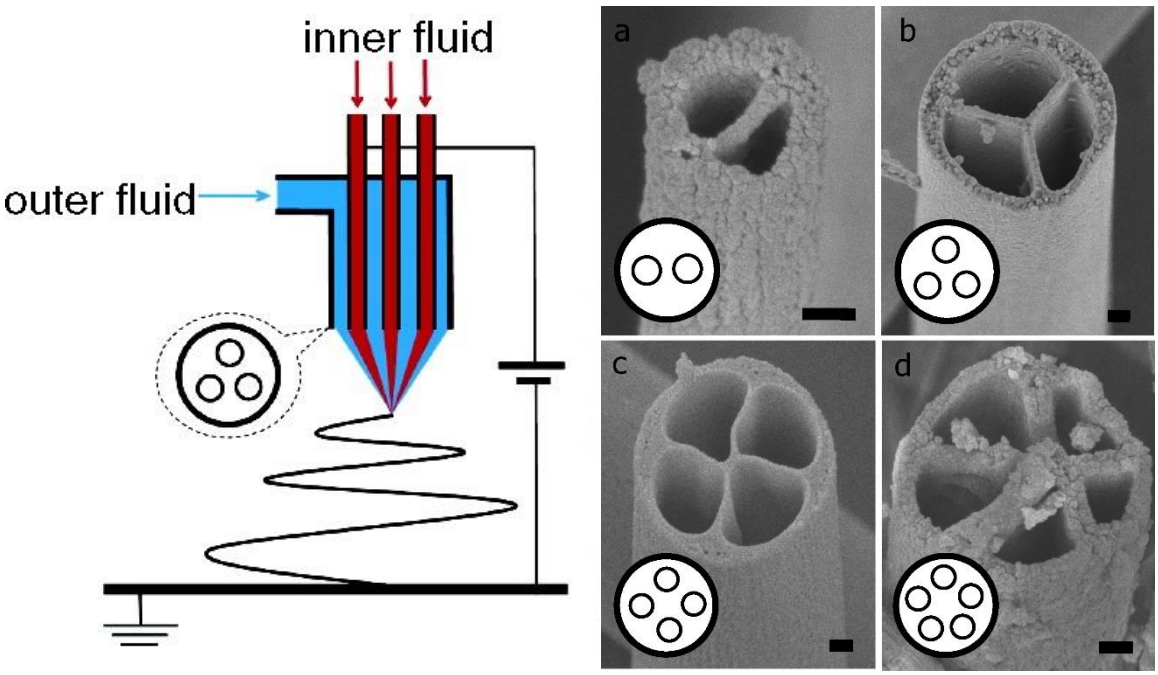

Figure 2.14: A multi-channel electrospinning diagram and SEM images of the resultant fibres. Scale bars are 100 nm[67]

These multi-channel fibres could be used in a variety of applications. They could be used to provide insulation in textiles, and may perform better than hollow fibres as the reinforcing struts would help to prevent the fibres from collapsing. The multiple channels could also be used to hold a myriad of drugs to be released through the fibre without prior mixing, or to hold different polymer precursors for use in self-healing applications.

2.5.4 Triaxial

A triaxial fibre can be distinguished from a multi-axial fibre as the layers of material share the same axis, alike to a coaxial fibre. Coaxially spinning two different materials has proven uses in research, thus adding an additional material layer could also have its uses. Adding a third concentric needle to a coaxial set-up can produce fibres with three layers: a core, intermediate layer, and a shell layer.

Lallave *et al*.[69] used a triaxial spinneret to electrospin hollow lignin fibres as a precursor to hollow carbon fibres. Glycerine was used as the core material to provide a template for the lignin solution (50 wt% in ethanol), which surrounded it, and finally, an ethanol outer sheath was used to prevent the lignin from solidifying too rapidly and causing blockages on the nozzle. The paper does not go into detail regarding the hollow carbon fibres, and focuses largely on creating solid carbon fibres, however, from a TEM image provided, it can be seen that hollow carbon fibres were created with a diameter of about 450 nm, with a hollow core of about 200 nm.

To prove the feasibility of triaxial electrospinning biodegradable polymers, Liu *et al*.[70] electrospun poly(ε-caprolactone) (PCL) surrounded by gelatine both in the core and shell layers. As gelatine is limited by its mechanical strength, PCL was used to strengthen the structure. The gelatine sheath allows greater cell compatibility, and the gelatine core can be used to store drugs for controlled release. The triaxial fibres were successfully imaged using an SEM, and exhibited diameters of approximately 1 μm. To view and confirm the triaxial structure of the fibres, other microscopy techniques were applied, these were: confocal fluorescence microscopy (CFM) and field-emission scanning electron microscopy (FIB-FESEM). When using dye in the gelatine, the structure was visible with CFM, but the poor resolution makes it difficult to measure the dimensions of each layer. FIB-FESEM uses a focused ion beam to cut through a fibre and reveal the inner structure. The three layered fibre is

clearly visible in these images, with the sheath, intermediate, and core layer diameters measuring 970 nm, 710 nm, and 230 nm respectively. Images from both methods can be seen in Figure 2.15.

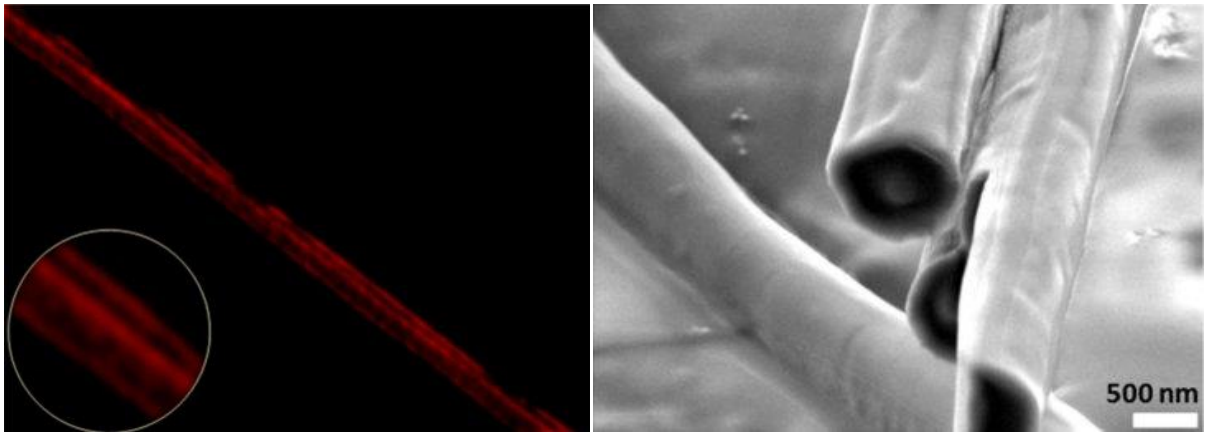

Figure 2.15: Images of a triaxial electrospun fibre with a gelatine core and sheath, and a layer of PCL in-between. CFM image with dyed gelatine (left), FIB-FESEM cross-section (right)

These fibres could be useful in terms of medical applications such as: slow release drug implants, due to the ability to incorporate drugs into the gelatine core, and bone and tissue scaffolds, due to the strength of the PCL, the biocompatibility of gelatine sheath, and the ability to include growth elements or drugs into the core to assist with the healing.

The most appropriate biocompatible polymer coatings are often not ideal for controlled drug release. To improve on this, an additional layer was developed by Han & Steckl,[71] building on the work by Liu *et al.*,[70] to ensure a slower controlled release. The core holds the drugs, a nonhygroscopic layer controls the release and lastly a hygroscopic, biocompatible shell to enable the initial burst release. The tri-

axial fibre arrangement, shown in Figure 2.16, was used to control these two rates of drug release.

The triaxial fibres were spun with a polyvinylpyrrolidone (PVP) core, and poly(ε-caprolactone) (PCL) intermediate and shell layers. Dye was mixed in with the sheath solution and with the core solution to simulate the release of drugs. The results showed that while coaxial fibres would release 80 % of the dye within 1 hour, the triaxial set-up required 24 hours to release the same amount, as after the initial burst, the release was more sustained.

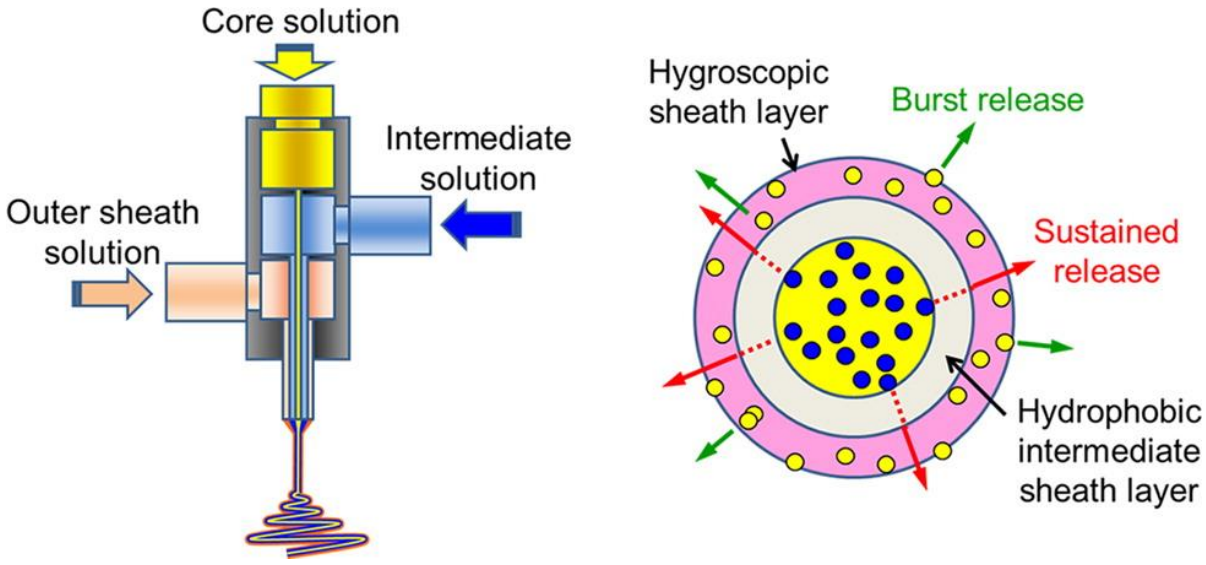

Figure 2.16: A diagram showing a triaxial electrospinning set-up and cross-section of a triaxial fibre for controlled, sustained drug release.[71]

This method could be used to control the release of two different drugs. For example, when used in a wound dressing, anaesthetic drugs could be released in the initial burst to dull pain, followed by a sustained release of antibiotics to prevent infection.

These experiments into triaxial electrospinning show that there is still much work that can be done with electrospinning. These methods present simple ways to combine different materials and properties into single fibres, opening up a myriad of potential uses for electrospinning.

2.6 High Throughput

The potential for having a high volumetric yield is an important aspect of this project, and most electrospinning research in general. When a useful end product can be produced for the consumer market, slow production can drive up costs making the product too expensive and not viable for market. It is therefore extremely important for production to meet a competitive level. As conventional electrospinning runs at very low flow rates and low concentrations, the deposition rate of polymer is slow, and unsuitable at industrial scale.

Both single polymer and coaxial fibre production can be improved by using multiple nozzles, but other needleless methods specific to each can provide higher throughput.

2.6.1 Single polymer

Elmarco's Nanospider™[72,73] can produce electrospun nanofibres thousands of times faster than conventional methods, depending on the size of the apparatus. This is a nozzle-less method consisting of a mandrel in a bath of polymer solution which rotates to coat itself in the solution. A high voltage is passed into the mandrel which

causes the polymer to collect into beads and eject from the surface upwards onto a grounded collector. Another method shown by Elmarco is to use a single charged wire as an electrode. The electrospinning solution is then coated over the wire using a delivery system moving back and forth over the wire as the polymer is ejected.

These methods have the disadvantage of not being able to produce continuous fibres as the solution applied is finite, and the jets stop and start throughout the process. However, due to the thin diameters and aspect ratio of the fibres produced, this can be considered negligible for most applications.

Another, less successful, bottom-up approach to mass production, first published in 2007,[74] pumps air through a polymer solutions to form bubbles on the surface of the polymer which deform into Taylor cones when an electric field is applied. This causes many Taylor cone bubbles on the surface of the polymer, and an equal number of jets of solution ejected on to the collector. This technique has similar issues with non-continuous fibres as the previous method. It may also have issues with premature solvent evaporation as a result of leaving a surface open to the atmosphere.

Although not strictly a means of mass production, blowing air around the jet can speed up the process by introducing an additional shear force on the fibre and droplet.[75] To do this, a similar setup of concentric needles for the production of coaxial fibres can be used, but instead of using the outer needle to spin a shell

polymer, high pressure air is pumped through. Electroblowing can also aid in the production of previously non-electrospinnable polymers, such as hyaluronic acid.[76]

2.6.2 Coaxial

With coaxial electrospinning being a newer technique that single polymer electrospinning, and with fewer commercial applications requiring the need for the coaxial process, research to scale up the production of coaxial electrospun fibres is in its infancy. This is, however, very important it improve the commercial viability of any research involving coaxial electrospun fibres. There are currently two techniques that can be found in the literature which has had success with this endeavour.

Establishing a similar technique to the Nanospider, Forward *et al*.[77] produced coaxial fibres. Metal wire electrodes mounted on a spindle are passed through a bath of two immiscible polymer solutions, where one sits above the other. The lower layer of solution coats the wire and the upper layer coats the lower layer of solution around the wire. The electric field then draws the solution into Taylor cones across the wire, and coaxial fibres are drawn up towards the collector. The thickness ratio of each layer on the wire corresponds to the core to shell ratio on the resultant fibres, and can be varied with the capillary number of the solutions used. The non-continuous nature of this technique may result in an uneven distribution of core to sheath polymer as the droplet is drawn into a fibre and reduces in size. It also limits the polymers and solutions which can be used, and how they can be arranged in the fibre, as the less dense solution will always be the sheath.

Yan *et al*.[73] developed a method to produce coaxial nanofibres with a 300 times volumetric throughput increase when compared to typical coaxial needle setup. For this method, rather than using a coaxial needle, a "coaxial" slit was used; a slit within a slit. When a high voltage was applied, multiple Taylor cones formed across the slit, and jets of polymer solution were ejected on to a collector. The pressure drops around the formation of a jet causing more solution to flow towards these points, ensuring a constant flow. This technique manages to produce continuous coaxial fibres with a vast yield. Like much of coaxial electrospinning it has only been developed recently, so research is still ongoing, and has yet to make it to market.

2.7 Composites

A composite is a material containing two or more constituents: a filler material and a binder. Composites are present in nature: for example, wood consists of cellulose fibres which are bound together with lignin. While the filler material is usually a strong fibrous material, other materials can be used to take advantage of their properties. For example, metal particles can be added to a resin to increase its thermal conductivity.

Fibrous materials are effective because many materials exhibit higher strength and stiffness than their bulk counterparts. This was proven experimentally in 1920 by Griffith using glass fibres.[78] The experiment showed that the tensile strength of the glass fibres increases as the diameter of the fibres decreases (Figure 2.17). Extrapolation of the experiment showed that the tensile strength of the fibres

approached the theoretical strength of the bonds between the atoms. This is because as the diameter of the fibres decreases, there can be fewer defects within the sample to create weakness and failure points. These defects can include small cracks or voids in the material, or dislocations in the atomic lattice. These weaken the structure by causing stress concentrations in these areas, resulting in premature failure.[2]

In addition to this, polymers are comprised of long molecular chains which are usually randomly orientated in their bulk form. When drawn out into fibres, these polymer chains can align in the direction of the fibres, giving the polymer fibres increased strength over the bulk material due to stronger intermolecular bonds.[79,80]

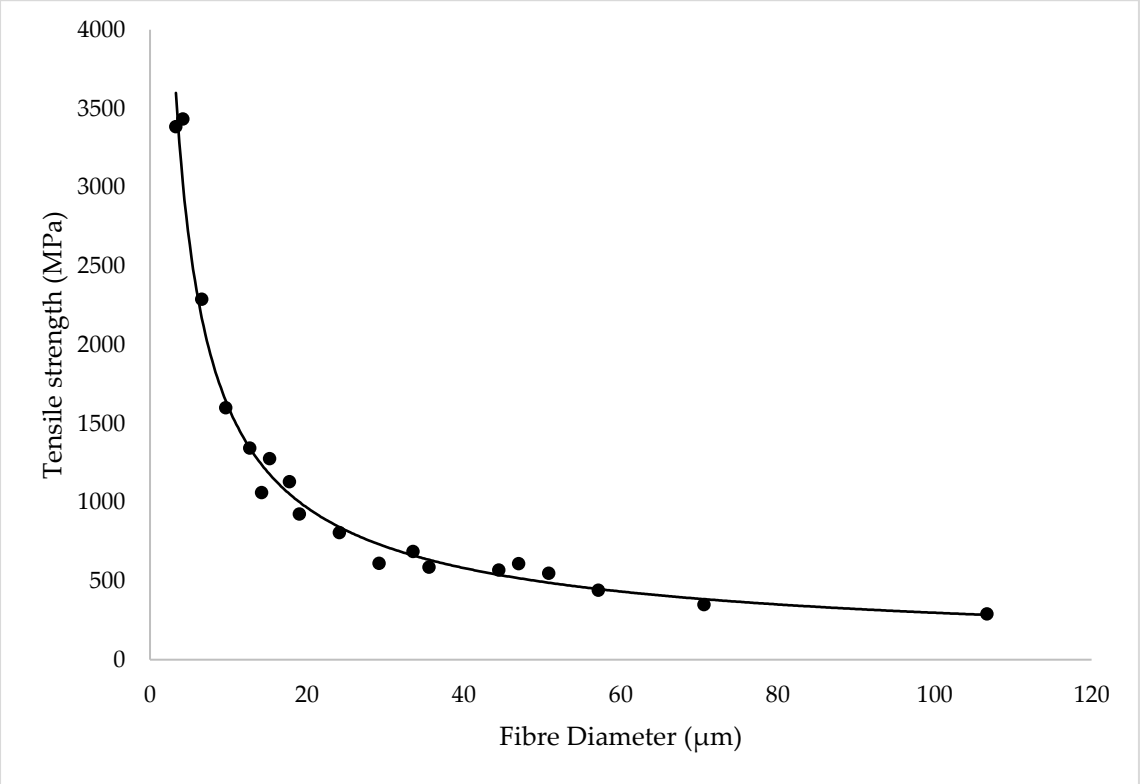

Figure 2.17: Tensile strength of glass fibres with changes in diameter. Data adapted from Griffith.[78]

Polymer matrix composites (PMC) are often reinforced with glass or carbon fibres, and are becoming more and more prevalent in today's industry with demand rising due to the need for these lightweight, and strong materials. Glass fibre reinforced polymer (GRP) is cheaper to produce than carbon fibre reinforced polymer (CRP), but offers less strength per mass of material, making it less popular in high end applications. However, GRPs remain the largest group of materials in the composites industry, accounting for over 95 % of all composites. In 2014, 8.8 megatonnes of GRPs were produced worldwide. Over the past 10 years, demand for GRPs has remained steady, however, the demand for CRPs is rising. In 2014, 83 kilotonnes of CRPs were produced, over double the demand from 5 years before (41 kilotonnes). Furthermore, this is expected to rise to 175 kilotonnes by 2021.[81]

The recycling of these materials poses current and future issues due to rising usage. Glass and carbon fibres and the thermoset polymers which are commonly used, are not biodegradable, so to avoid landfill they must be either recycled or reused. Recycling these materials is difficult; firstly due to the need to separate the constituent parts, and secondly, once separated, the fibres are shorter and weaker than the virgin fibres. Thermoset polymers, which are often used in PMCs, are also difficult to recycle as they cannot be remoulded.

The quantity of research into electrospun composites has been low. This is surprising considering the ease of using electrospinning to produce some of the thinnest fibres currently possible, which are perfect for use in fibre reinforced polymer (FRP)

composites due to their high strength. Post processing techniques can be also be applied to electrospun fibres to create more than just thermoplastic polymer fibres, for example, polyacrolonitrile (PAN) fibres can be heat treated and carbonised to form carbon fibres,[82,83] and metal particles included in the electrospinning solution can be fused together to create metal fibres.[84]

Bergshoef & Vancso[85] used electrospinning to produce nylon nanofibres for use as reinforcement in a phenolic epoxy resin matrix. The composite films produced were fully transparent as the electrospun fibres (with diameters of 50-200 nm) were thinner than the wave length of light (400-700 nm). The nylon fibre reinforcement increased the Young's modulus of the epoxy resin from 2.5 MPa to 91 MPa. The yield strength, however, was not reported to have changed, remaining at 16 MPa.

Kim & Reneker[86] produced composites reinforced with electrospun poly-benzimidazole fibres. These were embedded in an epoxy matrix and a styrene-butadiene rubber matrix using vacuum and compression moulding respectively. The addition of 15 wt% fibres increased the tensile strength of the rubber by 33 % and the Young's modulus by almost 10 times from 1.8 to 19.8 MPa. For the epoxy composite, the addition of 15 wt% fibres increase the Young's modulus by 27 %, however, the tensile strength was not mentioned in the paper.

Electrospun fibres have also been combined with other composite to modify their properties. Li, *et al.*[87] electrospun polysulfone (PSU) nanofibres onto carbon fibre/epoxy pre-pregs, improving the toughness of the materials by up to 281 % with

the addition of 5 wt% electrospun fibres. Electrospinning in this case, however, was only used a delivery and dispersion method for the PSU and not for the strength of the fibres; the nanofibres were dissolved by the epoxy resin, and separated out during curing into spherical particles.

Zhang, *et al*.[88] electrospun polyetherketone cardo (PEK-C) onto carbon fibre sheets, layered with epoxy resin, and cured in a hot press. Again, as the fibres dissolved upon curing, they were not used for their strength, but, this time, for the porosity of the fibre mat. By introducing an electrospun interlayer, the epoxy resin could be infused more evenly throughout the composite, and in this experiment, resulted in a composite with improved interlaminar fracture toughness.

Magniez, *et al*[89] electrospun a layer of poly(hydroxyether of bisphenol A) phenoxy nanofibres onto a layer of pre-preg carbon fibre material. During curing, the electrospun fibres diffuse through the epoxy resin. Improved fracture toughness is reported for in mode I and mode II by up to 150 % and 30 % respectively.

This concept has been used by a New Zealand based company called *Revolution Fibres* in their *Xantu.Layr* product line. They use electrospun mats of an undisclosed polymer to layer between sheets of pre-preg carbon fibre material.[90] The addition of the non-woven, unaligned nanofibres are reported to increase the fracture toughness of the carbon fibres composite by up to 170 % for mode I and up to 69 % for mode II.[91] This product has already been successfully used in a range on *Kilwell* fishing rods, asserting a two times maximum load compared to a plain rod, increased

flexural strength, interlaminar strength, and impact resistance, with no increase in weight or thickness.[91] Due to the commercial nature of the product, it is difficult to find more detailed information on the production and properties.

The ability to coaxially spin two different materials is an attractive concept, and yet there have been few papers published which investigate the possibility of creating a composite this way. Nothing has been published on the effect of using electrospinning to create a pre-impregnated (pre-preg) composite. A pre-preg mat is a composite fibre mat with the matrix materials already present. This enables simpler and easier formation of the fully cured composite. A fibre mat akin to a pre-preg composite can be produced by coaxially electrospinning two different polymers with a lower melting point polymer shell. The fibre mat could then be heated, only melting the shell polymer, and forming a matrix around the core polymer. Producing and optimising polymer composites in this way is the main focus of this thesis.

2.7.1 Self-reinforced composites

Thermoplastic composites are gaining traction due to being lightweight and low cost. Wetting of the reinforcing fibres and interface adhesion can be improved if the same thermoplastic is used in the matrix and the reinforcing fibres.[92] This is known as a self-reinforced composite. The challenge when making these is ensuring that the matrix can flow around the fibres while the fibres stay solid without deforming. This can be accomplished by using polymers with different tacticity or crystalline

structure, resulting in minor difference in melting temperature, allowing for a small window of processing temperature, or an increase in solvent resistance in one form of the polymer. These composites are typically produced by film stacking with a film of lower melting point with the reinforcing fibres.[92] However, this can produce poor results due to the viscosity of the thermoplastic melts preventing even distribution of the matrix and the fibres.[2,93]

Despite the complexities of producing these types of composites, they have distinct advantages. Firstly, as the fibre and the matrix are comprised of the same material, these composites can achieve a near perfect interface between the fibres and the matrix, ensuring good adhesion, and good distribution of strain.[92] Secondly, the end-of-life and recycling of these materials is simple, as different materials do not need to be separated.

There are methods of producing the fibres with the matrix already distributed, similar to pre-preg carbon fibre sheets. This alleviates the need for the matrix of thermoplastic melt to penetrate around the reinforcing fibres.

The PURE® composite developed by Lankhorst BV and DIT BV is a polypropylene (PP) self-reinforced composite created by co-extruding two different grades of PP and cold drawing them into fibres, followed by hot pressing from 130 – 180 °C.[94] Another self-reinforced PP composite called Tegris® produced by Milliken® is manufactured in a similar way to the PURE® composite, with a pressing temperature of 120 °C. This product has found use in ballistic protection, sports

equipment, suitcases, and wind turbines.[95] Both of these composites advertise similar mechanical properties of the consolidated sheets, and Young's modulus of 5 – 6 GPa, and tensile strength of 200 MPa.[96,97]

Alternatively, a "hot-compaction" method has been realised, where fibres are pressed at specific temperature and pressure, causing only a surface of the fibres to melt, and upon cooling, is recrystallised into to the matrix. This was first conducted successfully with polyethylene fibres.[98–100] This process has since been commercialised using polypropylene fibres to produce a woven, self-reinforced thermoplastic composite known as Curv®, it is currently used on a range of Samsonite® suitcases.[101–103]

3 Experimental

This section describes in detail the methods used for the experimental work. It is broken up into a "General" section for practises which will be repeated throughout the thesis, and individual sections to methods specific for each experiment.

3.1 General Methodology

Much of the preparation work for the electrospinning process was repeated in the same manner for each experiment. Standard laboratory personal protective equipment was worn at all times (unless specified), and consisted of: a lab coat, nitrile gloves and safety spectacles.

3.1.1 Polymer solutions

The solvent used to dissolve each of the polymers used was a tetrahydrofuran (THF) AnalaR NOMAPUR (supplied by VWR). The polymers used were polycaprolactone (PCL) (M_n = 80,000 g mol^{-1}) (supplied by Sigma Aldrich), and poly(lactic acid) (PLA) (M_n = 50,000 g mol^{-1}) (supplied by a local company). All polymers and solvents were used at received, and without further purification.

The polymers were dissolved in the solvent under reflux, on a temperature controlled hot plate under an inert nitrogen atmosphere. The concentration of the solution was confirmed by evaporating the solvent under vacuum. More solvent was then added to the solutions to make up for any losses during the dissolution process. The concentration was measured again to confirm the final value.

3.1.2 Single Polymer Electrospinning

Single polymer electrospun fibres were produced using a simple laboratory set-up confined within a fume hood for safety (Figure 3.1). Polymer solution was loaded into a 10 ml polypropylene (PP) syringe, and driven at a constant rate using a syringe pump (Cole & Palmer, model number: 12406360). A stainless-steel gauge 16 needle was blunted and attached to the end of the syringe. The live wire of the high voltage direct current (HVDC) power supply (Glassman FC-series) was attached to the needle using a crocodile clip, and the wire was secured in place using a retort stand and clamp. The grounding wire for the high voltage supply was attached securely to the fume hood, copper water supply pipes, and to the collector. This provides a reference frame for the power supply to ensure that the voltage read out is accurate, and to ensure that the electrically charged fibres were attracted to the grounded collector. The collector was a bespoke aluminium drum, width 150 mm, diameter 50 mm. This was attached to a 12 V DC motor which was connected to a variable voltage bench power supply.

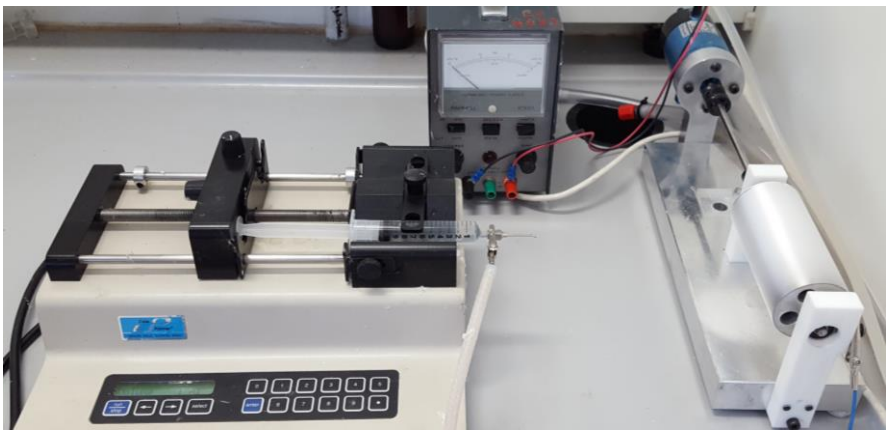

Figure 3.1: Single polymer electrospinning set-up. In this set-up the high voltage power supply is situated outside of the fume hood and is not pictured.

Once the process had been running for the allotted time, the high voltage supply was turned off, followed by the syringe pump and the rotating collector. To remove the electrospun fibre mat from the collector, an 80 mm wide section of the mat was chosen where the mat was thickest, generally around the centre of the collector. This section was cut using a sharp blade while manually rotating the collector. A cut was then made in the section across the mat to separate the mat from the drum. Although rare, if there were any imperfections on the fibre mat, such as a droplet splatter, the mat could be cut across at this point so this would be at the edges of the sample rather than in the middle.

3.1.3 Coaxial electrospinning

The coaxial fibres were electrospun using a slightly modified set-up which can be seen in Figure 3.2. Compared to the single polymer set-up where only a needle was attached to a syringe, two syringes were attached via PTFE tubing to a custom-made PTFE coaxial spinneret. Initially, the same dual syringe pump was used with two syringes mounted; one for the shell and one for the core fibre, however, this was later changed to two syringe pumps; one for each solution. The single syringe pump set-up was used to test the viability of the coaxial fibre production, and potentially vary the relative flow rates of the two solutions by using syringes with different diameters. However, this did not provide enough control over the flow rates, so the second syringe pump was added. The body of the coaxial spinneret was CNC milled out of a block of PTFE to ensure resistance to solvents, and to allow for thorough

cleaning due to its non-stick properties. The back of the spinneret was CNC milled out of aluminium, to allow for conduction of the high voltage supply. A blunted stainless-steel gauge 21 needle was attached to this back plate to deliver the core polymer solution and to provide a path of electrical conductivity through the body to the tip of the spinneret. The tubing was attached to the spinneret using threaded bar to screw into the spinneret components, and to grip the inside of the PTFE tubing. A concentric hole was drilled through to allow for polymer solution delivery. To deliver the sheath solution, a 100 µl polypropylene pipette tip was attached to the end of the spinneret and trimmed to the length of the inner core needle; opening up the inner diameter of this to 2 mm. Figure 3.3 shows the computer aided design (CAD) drawing and a photo for the finished product, fully assembled.

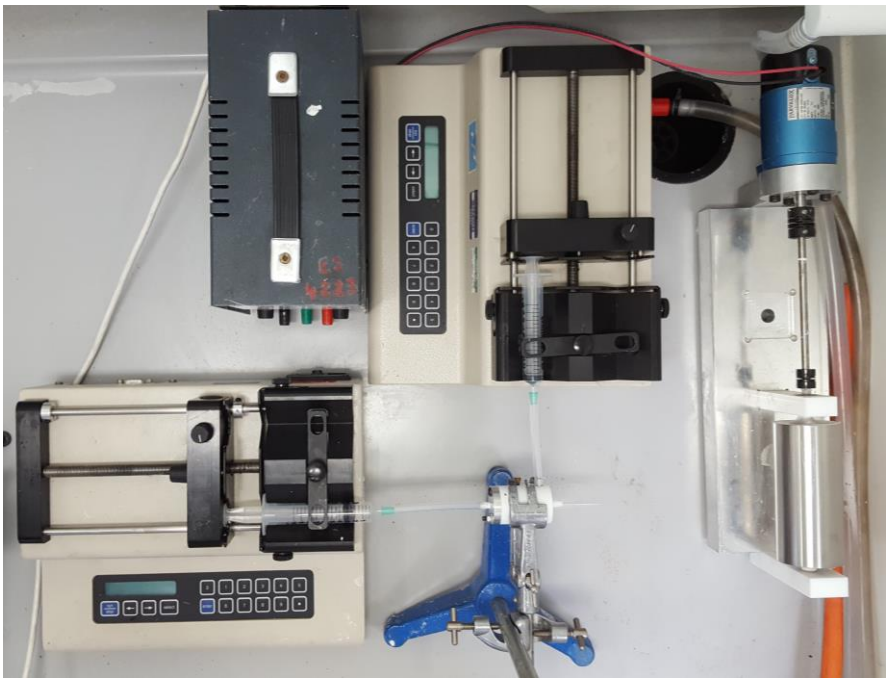

Figure 3.2: Coaxial electrospinning apparatus

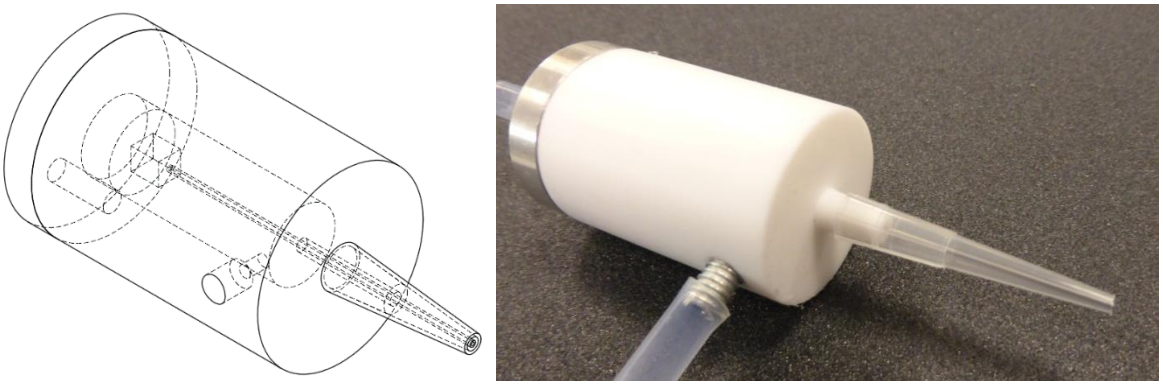

Figure 3.3: Drawing of the coaxial spinneret (left) and the finished part (right)

3.1.4 Discussion of Parameters

Electrospinning requires a fine balance of parameters in order to successfully electrospin a polymer solution. Changes in a polymer solution can require alterations in the input parameters due to a differences in viscosity, surface tension, and dielectric properties. To find out the required parameters, a set procedure was followed.

Firstly, the distance to the collector was to set to 100 - 200 mm, a typical range for electrospinning. The flow rate of the polymer solution was set to a higher level than typically required, up to 10 mL h^{-1}, and the voltage was slowly increased until a Taylor cone was observed and a jet was ejected from the droplet of solution, indicating electrospinning had started. The current on the HVDC power supply was limited to the minimum setting for safety, although during experimentation, the current read out was consistently displaying 0.00 mA. The flow rate on the syringe pump was then slowly decreased (or increased as required) to match the rate at which the polymer was ejected from the nozzle to ensure a steady droplet. The

electrospinning process would be observed, and the collector would be moved backwards until there was enough spread of the fibres for it to be sufficiently coated. The flow rate and electrospinning voltage would be adjusted again as required to ensure a consistent stable jet. The electrospinning was observed for the duration and the needle tip was wiped clean with the HVDC supply turned off when required to prevent any blockages from premature evaporation of the solvent.

Fibre alignment was an important aspect in this work, and the speed at which the collector was rotating was an important factor in ensuring this alignment. Again, the speed at which the collector needs to rotate to correctly align the fibres will differ between experiments, as the rate at which the fibres are deposited vary according to other parameters. Once successful electrospinning was established in the previous steps, the collection speed of the fibres was initiated slowly, with the motor voltage set low at 2 or 4 V, and with addition fibre mats collected at increasing voltages up to the maximum of 12 V. The rotational and linear speed of the collector that these voltages corresponded to was measured using an optical tachometer as shown in Table 3.1.

Table 3.1: Motor input voltage and corresponding collection velocity

Motor input voltage (V)	RPM	Linear velocity (m/s)
2	498	1.30
4	1158	3.03
6	1860	4.87
8	2622	6.86
10	3312	8.67
12	4044	10.58

These fibre mats were analysed using SEM and image analysis (see section 3.1.5) in order to measure the angles of the fibres with respect to the rotation of collector. This was conducted to find the point at which the fibres are sufficiently aligned. Fibres cannot always be collected at the equipment's maximum collection speed to ensure production of aligned fibres, as if this is faster that the deposition speed, it can stretch or break the fibres as they are collected.

Once all the parameters had been decided for the experiment, the electrospinning process could be started more quickly. First the collection distance was set, then syringe pump was switched on, followed by the rotating collector. Once all the equipment was checked, the high voltage supply was turned on, and a timer was started to ensure the accuracy of the running time.

All electrospinning was conducted under atmospheric conditions of 19 - 23 °C and 40 - 50 % relative humidity.

3.1.5 Analytical Techniques

To characterise the electrospun fibre mats and the composites produced scanning electron microscopy and tensile testing were primarily used.

Microscopy

Due to the scale of the fibres being produced, the electrospun mats and composites were characterised using a scanning electron microscope (SEM). This will be used to analyse the fibre diameters and alignment of the mats, and the structure of the composites once formed. A scanning electron microscope is able to view objects at a much higher resolution and greater depth of field than a visible light microscope due to the limiting factor of the wavelength of light, resulting in diffraction and a theoretical resolution of about 200 nm, compared to that of an SEM which can be less than 1 nm. SEM also allows for greater depth of field, important to observe the uneven nature of the fibre mats.

The samples were mounted on to individual 12.5 mm aluminium SEM stubs using 12 mm carbon adhesive tabs. Sliver paint was applied to one of the sides of the sample to increase conductivity. Once dry, the samples were placed in a gold splutter coater for 30 seconds. This makes the surface of the polymer fibres conductive to prevent build-up of electrons in the SEM (an effect known as "charging") which can cause the sample to burn and distort the image. Once prepared, the samples were placed in the SEM (Zeiss, Gemini) and analysed. Typical

settings used were 10 kV, 30 μm aperture size, and observed with a secondary electron detector.

For some samples, a desktop SEM (Hitachi TM3030) was used. This provides lower resolution than the Zeiss Gemini, but the samples do not require as much preparation because the low voltages used do not require the samples to be conductive.

An SEM, however, can only image the surface of a material, so in order to investigate the structure of composite materials, a clean cross section of the material was required. To obtain this cross section, a small volume of liquid nitrogen, about 100 ml was decanted into a Dewar flask. The composite samples to be analysed were cut into 5 mm strips and immersed into the liquid nitrogen for 30 seconds to bring them to well below the glass transition temperatures of the both polymers. The composite strips were then snapped in half while immersed in the liquid nitrogen using two pairs of tweezers until a suitably straight fracture surface, perpendicular to the fibre alignment, was created. The cryogenically fractured composite samples were mounted vertically, and gold sputter coated before being analysed by SEM.

All SEM images were analysed using the software "*ImageJ*". This software allows for the measurement of dimensions using the image and scale bar provided by the SEM.

Mechanical Testing

Mechanical testing was conducted on the composite materials to compare the tensile properties of different compositions and processing techniques.

A universal testing machine (Shimadzu AGS-X) was used to characterise the samples. The machine was outfitted with a 500 N load cell, and 500 N rated polymer film grips. In later tests, a camera extensometer strain gauge was used to more accurately measure the extension of the sample. Trapezium X software was used on a desktop computer to control the testing machine.

The grips were moved apart to a distance of 25 mm, and the stroke of the machine was zeroed. The testing speed was set to 1 mm min^{-1}, a slow testing speed to ensure high resolution in the results. The dimensions of each samples were also inputted into the software, so that the stress and strain could be calculated, and outputs such as the Young's modulus, tensile strength, and elongation as break could be found.

ISO standard 527-5[104] details the approved tensile test conditions for unidirectional fibre-reinforced polymer composites. Instead of the more standard "dog-bone" shape, the test sample should be cut into thin rectangular strips that are 15 ± 0.5 mm wide, 250 mm long, and 1 ± 0.2 mm thick. However, due to the nature of the samples, their length and thickness could not conform to this. The thickness could not be accurately controlled, and the samples made were not long enough. The standard also suggests that optional adhesive tabs could be attached to each end to ensure the failure occurs across the middle of the sample, rather than at the grips.

3.1.6 Confirmation of core-shell coaxial structure

To confirm the core shell structure of the fibres, a section was cut using a scalpel and imaged using scanning electron microscopy. Although the images showed separation of the core and shell where the fibres had been damaged by the scalpel, more conclusive proof of the structure would be desirable. To this end, poly(vinyl alcohol) (PVOH) (Mowiol® 56-98, M_w = 195,000 g mol^{-1}), obtained from Sigma Aldrich, was dissolved in water to form a 10 wt% aqueous solution. The PVOH matrix was required to mechanically stabilise the fibres for imaging. PVOH was chosen as it could be dissolved in water, which would not affect the PCL or PLA in the fibres. This solution was applied to 5 x 25 mm strips of electrospun coaxial fibre mat, with the fibres aligned along the length of the strips. This was left to dry at room temperature to avoid any damage to the coaxial fibres. Once dried, the strips were immersed in liquid nitrogen and snapped and imaged under SEM as described in the previous section.

3.2 Fibre volume fraction

This section details the specific experimental details regarding the experiments with fibre volume fraction. The general methodology section 3.1 will be referred to when these techniques were used.

3.2.1 Preparation

Polymer solutions were created by dissolving polymer granules into a solvent as described in the general methodology section 3.1.1. Polycaprolactone (PCL) and poly(lactic acid) (PLA) were dissolved into tetrahydrofuran (THF) at concentrations of 15 wt% and 25 wt% respectively. These solutions were made up to the lowest concentration of polymer while maintaining the viscosity required to successfully electrospin fibres.

3.2.2 Electrospinning

As discussed in the introduction (section 1.4), due to their thermal and mechanical properties, coaxial fibres consisting of a PCL sheath, and a PLA core were electrospun using a set-up of: a Glassman high voltage power supply, a custom made rotating mandrel collector, and a custom made coaxial spinneret fed by two separate syringe pumps as described in section 3.1.3. The high voltage supply was set to 8 kV, the lowest voltage that could be used to break the surface tension on the polymer solution and produce a consistent Taylor cone and electrospinning jet. The collection distance used was set to 200 mm to ensure adequate horizontal coverage of the rotating collection mandrel. Each mat was electrospun for one hour.

To create unidirectional fibre reinforced composites, the electrospun fibres must aligned on the rotating collector. To investigate the motor speed required to align the fibres, the fibre volume ratio of 0.75 was chosen, as it was in the middle of the range to be tested. This was electrospun, and collected at a range of speeds, between 4 V

and 12 V in steps of 2 V. The fibre mats were imaged using scanning electron microscopy (SEM), and the images were analysed using ImageJ software. The angles of 100 fibres over three images were measured manually and the standard deviation of these angles was calculated.

Using a separate syringe pump for both the core and sheath polymer solutions allowed precise independent control over the flow rates. This was the method used to vary the ratio of each polymer in the fibres produced. To ensure fair testing, only the flow rates of the polymer solutions were varied during experimentation.

The relative flow rate for each polymer solution was calculated taking into account the concentration of the solutions and the polymer density. This calculation is shown in equations 3.1 and 3.2. The total flow rate was kept around 5 ml h^{-1} and altered slightly for each experiment as necessary to ensure a constant electrospinning jet. The flow rates used in the experiment are listed in Table 3.2.

$$\phi = \frac{1}{1 + \left(\frac{\rho_p}{\rho_s}\right)\left(\frac{1}{w_f} - 1\right)} \tag{3.1}$$

$$Q_{PCL} = \frac{Q_{PLA}\phi_{PLA}\left(1 - V_f\right)}{V_f\phi_{PCL}} \tag{3.2}$$

Where:

ϕ is the volumetric concentration of the polymer solution
ρ_p is the density of the polymer
ρ_s is the density of the solvent
w_f is the mass concentration of the solution
Q_{PCL} is the volume flow rate of the PCL solution
Q_{PLA} is the volume flow rate of the PLA solution

ϕ_{PCL} is the volumetric concentration of the PCL solution
ϕ_{PLA} is the volumetric concentration of the PLA solution
V_f is the volume fraction of PLA in the sample produced

Table 3.2: Solution flow rates for electrospinning

Fibre fraction	PLA Flow Rate (ml h^{-1})	PCL Flow Rate (ml h^{-1})	Total Flow Rate (ml h^{-1})
0.50	2.00	3.24	5.24
0.60	2.50	2.70	5.20
0.65	3.00	2.62	5.62
0.70	3.00	2.08	5.08
0.75	3.50	1.89	5.39
0.80	3.50	1.42	4.92
0.85	4.00	1.14	5.14
0.90	4.00	0.72	4.72
1.00	5.00	0.00	5.00

Only maximising volume fraction was of interest, so volume fractions lower than 0.50 were not considered to be of interest for this study. It was assumed that the maximum volume fraction would be of a similar value to that found in literature, so small divisions of 0.05 were measured around 0.60 to 0.90 for better resolution of data. Divisions of 0.10 were used outside of this to obtain a more general trend line. Six mats were produced for each fibre volume fraction

3.2.3 Composite forming

As one composite sheet was to be made up of three electrospun sheets, these were sorted into stacks to be pressed. Each stack of three mats was trimmed to the same

width, and cut in half perpendicular to the longest side to fit into the hot press. This produced four stacks of three layers (about 75x75 mm) for each volume fraction.

The fibre mats were placed between two sheets of polytetrafluoroethylene (PTFE) release film and placed in a Rondol hot press between two square blocks of steel (100x100x15 mm).

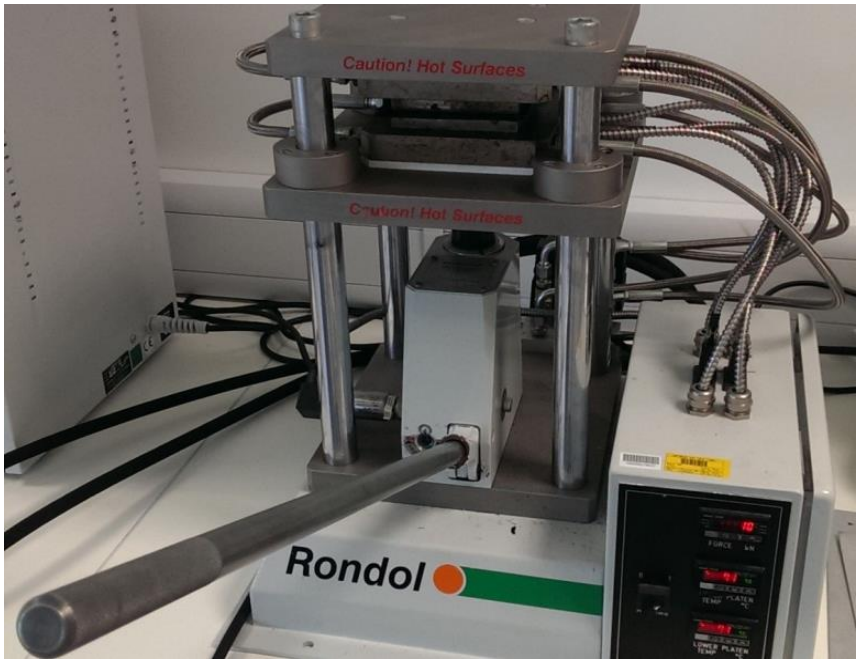

Figure 3.4: Rondol bench top 10 tonne heated hydraulic press

The top and bottom plates of the hot press were heated to 80 °C, and the electrospun mats were pressed with 10 kN of force, equating to 1.78 MPa of pressure across the sample. This was applied for 30 minutes before the heating element was switched off, and the sample was left to cool under pressure in the press to 40 °C to ensure the polymers were at a stable state (with no melting points or glass transition temperatures between removal and room temperature) before removing. This was done under atmospheric conditions over the course of about 40 minutes as the hot

press did not have a functional chiller. The cooling profile of the hot press was recorded and is displayed in Figure 3.5.

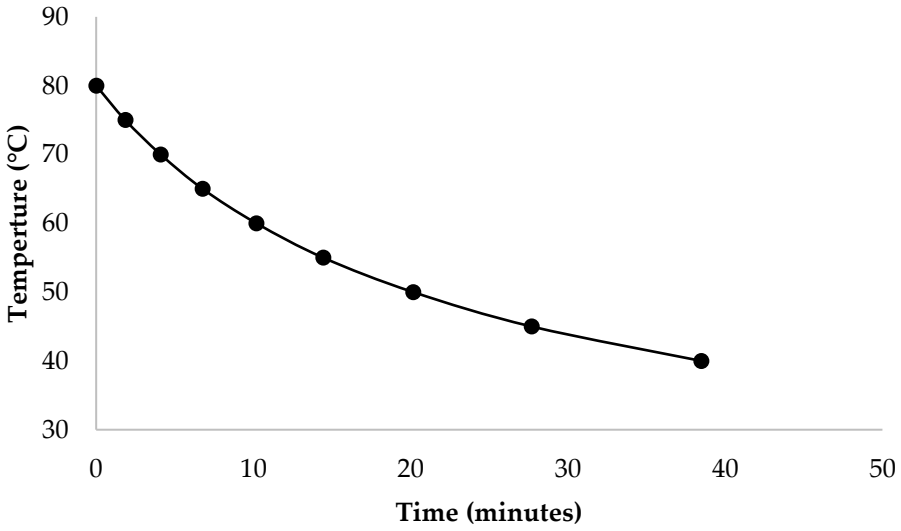

Figure 3.5: Cooling profile of the hot press

3.2.4 Materials characterisation

Tensile testing

The sides were trimmed straight and the composite was cut into four 15 mm strips parallel to the orientation of the fibres. The thickness of the strips was measured using a micrometer with an average taken from five points on each sample. The samples were then tested using the method described in general methodology section 3.1.5.

Thermogravimetric analysis

Thermogravimetric analysis (TGA) was conducted on samples from the electrospun fibre mats using a METTLER TOLEDO TGA. Although this was intended to be used

to characterise the volume fraction of the polymers in the sample, it also provides important information about the heat degradation characteristics of the polymers. The degradation temperature of each polymer was investigated, and a heating method was devised to take these temperatures into account.

The samples were placed in the TGA and run under a nitrogen atmosphere. The heating method is displayed in Figure 3.6. It employs faster heating at 25 °C min^{-1} when no degradation is taking place to improve process time, and slower heating at 5 °C min^{-1} during degradation to ensure adequate resolution around the degradation temperatures.

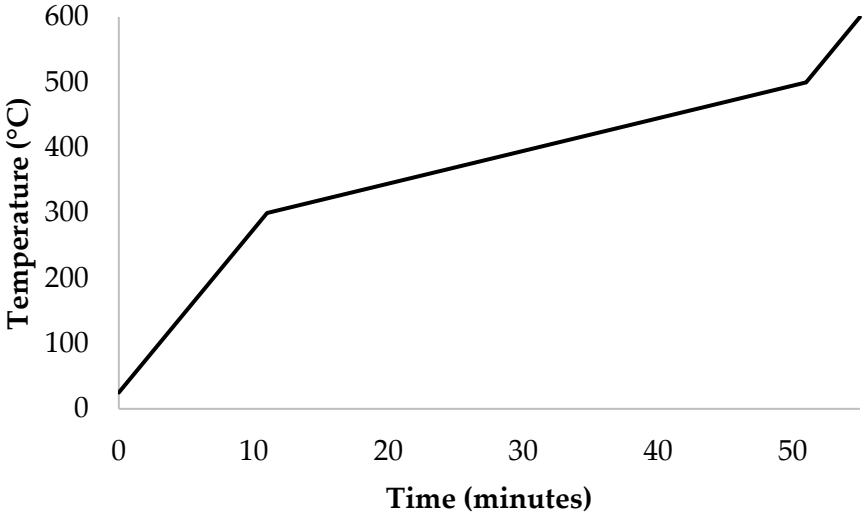

Figure 3.6: TGA heating rate

Nuclear magnetic resonance

Nuclear magnetic resonance (NMR) was also used to characterise the fibre volume ratio of the electrospun coaxial fibres. In the case where the degradation temperature of the two different polymers overlaps, NMR will present a clearer view of the

content of the sample. A small section of each electrospun mat was dissolved in deuterated chloroform in an NMR tube, and placed in a Bruker DPX400 (400 MHz) hydrogen NMR for analysis. For a clear output result, each polymer must have at least one hydrogen atom at a different energy level to the other polymer. This will allow two distinct peaks to appear when the fibre mat is analysed.

The signal area will relate to the number of hydrogen atoms in the various energy states (attached to the different carbon atoms). To analyse the signal, two distinct, separate peaks will need to be apparent for each polymer. The areas of these peaks will need to be divided by the number of corresponding hydrogen atoms assigned to that peak. These values can then be compared to find the molar ratio of the two polymers in the solution. This calculation is commonly used in NMR analysis to calculate the product yield from synthesis reactions, particularly when creating a polymer from a monomer.[105,106] This can then be converted into the volume fraction by taking into account the molar mass of the polymer's repeating unit, and the density of the polymer. These calculations are shown in equations 3.3 – 3.5.

$$M_f = \frac{\frac{A_{PLA}}{H_{PLA}}}{\frac{A_{PLA}}{H_{PLA}} + \frac{A_{PCL}}{H_{PCL}}} \tag{3.3}$$

$$w_f = M_f \left(\frac{M_{PLA}}{M_T}\right) \tag{3.4}$$

$$V_f = \frac{1}{1 + \left(\frac{\rho_{PLA}}{\rho_{PCL}}\right)\left(\frac{1}{w_f} - 1\right)} \tag{3.5}$$

Where:

M_f is the molar fraction of PLA
A is the area (intensity) of the NMR peak
H is the number of hydrogen atoms in the peak
w_f is the mass fraction of PLA
M_{PLA} / M_{PCL} is the molecular mass of the repeating polymer unit
M_T is the average molar mass of the polymer mixture
ρ is the density of the polymer
V_f is the volume fraction of PLA in the sample

The area of the peaks was measured using ACD/Labs NMR analysis software, and used in the equations to find the fibre volume ratio of the tested composite.

3.2.5 Rule of Mixtures

To calculate the theoretical material properties of the composite using the rule of mixtures, these properties need to be measured for the PLA fibres and the PCL matrix. PCL pellets were hot pressed, cut into strips and tensile tested, all under the same conditions as the composite forming process. A total of 10 strips were processed for tensile testing.

Although testing of individual PLA fibres would ensure accuracy of the equation, this was not necessary due to the large diameter of the fibres. Research has shown that the mechanical properties of fibres above 1 μm are close to bulk properties of the polymer.[107] The PLA could not be processed in the same way as the PCL because it was too brittle and, when formed into thin sheets, it was difficult to cut into even strips and was prone to fracture when gripped for tensile testing. To ensure adequate durability for tensile testing, the PLA pellets were injection moulded into

dogbones using a Thermo Scientific HAAKE™ MiniJet Pro Piston Injection Moulding System (Figure 3.7). The polymer was melted at 200 °C and injected at 200 psi into a dogbone mould set to 85 °C. All dogbones produced were inspected for air bubbles or incomplete moulding, and any defective samples were discarded. A total of 10 PLA dogbones were produced and tested.

Figure 3.7: Mini injection moulding system, Thermo Scientific HAAKE™ MiniJet Pro (left), PLA dog bone samples produced (right)

Using the rule of mixtures, the tensile testing results from the two separate polymers can be used to calculate the theoretical tensile properties of the composite. There are two equations for the rule of mixtures, one specifies the upper bound (equation 3.6), and another, the lower bond (equation 3.7). The lower bond indicates the transverse loading of the unidirectional specimen, where the fibres are not reinforcing the matrix. This indicates that for results before the lower bond, the composite is not being properly reinforced.

$$E_c = fE_f + (1 - f)E_m \tag{3.6}$$

$$E_c = \frac{fE_m}{(1 - f)E_f + fE_m} \tag{3.7}$$

Where:

f is the volume fraction of the PLA fibres
E_f is the material property of the fibres
E_m is the material property of the matrix

The rule of mixtures was calculated for all values of the fibre volume ratio used in the experimentation. The Young's modulus and the tensile strength of the composites was then compared to the theoretical values calculated from the rule of mixtures.

3.3 Composite forming variation

This section details the specific experimental details regarding the experiments with composite forming process. The general methodology section 3.1 will be referred to when these techniques were used.

To more efficiently test the variation in processing techniques Taguchi experimental design was employed. With three variables and threes levels for each variable, an L9 array (Table 3.3) was used, resulting in nine variations of the experiment. Six mats coaxial fibre mat were electrospun for each experiment in order to produce enough samples for tensile testing, resulting in a total of 54 mats.

Table 3.3: Taguchi matrix of experiments required for test the composite forming process

Experiment number	Cooling rate (K min^{-1})	Pressure (bar)	Temperature (°C)
1	10	1	70
2	10	5	90
3	10	10	110
4	5	1	90
5	5	5	110
6	5	10	70
7	1	1	110
8	1	5	70
9	1	10	90

Different cooling rates were selected as they may have an effect on the crystalline structure of the polymers. The lowest cooling rate was selected to be similar to that used in previous experiments using a different hot press. The pressure of the hot press changes how the matrix material penetrates the fibres. Low pressure reduce penetration, while high pressure increases it. The lowest pressure was selected to be the same as the pressure from vacuum forming to show whether vacuum forming could also provide good composite consolidation. The maximum temperature used was set to just before where crystalline structures in the PLA formed by previous processing break apart.

3.3.1 Preparation

Polymer solutions were created by dissolving polymer granules into a solvent as described in the general methodology section 3.1.1. Polycaprolactone (PCL) and poly(lactic acid) (PLA) were dissolved into tetrahydrofuran (THF) at concentrations

of 15 wt% and 25 wt% respectively. These solutions were made up to the lowest concentration of polymer while maintaining the viscosity required to successfully electrospin fibres. The concentration of the solutions was confirmed by evaporating the solvent of a sample under vacuum.

3.3.2 Electrospinning

Coaxial fibre mats were electrospun as in previous experimentation, selecting the highest fibre volume ratio from the previous experimentation from chapter 4. The polymers used were the same as discussed in the general methodology in section 3.1, PLA and PCL dissolved in tetrahydrofuran (THF) at 25 wt% and 15 wt% respectively. Using a separate pump for each one, these solutions were pumped from 10 ml polypropylene (PP) syringes into the custom made coaxial spinneret at 3.50 ml h^{-1}, and 1.89 ml h^{-1} respectively to obtain a fibre volume ratio of 0.75. The coaxial solution was drawn into a fibre using the HVDC power supply set 8 kV. The fibre was collected across 200 mm onto a rotating mandrel set to 6.8 m s^{-1}. Each mat was collected for one hour before being cut from the mandrel and being laid flat. A total of 54 mats were electrospun.

3.3.3 Hot Pressing

For a more controlled process, a different hot press was used in this experiment compared with in the previous experimental section 3.2. The press used for this set of experiments was a Collins Platen Press P 200 P/M. This was a computer controlled press with the ability to control the heating and cooling rate, and pressure profiles.

Figure 3.8: Automated hydraulic press, Collins Platen Press P 200 P/M

Nine different programs were written on the machine corresponding to the nine experiments in Table 3.3. The samples were given 2 minutes to heat up, followed by a 50 second degassing step to remove air pockets before the pressure was applied. After this the pressure was applied constantly for the rest of the process, including 5 minutes at the highest temperature, and during the cooling stage.

The electrospun mats were layered in stacks of threes and cut in half across the width of the sample to fit into the hot press. The halved stacks of three mats were sandwiched between two sheets of PTFE release film and sheet aluminium and placed in the hot press. The two halves of each sample were processed using the same heating and pressure cycle; this was repeated for another set of three electrospun mats using the same cycle. The hot pressed mats were cut into 15 mm strips with a knife using a template.

3.3.4 Analysis

Differential scanning calorimetry (DSC) was used to investigate how the crystalline structure of the polymers was affected by the heating process. A strip from each hot pressed samples was cut horizontally from the bottom and cut into smaller pieces to fit inside a 100 μl aluminium pan. The sample pan was place alongside a reference pan (an empty pan and lid) inside a Mettler Toledo DSC1. The DSC was programed to heat at 10 K min^{-1} from 25 °C to 200 °C, held at 200 °C for 5 minutes and cooled down to 25 °C at 20 K min^{-1} (Figure 3.9). A heating rate of 10 K min^{-1} is a standard heating rate in DSC measurements. The cooling rate was set to be faster to speed up the measurement, as this was not an important aspect of the material characterisation for this experiment. A maximum temperature of 200 °C was used, as this was higher than the glass transition temperature (T_g) and the melting point (T_m) of both polymers. This ensured a complete cycle, and was well below the degradation temperature (which was investigated using TGA in previous experimentation) of both polymers to avoid damage to the machine. The sample pan was then discarded, and the process repeated for the other samples.

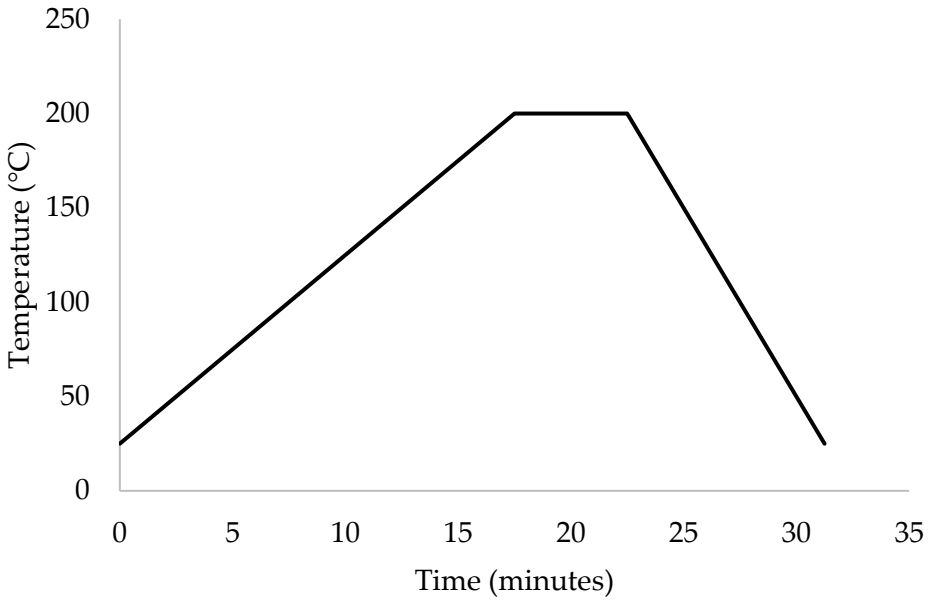

Figure 3.9: Heating and cooling profile used during DSC analysis of the hot pressed composites

The results curves were analysed using StarE software supplied by the manufacturer to measure peaks and onset temperatures, and to integrate the curves. The raw data was exported and graphed using Microsoft Excel.

3.4 Coaxial and layering

This experimental section covers the details about how the tensile properties of the composite material produced by the coaxial electrospinning technique compared to electrospinning a single polymer and layering the matrix material after, during the hot pressing. The general methodology section 3.1 will be referred to when these techniques were used.

3.4.1 Preparation

Polymer solutions used to electrospin the coaxial fibres were created by dissolving polymer granules into a solvent as described in the general methodology section

3.1.1. Polycaprolactone (PCL) and poly(lactic acid) (PLA) were dissolved into tetrahydrofuran (THF) at concentrations of 15 wt% and 25 wt% respectively.

Due to changes in the electrospinning process and the removal of the sheath polymer solution during the single polymer electrospinning of PLA, the PLA fibres produced were an order of magnitude larger than the fibres produced by the coaxial electrospinning process. To prevent this from causing a discrepancy in the results, the fibre diameters must be reduced. This was done by altering the variables of the electrospinning process, along with the solvent used to dissolve the polymer. By reducing the volatility of the solvent, the fibres would take longer to solidify, allowing them to stretch more during electrospinning and reducing the diameter. It was found in the literature that a 3:1 ratio of a solvent and dimethylformamide (DMF) was commonly used in solution with the polymer due to its high dielectric constant and conductivity.[108–111] For this experiment N,N-Dimethylformamide (supplied by Fisher Scientific) was mixed with THF in a measuring cylinder in a 3:1 ratio, with three parts THF and four parts DMF by volume. The PLA polymer granules were then dissolved in the same fashion as described in general methodology section 3.1.1. At the end of the dissolution process, the concentration of the solutions was confirmed by evaporating the solvent of a sample under vacuum as usual; however, due to the different boiling point of the two solvents used, the 3:1 ratio of solvents could not be added to the solution to compensate for lost solvent. It was assumed that the majority of any lost solvent was THF as it has a much lower

boiling point (66 °C) than DMF (152 °C), so only THF was added to the solution. These solutions were used for electrospinning within a week of being made in order to minimise the volume of solvent lost in storage which would disturb the ratio further. Solutions of PLA and the THF:DMF solvent were made and electrospun at concentrations from 15 wt% in 5 wt% increments until an acceptable fibre diameter was created.

3.4.2 Electrospinning

Coaxial fibre mats were electrospun in the same way as described in general methodology section 3.1.3, selecting the highest fibre volume ratio from the previous experimentation from chapter 4. The polymers used were PLA and PCL dissolved in tetrahydrofuran (THF) at 25 wt% and 15 wt% respectively. Using a separate pump for each solution, they were pumped from 10 ml polypropylene (PP) syringes into the custom made coaxial spinneret at 3.50 ml h^{-1}, and 1.89 ml h^{-1} respectively, in order to obtain a fibre volume ratio of 0.75. The coaxial solution was drawn into a fibre using the HVAC power supply set 8 kV. The fibre was collected across 200 mm onto a rotating mandrel set to 6.8 m s^{-1}. Each mat was collected for one hour before being cut from the mandrel and being laid flat. Eight coaxial electrospun fibre mats were produced.

Single polymer PLA fibres were produced from the various solutions created in the preparation stage. These were produced in the same way as described in general methodology section 3.1.2. Solutions from 15 – 25 wt% were electrospun at 8 – 10 kV,

with collection distances at 150 – 200 mm, and the flow rate varying between 1 – 3 ml h^{-1}. The solution concentration of 25 wt%, which was used for the comparison was electrospun at 10 kV, 3 ml h^{-1} flowrate, and 200 mm collection distance. Experiments were conducted to align these fibres in the same way as discussed in section 3.1.4, resulting in a collection speed of 10.58 m s^{-1}, with the motor set to 12 V.

3.4.3 Composite forming

The coaxial fibre mats were formed into a composite sheet using the same method as used in chapter 5, Composite forming variation. The parameters used were the same as in the experiment which produced the composite with the highest tensile strength: 70 °C and 1 bar. As there was no trend in the cooling rate, the fastest cooling rate of 10 K min^{-1} was used to increase the speed of production.

To create the composite from the PLA fibre mats, sheets of PCL needed to be made to melt around the PLA. Initially, this was done by electrospinning PCL fibre mats and melting these in a hot press with the PLA fibre mats, however, this produced unexpected results due to poor control over the fibre volume ratio. To control the fibre volume ratio of these composites, the PLA fibre mats to be used in the composite were weighed using a four-point balance, and the mass of the PCL required to make up the fibre volume ratio was calculated. The initial target was to sandwich the PLA fibre mats with sheets of the PCL matrix, however, the mass of the PCL to be included with these sheets was so low that it was difficult to produce

sheets thin enough. Both methods of hot pressing PCL granules and drying from a solution were tried. By drying from a solution, the mass of PCL in the mould could be calculated before drying, however, the end result of these PCL sheets once dried were uneven and fragile, and could not be separated from the medium without breaking. Hot pressing the granules was more successful, and the correct mass and size of the sheets was produced through an iterative process of pressing the material into a sheet, cutting to size, measuring the mass, and repeating until the result was as required. Although this produced thin sheets, they were not thin enough to be applied to both sides of the PLA fibre mats, so a single sheet of PCL was used in the formation of these composites with two sheets of the PLA fibre mats on the outside. These PCL sheets were created by pressing at 120 °C and at pressures of up to 90 bar.

The stack comprising of two PLA fibre mats and the PCL sheet was pressed into a composite using the same method as the coaxial fibres: at 70 °C, 1 bar, and a cooling rate of 10 K min^{-1}.

3.4.4 Tensile testing

To produce more accurate results for the final experimentation, each sample was tabbed to reduce breakage at the grips and a camera extensometer was used. The camera negates any slippage caused by the tabs, and removes the contribution of any deformation in the frame of the testing machine.

The composite tabbing procedure was tested using a variety of methods, by tabbing using adhesive and using tapes. Loctite super glue and Bostik all-purpose adhesive were tested, however, these contained a solvent which would dissolve and damage the polymer. Tapes used were Scotch magic tape, Gorilla (gaffer) tape, unbranded masking tape, and two types of Scotch branded industrial strength masking tape. For the final composite testing, the unbranded masking tape was used.

The composite sheets produced were cut into 15 mm strips parallel to the direction of the fibres and labelled accordingly. Each strip was tabbed using the unbranded masking tape by sticking the tape on both sides and on each end of the strip, with a 25 mm section of composite left untouched in the centre for the tensile testing. The thickness of the samples was measured in this section in five places using a micrometer, and averaged as in previous experimentation. The masking tape tabs were applied at least three days before testing to allow for the adhesive on the tap to dry sufficiently and create a strong bond with the composite.

The tensile testing machine was setup as in general methodology section 3.1.5. A few extra steps were taken regarding the camera extensometer. The camera was moved into a position so that the camera frame was over the sample. LED lighting was moved into position to illuminate the sample from various angles to reduce shadows. The brightness of the lighting, and the focus and exposure settings of the camera were adjusted to provide a clear image of the sample. In the software, the camera was set to a high precision mode, and with an automatic calculation of the

gauge length. To calculate the gauge length and to measure the extension of the sample during testing, the sample must have two reference position marked on to it. To mark this these points on the samples, either a sticker or a marker pen is commonly used. A number of markers were tested on the composite, however, due to solvent present in the inks, (even a "water-based" brand) these created a weak point in the material, at which breakage of the samples consistently appeared at these marks. As a result, two stickers with a black background and a horizontal line of white diamonds were placed 20 mm apart on each sample for the reference positions.

Stress-strain curves were plotted using the strain measured from the camera extensometer, and processed in the same way as described in general methodology section 3.1.5.

4 Fibre volume fraction

4.1 Introduction

According to the rule of mixtures theory, in a perfect composite, tensile strength and Young's modulus will increase linearly as the fibre volume fraction increases from 0 to 1 (all matrix and no fibres to all fibres and no matrix).[112,113] Reality does not always follow theory, and while this may hold true for intermediate fractions, other interactions cause different results at the extreme ends of the scale.[2,113–115] Various experimental studies have shown this linear relationship between the fibre volume and the tensile properties for different kinds of fibre composites.[116–119] Most long fibre reinforced composited have fibre volume ratios between 0.30 and 0.70.[2]

The effect of the fibre volume fraction on the tensile properties of a composite can be calculated theoretically using the rule of mixtures. This uses equations taking into account the tensile properties of the individual components of the system, the fibre material and the matrix material. These equations (3.4 and 3.5) can be found in methodology section 0.0.0. These equations create a linear relationship between the fibre volume ratio and the material property from the material property value of the matrix to the material property value of the individual fibres. This assumes equal strength of all fibres, linear elastic behaviour until failure, and equal strains in the fibre, matrix and the composite. In reality, fibre diameters will vary and defects will be present resulting in a variation in strength across the fibres, elastic behaviour

decreases as strain increases (strain hardening), and non-perfect adhesion at the fibre-matrix interface will create an uneven distribution of strain across the fibres and the matrix.[113]

Reinforcement below certain volume fractions of fibres, usually around 0.1,[115] can weaken the matrix. If the volume of fibres is not significant enough to carry the applied load, the fibres can break before the matrix reaches its limit, causing the matrix to perform as if the fibres were holes in the structure, triggering the material to fail in what is known as a matrix controlled failure, rather than the more preferable fibre controlled failure.[120,121] This volume fraction is known as the critical fibre volume. On the other end of the scale, above certain volumes of fibre, the matrix cannot transmit the load effectively to the fibres, resulting in poor distribution of stress. This can cause individual fibres which are subjected to higher stress than the average throughout the material to break prematurely, placing more load on the neighbouring fibres and causing a cascade of fibre breakage across the composite. This type of failure can be modelled as cumulative weakening, or fibre break propagation.[2] Theoretically, with perfectly circular, aligned fibres with equal diameter in contact with each other in a hexagonal (or triangular) pattern, the maximum volume fraction for a composite is 0.907.[2] This packing arrangement is depicted in Figure 4.1.

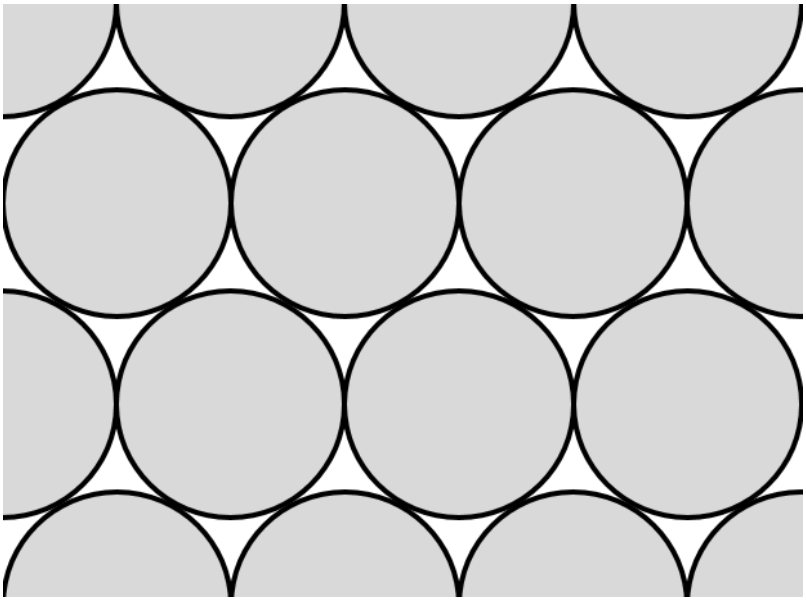

Figure 4.1: Hexagonal packing of unidirectional fibres

In reality, this is not practical as uneven fibre geometry and distribution, and misalignment of fibres within the matrix make it difficult to achieve fibre volume fractions above 0.65.[115]

In polymer matrix composites, different processing techniques can produce different fibre volume fractions. An aligned continuous fibre composite will exhibit higher maximum volume fractions compared with unaligned or short fibre composites. This is due to the spacing around the short and unaligned fibres and the need for more matrix material to fill these gaps.

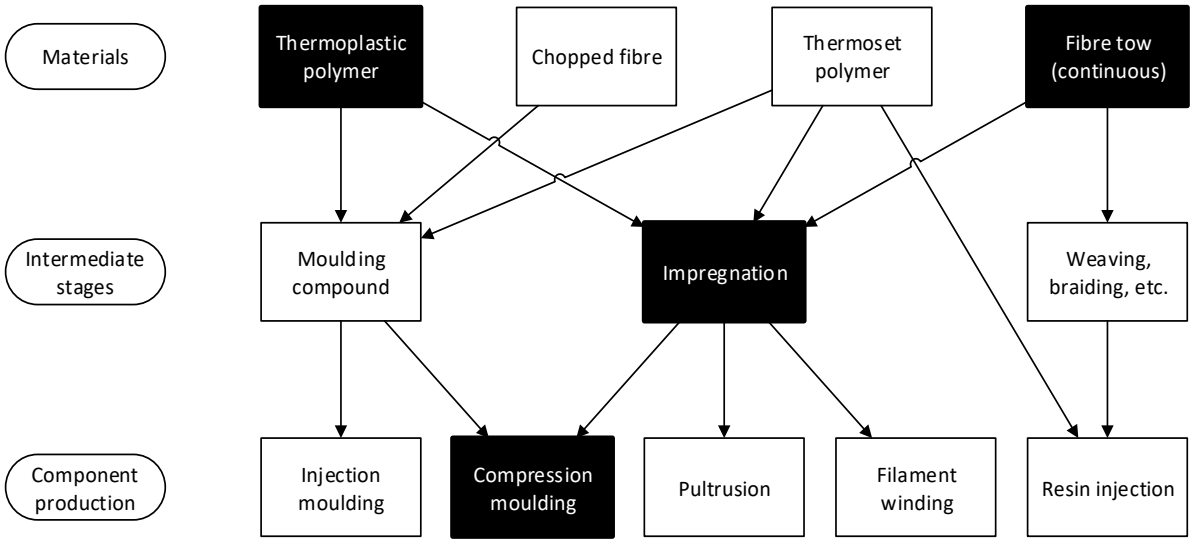

Figure 4.2: Schematic overview of composite forming processes for thermoplastic and thermoset matrices. Adapted from Hull[2]

Fibre reinforced thermoplastics are usually produced using either injection moulding for short fibres, or hot press moulding for continuous fibres.[2] Figure 4.2 shows a schematic diagram of composite materials and potential processing methods. The highlighted process is concerned with the work conducted here, as the matrix is a thermoplastic, the fibres are continuous, the co-axial electrospinning can be considered to be a form of impregnation, and the fibre mats are consolidated using compression moulding.

Thermoplastic matrix composites typically have lower maximum fibre volume ratios and must be formed at higher temperature and pressure compared to thermosets. This is due to the higher viscosity of thermoplastics which makes it more difficult for the matrix to penetrate through the fibres.[2]

It is expected that the co-axial electrospinning technique used in this work will lead to high fibre volume fractions due to the careful positioning of the matrix material

around the fibres allowing for even distribution of the matrix during the hot pressing as only a low amount of flow is required.

4.2 Electrospinning Polymer Fibres

Prior to coaxial electrospinning, each of the polymers were electrospun individually to ensure the compatibility of the polymer solutions with the electrospinning process. The solutions were made up to the concentrations described in the methodology section 3.2.1, using the solvent THF, around a viscosity consistent with previous electrospinning experience. These solutions were electrospun with increasing viscosity until consistent fibres were produced, at 15 wt% for PCL and 25 wt% for PLA. This was confirmed by scanning electron microscopy, as seen in Figure 4.3. The structures on the left were also seen in the literature discussed in section 2.3.1, and indicated that the solution is below that required to produce smooth fibres. To ensure that the coaxial structure could be maintained it was also confirmed that these two solutions were immiscible by mixing the two solutions in a vial and allowing them to separate overnight. Although the solutions being used contain the same solvent, the polymers themselves are immiscible.[122]

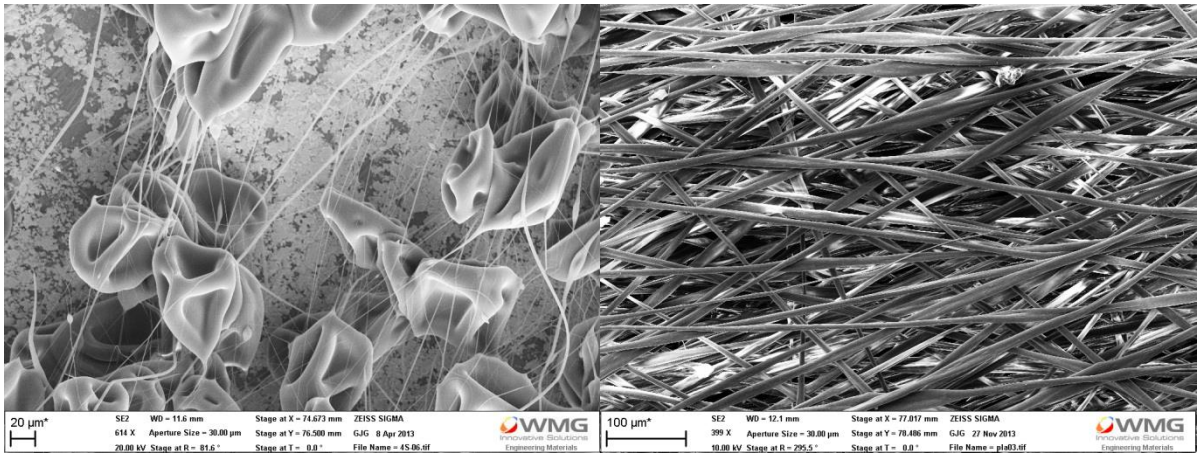

Figure 4.3: PLA electrospun from a solution of 15 wt% PLA in THF (left), and from 25 wt% PLA in THF (right)

A series of coaxial electrospun fibre mats were generated using the methodology outlined in section 3.2.2. This was the first time this equipment was used to produce coaxial electrospun fibres. The design for the coaxial nozzle was produced in house using SolidWorks software, and machined out of a piece of solvent resistant PTFE (Figure 3.3). The core solution was delivered by a stainless steel blunted gauge 20 needle, and the sheath solution was delivered through a polypropylene nozzle attached to the PTFE part which was cut to size to line up with the end of the needle. The polypropylene nozzle and the stainless steel needle were lined up concentrically by eye before each experiment.

In order to control the fibre volume ratio of the composite produced, the volume of each polymer within the fibre needed to be varied. This could be conducted by varying the concentration of one (or both) of the polymer solutions, however, this would be time consuming and unnecessary. A simpler method is to vary the flow rate at which the polymer solutions are delivered to the tip of the electrospinning

needle. While the total flow can remain consistent, the ratio of the two polymer solutions can be varied. Initial attempts used only one dual syringe pump, with the solutions loaded into syringes with different diameters to vary the flow rate of the two solutions. This did not provide enough flow rate variation and control for the final experiment, so a second syringe pump was used to be able to control the flow rate of the two solution independently.

To determine the electrospinning parameters, the total solution flow rate was increased with the electrospinning voltage until a consistent fibre jet was formed as described in methodology section 3.2.2. The collector was moved at 25 mm increments away from the nozzle until the collection drum could be covered by the electrospun fibres, which was at 200 mm from the nozzle. Although increasing distance will increase the spread of the fibres, it also has the negative effect of the fibres settling less on the collector and more on the surrounding area, so a balance needs to be achieved. Due to the increase collection distance, the electrospinning voltage was increased again to its final value of 8 kV, to ensure that a single consistent jet was produced.

All the electrospinning was conducted inside a fume hood to ensure that the fumes from the evaporating solvent were extracted safely. During the electrospinning, however, it became apparent that the airflow produced by the fume hood was adversely affecting the movement of the fibre jet as it moved from the nozzle to the collector. The fibre jet was being pulled towards the back of the fume hood as the

airflow overpowered the static charge attracting the fibre jet towards the grounded collector. To prevent this from affecting the electrospinning process, the fume hood was switched off for the duration of the electrospinning experiment, and turned on for a short time whenever the process was not running in order to ventilate the fume hood.

To confirm the core shell structure of the fibres, a section was cut using a scalpel and imaged using scanning electron microscopy. It was found that where the damaged had occurred the shell could be separated from the core, revealing the structure. This can be seen in Figure 4.4. Although the separation between the core and shell may be apparent here, further steps to confirm the structure proved to be more successful.

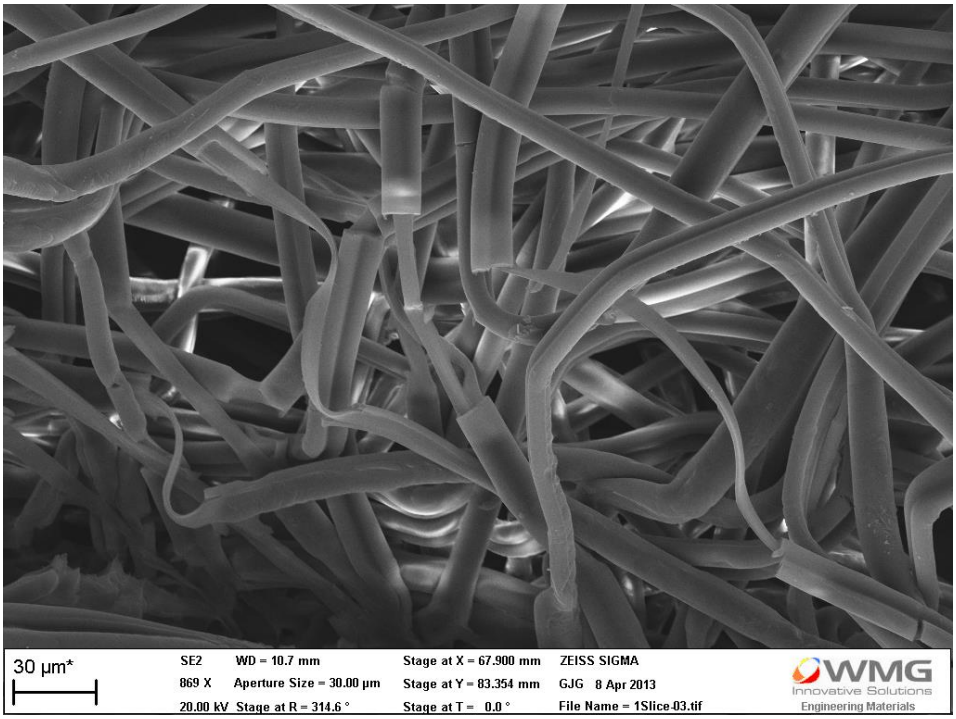

Figure 4.4: Coaxial fibres showing separation of core and shell from intentional damage.

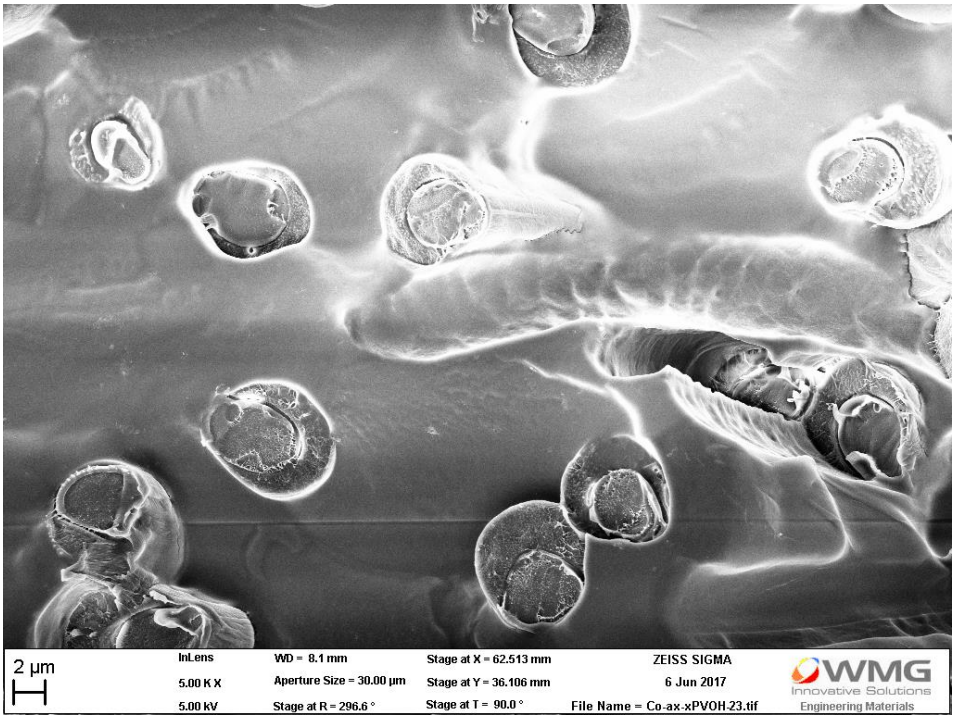

Figure 4.5: A cross-section of coaxial fibres embedded in a matrix of PVOH.

Figure 4.5 show the results of cryo-breaking the coaxial fibres while embedded in a PVOH matrix. While the fibres are sparsely distributed amongst the PVOH matrix, defined boundaries can be seen between the matrix, the PCL shell and PLA core. Although the PLA cores of the fibres are not exactly concentric with the PCL shells, this is not essential for the purposes of this project, as the PCL shell will be melted around the PLA core at another stage. Further work could be conducted on this stage of the process to create perfectly concentric shells and cores by altering the electrospinning nozzle.

The diameter of the fibres was not considered as an aspect of the electrospinning control here. Although the fibres were measured for reference, there was no attempt made to increase or decrease the fibre diameters at this stage as it was not a requirement in the experiment; only that the fibre diameter remained consistent

throughout. The coaxial fibres produced had an average diameter of 6.30 μm with a standard deviation of 1.15. This is quite large for electrospun fibres, which can be electrospun down to 10 nm,[7] however, by using such a volatile solvent (THF), high concentrations, and electrospinning two solutions, this is not unexpected. This potential to easily decrease the diameter of the fibres is a distinct advantage in the production of fibre reinforcement in composites due to the Griffith's criteria, and effects mentioned in section 2.7,[113] however it will not be capitalised on here to preserve consistency in the testing and due to equipment limitations. Thinner fibres would require further stretching of the solution jet, resulting in faster deposition rates. To combat this the speed of the collector needs to be increased, however, the equipment used here was not capable of the speeds required. Small changes in the electrospinning process, which are made to alter the variable being studied, will cause other small changes in the fibres produced. If the fibres being tested are approaching the region of nanofibre, small changes in the diameter of the fibres will make a much larger difference in the tensile properties compared to fibres with diameters in the micron range.[107]

4.2.1 Fibre Alignment of Electrospun Mats

Another important parameter when testing composite strength is the fibre alignment. This was measured from SEM images of the fibres by tracing out the fibres in ImageJ and measuring the angles of the lines. These lines can be seen in Figure 4.6. The results in Table 4.1 show that the standard deviation of the fibre

angles decreases as the speed of collection is increased, showing an improvement in the alignment of the fibres. This is in-line with literature on electrospinning fibre alignment[9,10]. There appears to be little change in alignment after reaching a collection speed of 6.86 ms^{-1}, so this can therefore be considered to be the point at which adequate fibre alignment has been achieved. Although the faster collection speeds show aligned fibres, the increased speed with the same rate of deposition can cause the collector to pull on the fibres, stretching or breaking them (Figure 4.8).

Table 4.1: Alignment of coaxial electrospun fibres by standard deviation from the average angle of the fibres

Input Voltage (V)	**Linear velocity (ms^{-1})**	**Fibre angle StDev (°)**
6	4.87	8.9
8	6.86	4.1
10	8.67	4.1
12	10.58	4.0

These changes in alignment can be seen in Figure 4.6 and Figure 4.7. The samples are aligned so that the vertical is parallel to the direction of rotation of the collector. The fibres in Figure 4.6 were collected at 4.87 ms^{-1} and in Figure 4.7, at 6.86 ms^{-1}. Although the fibres in Figure 4.6 are straight, they are less consistently aligned when compared to the fibres in Figure 4.7.

Figure 4.6: Coaxial electrospun fibres collected at a linear drum speed of 4.87 ms^{-1}. Yellow lines drawn on using ImageJ to calculate fibre alignment.

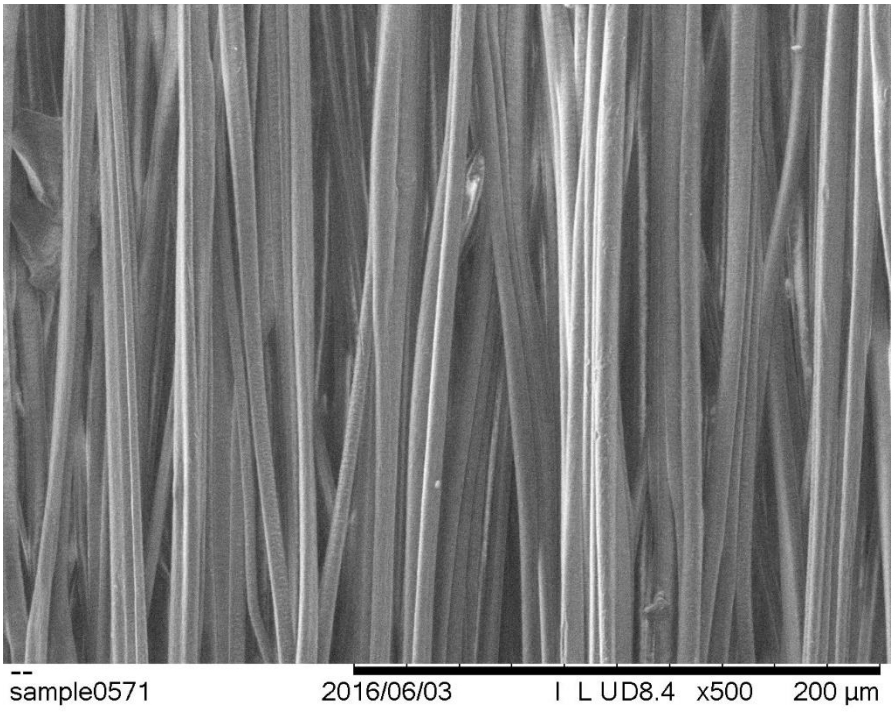

Figure 4.7: Coaxial electrospun fibres collected at a linear drum speed of 6.86 ms^{-1}

The fibres collected at higher speeds exhibited slightly less deviation (from 4.1° to 4.0°) in the alignment, however, this can cause damage to the fibres, which can be

seen in Figure 4.8. In the area highlighted, the fibre has been stretched during the collection process and has undergone a necking process; reducing the uniformity of the composite, and introducing a weak point in the fibre which can lower the strength of the overall composite.[113]

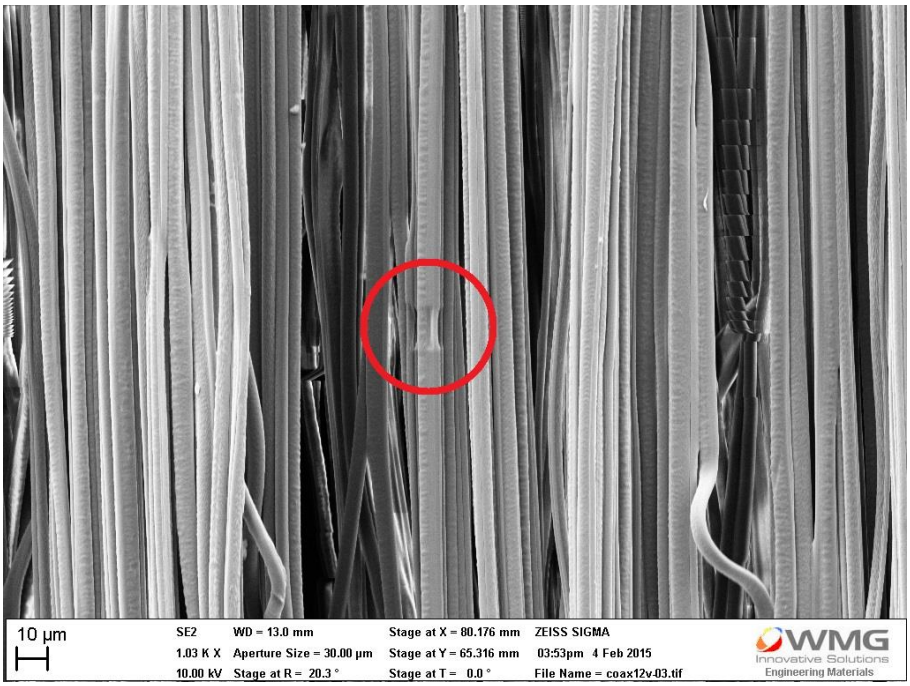

Figure 4.8: Coaxial electrospun fibres collected at a linear drum speed of 10.6 ms^{-1}

4.3 Characterisation of Electrospun Fibre Mats

4.3.1 Thermogravimetric Analysis

It is important to characterise the actual fibre volume fraction rather than relying on the theoretical values from the flow rate calculations. Thermogravimetric analysis (TGA) was initially used to investigate the composition of the electrospun fibres by constructing a calibration curve of known volume fractions of each polymer (See Appendix, Figure 9.1 and Figure 9.2).

The temperature at 80 % mass loss ($T_{d(80\%)}$) was plotted for all known volume fractions and the intended volume fractions from the fabricated electrospun samples were then compared against this. Whilst there is a trend of $T_{d(80\%)}$ decreasing as the volume of PLA is increased in both cases, the variance of the data is such that it could not be used as an accurate, predictive model. This variance can be attributed to the face that PLA has a slightly lower degradation temperature compared to PCL, and yet is encased within the PCL. This could hinder the time taken for the PLA to degrade by providing insulation, and it could also delay any gaseous compounds being emitted. This effect would be more pronounced in the higher fibre volume ratio samples. These results do, however, show that there was little mass loss prior to the degradation points of the polymer, showing that there was no residual solvent from the electrospinning process or moisture absorption.

4.3.2 ^{1}H NMR Analysis of Electrospun Mats

An alternative method was investigated based on solution phase ^{1}H NMR. Initially the ^{1}H NMR spectra of both the PCL and PLA samples were recorded individually (Figure 4.9 and Figure 4.10). As with the results from the TGA, these graphs show the high purity of the polymer composite as there is little noise between the peaks of the polymers.

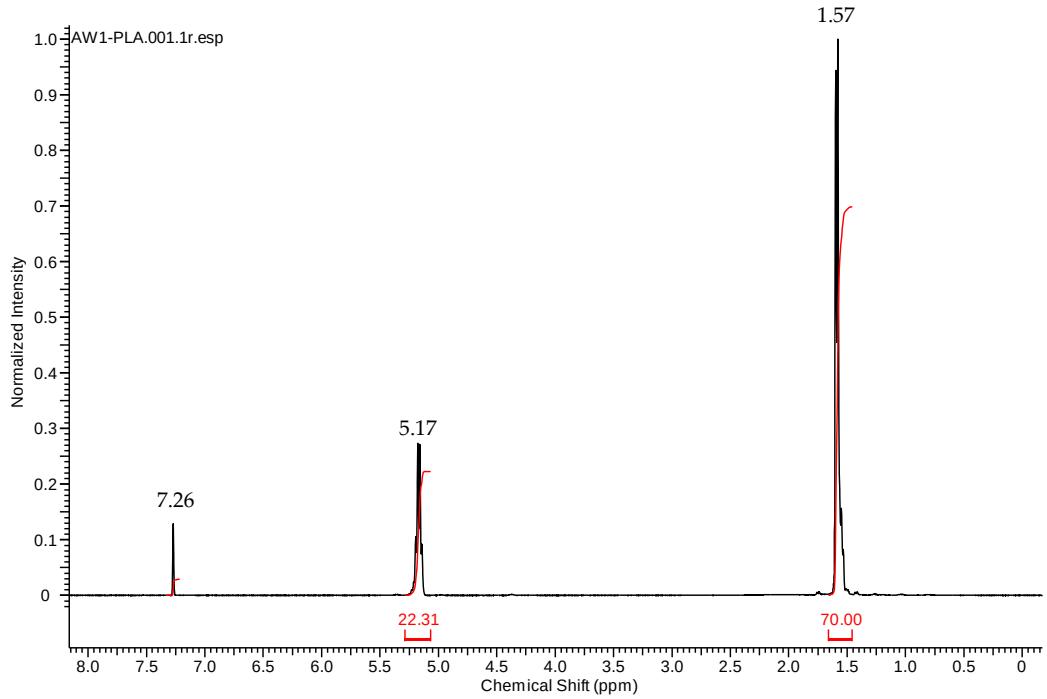

Figure 4.9: ^{1}H NMR spectra for PLA dissolved in d-chloroform

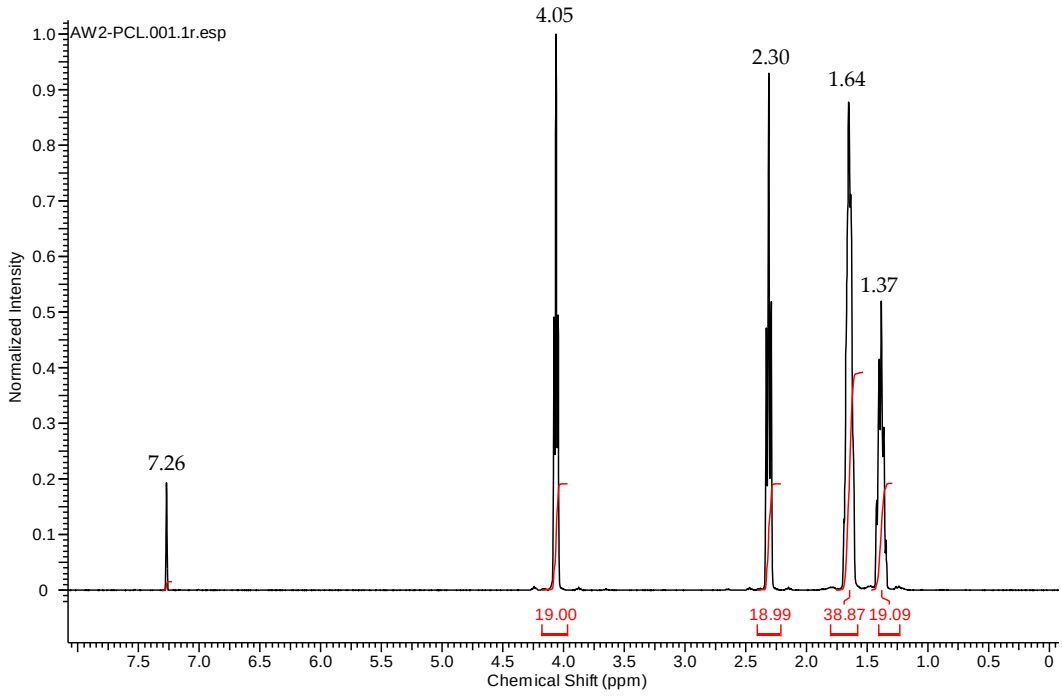

Figure 4.10: ^{1}H NMR spectra for PCL dissolved in d-chloroform

A comparison of these spectra in Figure 4.9 and Figure 4.10 shows distinct peaks for each polymer. The red number below each peak is the integral of the peak. The peak to the far left at 7.26 ppm is attributed to $CHCl_3$ ($CDCl_3$ was used as the solvent), and

is used in the spectra as a known value to calibrate the peaks against. The peak for the methine group next to the carbonyl functionality of PLA is at 5.17 ppm, whereas the corresponding methylene group on PCL is at 4.05 ppm. These are shown in Figure 4.11 with the relevant molecular group highlighted in red. This allowed for accurate measurements to be made about the content of the samples by comparing the relative areas of these peaks.

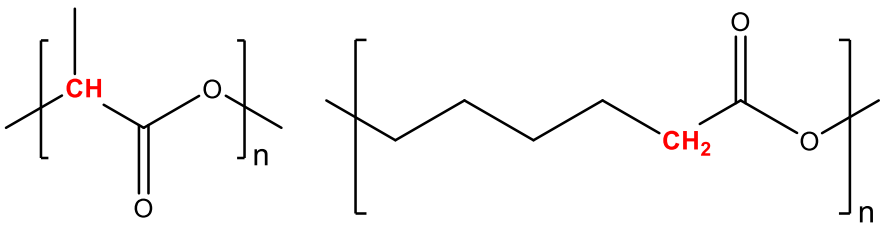

Figure 4.11: Repeating units for polymers, PLA (left), and PCL (right)

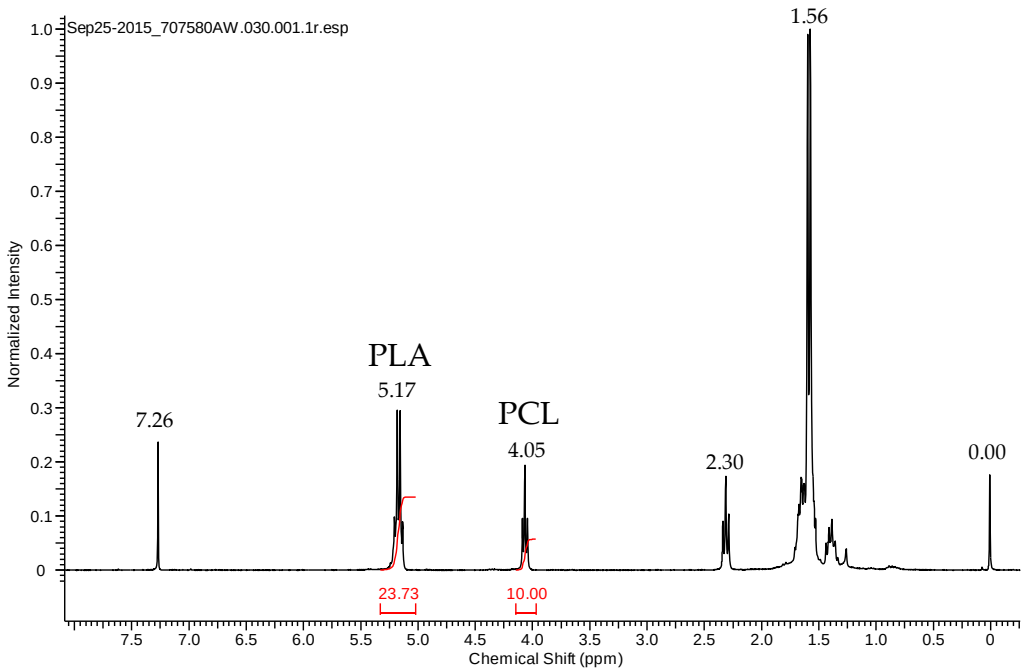

Figure 4.12: ^{1}H NMR spectra for 0.75 fibre volume ratio composite dissolved in d-chloroform

Figure 4.12 show the full NMR spectra of a sample of the electrospun polymer composite. In the spectra, the positions of the two peaks being used for the calculations are visible, and have been labelled with the integration value. This shows there is adequate spacing around these two peaks to take accurate readings.

The area of the peaks was measured using ACD/Labs 1D NMR analysis software, and used in the equations to find the fibre volume ratio of the tested composite. Using this methodology, the fibre volume ratios were calculated and displayed in Table 4.2.

Table 4.2: Fibre volume fractions of composite samples analysed by NMR

Intended	Measured	Difference
0.50	0.5086	0.0086
0.60	0.5584	-0.0416
0.65	0.6348	-0.0152
0.70	0.6742	-0.0258
0.75	0.7327	-0.0173
0.80	0.7654	-0.0346
0.85	0.8375	-0.0125
0.90	0.9213	0.0213
1.00	1.0000	0.0000

There is a small difference in the measured composition of the polymers and the theoretical composition calculated from the solution concentration and flow rate. This difference in most likely due to inconsistencies in the concentration of the polymer solutions. Although these solutions were carefully measured to confirm the concentrations, THF is a volatile solvent, so it evaporates quickly and can lead to this

slight variation in the concentration of the solvents. As a result of this during experimentation, the stored solutions were characterised weekly and THF was added to compensate for the loss of solvent due to evaporation.

4.4 Tensile Testing

Unidirectional fibre reinforced composites in industry are typically created to produce strength in tension, parallel to the fibre direction.[2,113,115] For this reason, tensile testing in this direction was considered to be the main focus of this work, aiming to create a composite with improved tensile properties.

The aligned coaxial electrospun fibre mats were consolidated into a composite using the hot-pressing procedure described in section 3.2.3. Figure 4.13 shows some of the composite sheets formed from the coaxial electrospun fibres. The sheets have been cut into 15 mm strips, using a utility knife and a template, for tensile testing.

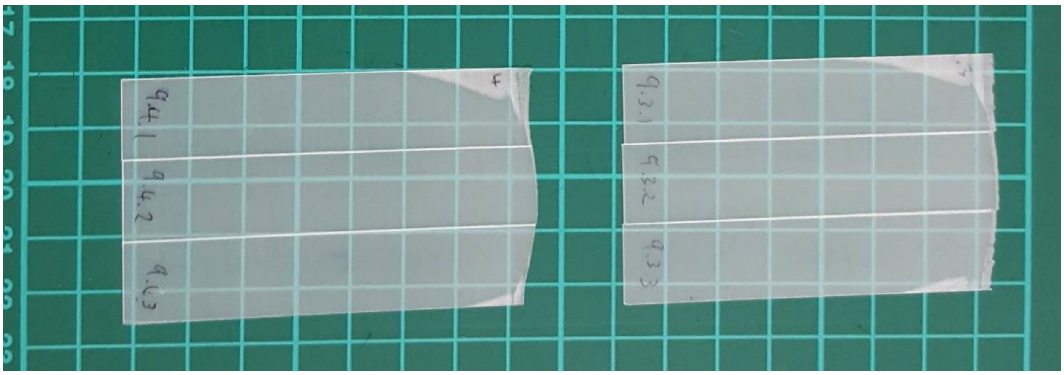

Figure 4.13: Consolidated coaxial electrospun composites cut into 15 mm strips and labelled for tensile testing. Each square on the mat is 10 x 10 mm.

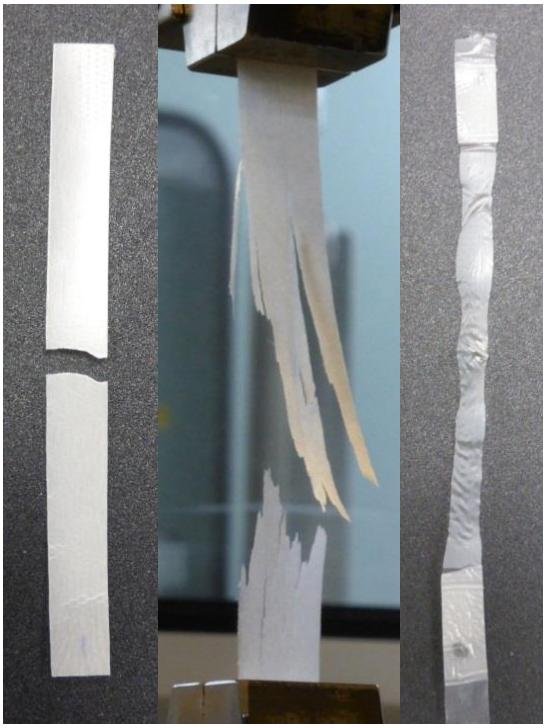

Figure 4.14: Results of tensile breakage on the composite (left) and its constituent parts, the PLA fibres (middle) and the PCL matrix (right). Each sample is 15 mm wide.

Figure 4.14 shows an example of how the composite breaks compared to its constituent parts. The fibres (middle) break individually at different points throughout the sample at low extension, whist the bulk PCL (right) undergoes necking throughout the sample with high extension. The composite breakage has a clean, horizontal break at low extension, as the fibres break, the stress also overcomes the matrix.

The tensile testing results have echoed what has been revealed in theory and in the previous literature with an increase in strength and modulus up to a point of maximum fibre volume, followed by a decrease in tensile properties. In all cases, the break point of the composite was at a higher stress than the UTS of the matrix alone, signifying that each composite was a fibre controlled failure. Figure 4.15 shows some

typical stress-strain curves from the results. The graph also shows how the composites compare to the bulk polymers, with bulk PLA at the top left, and PCL at the bottom right. PCL is ductile, and the curve in this example extends to 22 % strain, however, the curve in this graph has been truncated for clarity and to fit with the others.

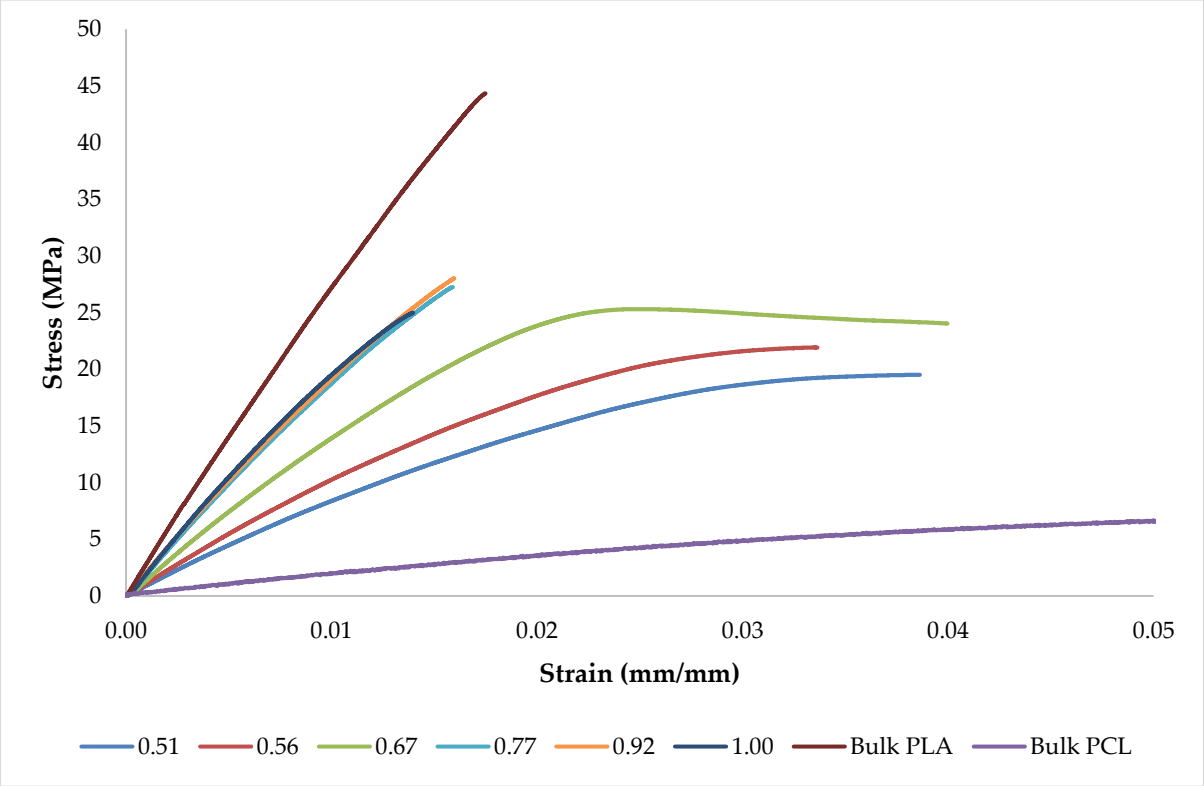

Figure 4.15: Typical stress-strain curves for the composites from a selection of fibre volume fractions, and compared with the bulk polymers. The bulk PCL curve extends to 22% strain, but it has been truncated in this graph for clarity.

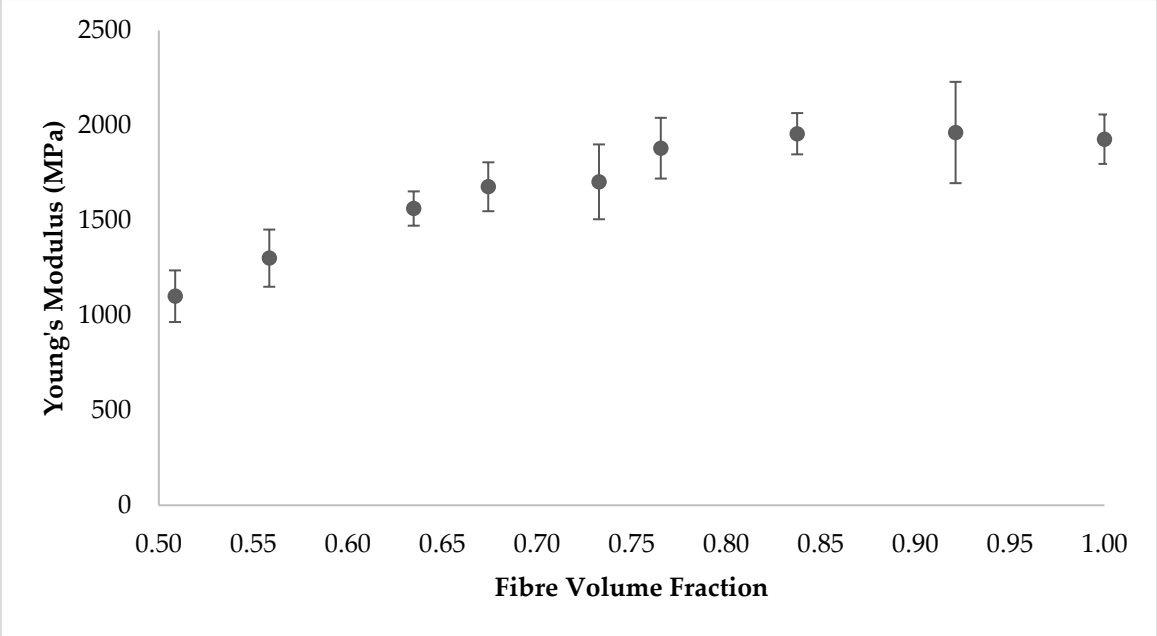

Figure 4.16: Young's modulus compared to volume fraction of PLA in the composite with standard deviation error.

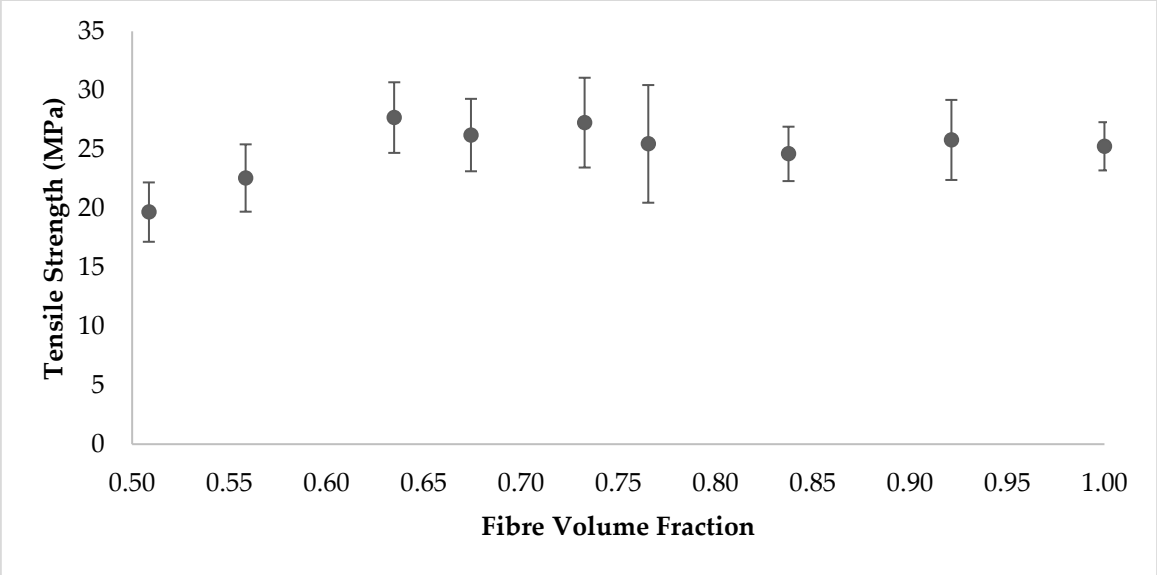

Figure 4.17: Tensile strength compared to volume fraction of PLA in the composite with standard deviation error.

The Young's modulus (Figure 4.16) appears to increase (stiffer material) in significant steps from 0.51 up to 0.73 fibre volume, from here to 1.00 (all fibres and no matrix); however, the increase is slowed as only minor increases, within experimental error, of Young's modulus is observed. The Young's modulus increases

due to the increased content of the stiffer PLA fibres. The increase slows down at higher volume fractions due to poorer distribution of stress on the fibres as a result of the reduction of matrix material. This poorer interaction results in PLA fibres stretching independently, or in a more localised fashion, rather than as a collective, resulting in a less stiffness than if all the fibres could work together.

From 0.51 fibre volume, tensile strength (Figure 4.17) increased up to its maximum at 0.73, 27.3 MPa, followed by a decrease as fibre volume increased further. As with the Young's modulus, the increase in tensile strength is mainly due to the increase of the stronger PLA fibres. The increase in fibre content at higher volume fraction has a more detrimental effect here than on Young's modulus, as there is a slight decrease rather than just a levelling off. The reduced matrix content results in poorer distribution of stress, and premature failure of localised groups of fibres under more stress. This, in turn, places a sudden increase of stress on the remaining fibres causing them to fail, rather than the preferred mechanic of the stress being distributed evenly across all the fibres leading to simultaneous failure at the greatest level of stress.

There is consistent degree of error throughout these results. This can be attributed to the variation in thickness across each of the electrospun fibre mats. During the electrospinning process, there is a tendency for a greater quantity of fibres to be deposited onto the middle of the collector rather than the sides. This is offset by maintaining as large a distance as possible between the spinneret and the collector,

and by increasing the spinning time to produce thicker mats overall, which reduce the difference between the thickest and thinnest sections of the mats. These variables are limited by the spinning process. The collection distance is limited by the voltage of the equipment and the surroundings to ensure collection on the drum. The duration of the spinning is limited by the insulating effect of the polymer fibres on the grounded collector. As when the fibres build up less of the polymer is encouraged to be deposited on to the collector due to the electrostatic charge. It was found during the experimentation that there was a very low rate of fibre deposition after one hour of electrospinning. There are other methods of processing to reduce this variation. The collection drum could be mounted on to a moving platform which would oscillate slowly and in a controlled pattern in the perpendicular direction to the fibre spinning; effectively moving the centre of the electrospinning process across the drum. Scaled up production techniques can also increase uniformity by having multiple points of fibre ejection from the solution. These techniques were not employed in this experimentation as the equipment was not available.

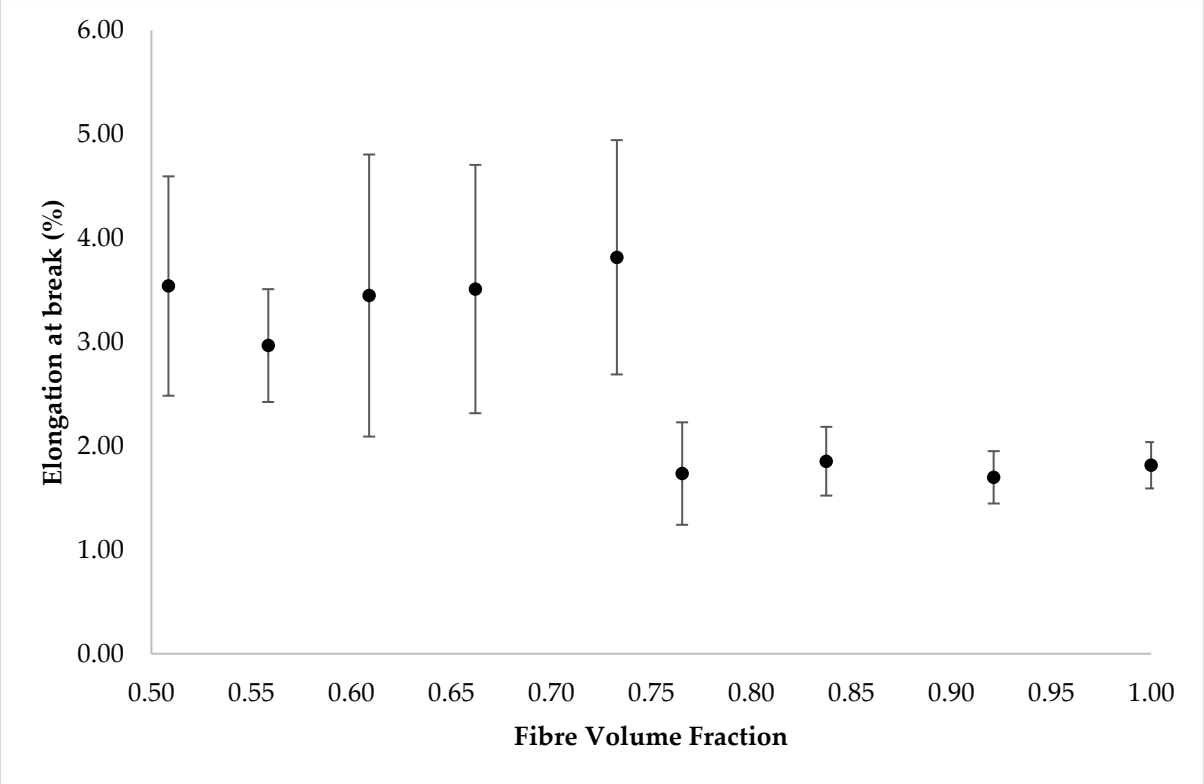

Figure 4.18: Elongation at break compared to volume fraction of PLA in the composite with standard deviation error.

The elongation (Figure 4.18) in the lower fibre volume fractions is a result of plastic deformation of the fibres (Figure 4.19). This is due the good distribution of stress, allowing the reinforcing PLA fibres to deform plastically in unison. However, at the higher volume fractions, there is no plastic deformation section in the curves (Figure 4.20) of the composites, showing that the stress is not well distributed. This could be due to voids being present in the composite. This leads to stress concentrations around the voids, and the breakage of individual components, resulting in cascading fibre failure and the sudden failure of the material.[2]

Although the error values are fairly even across the tensile strength and modulus results, for the elongation at break (Figure 4.18), there are large errors at lower

volume fractions (where the elongation was greater), and smaller errors at high volume fractions (where elongation was lower). This was observed at the lower volume fractions, as some samples would break soon after yield due to imperfections in the sample, but most would go on to higher elongations, and greater toughness. At the higher volumes fractions, all samples broke soon after the yield strength was reached. This indicated that although the lower volume fractions have larger elongation, from the plastic deformation of the fibres, this can be affected by defects, such as a variation of fibre diameters from the electrospinning process, or less than perfect fibre alignment.

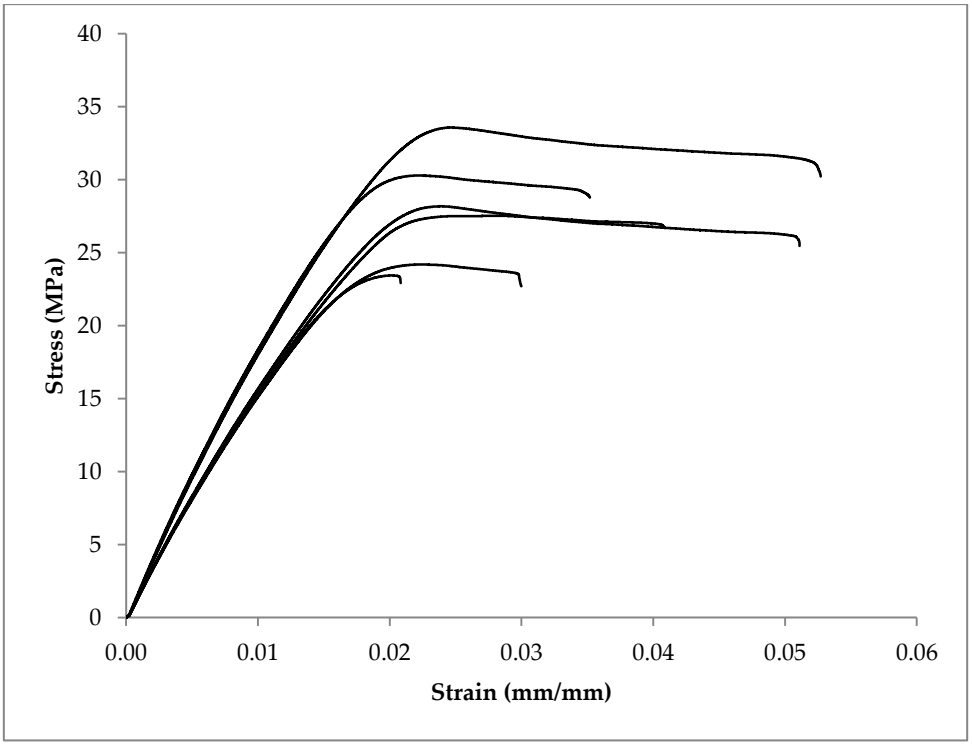

Figure 4.19: A sample of tensile test results for composite samples of 0.73 volume fraction of PLA

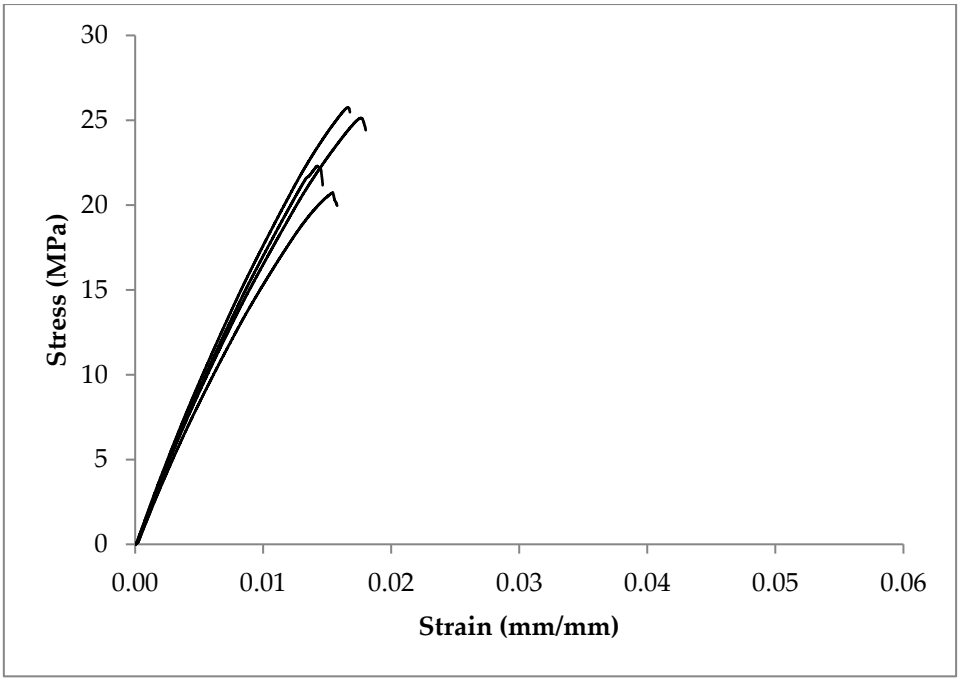

Figure 4.20: A sample of tensile test results for composite samples of 0.92 volume fraction of PLA

The tensile testing results here show that the maximum volume fraction found here is larger than the typical fibre volume fraction in continuous unidirectional fibre reinforced composites which is usually stated as between 0.60 and 0.70.[2] As mentioned in the introduction, a high maximum volume fraction was expected from this technique. Using the rule of mixtures, these results can be compared to theoretical calculations to see how well they fit and provide a more robust explanation for the maximum fibre volume ratio.

4.4.1 Rule of Mixtures

The theoretical maximum tensile strength of the composites was calculated from the properties of the individual component polymers by using the rule of mixtures. The actual tensile strength of the composites will be lower than this as a result of imperfections in the composite material due to variation in the strength of the fibres,

inelastic behaviour of the polymers, and uneven strain distribution across the fibres and the matrix.

There are variations of this rule, such as the Tsai-Hahn, Haplin-Tsai, and Cox models. These models use additional parameters to allow for the calculation to include addition information such as fibre geometry, packing geometry, and loading conditions. These models can also be adapted to determine the properties of discontinuous fibre reinforced composites.[113,123] The intention of the experiment here was to compare the composites produced with a perfect theoretical continuous fibre specimen, with perfect fibre geometry, packing, and adhesion to the matrix. These alternative methods are used to provide a closer approximation to the experimental results, so are not appropriate to use here. Results from this study could be used with these equations to produce theoretical results which would conform more accurately to the experimental data, allowing for a better prediction of the results.

Table 4.3 shows how the measured tensile properties of the composite compared to the upper bound of the rule of mixtures. The upper bound was calculated using the bulk properties of the materials with equation 3.6 in section 3.2.5. A value of 100 % in this table would show an exact match to the rule of mixtures, indicating a perfect composite with perfect adhesion between the fibres and matrix, and perfect fibre alignment. The aim is to get a close to this as possible.

Table 4.3: Actual composite test results compared to the theoretical maximum calculated by the rule of mixtures

Fibre volume ratio by NMR	**Test compared to Rule of Mixtures**	
	Young's Modulus (%)	Tensile Strength (%)
0.51	71.98	73.16
0.56	78.35	78.71
0.61	87.10	90.89
0.66	86.73	81.00
0.73	80.33	78.18
0.77	85.22	70.65
0.84	81.64	63.76
0.92	75.00	62.03
1.00	68.25	56.90

All the test results of the formed composite are lower than the upper bound of the rule of mixtures values as expected, and a trend is apparent with lower percentages at the extremes of the fibre volume ratio, and a peak in-between.

Figure 4.21 and Figure 4.22 show lines for the upper and lower bound calculations of the rule of mixtures, with the measured tensile properties displayed. Although the increase in fibre volume increases the tensile properties as per the rule of mixtures,[2,112,113,115] the uneven distribution of stress weakens the composite. While the lower volume fractions remain within the lower bound, some of the high volume fractions are below this. It is clear that for these fibre volume fractions, the materials no longer have enough matrix material to bind the fibres, and may no longer be considered to be working fibre reinforced composite materials.

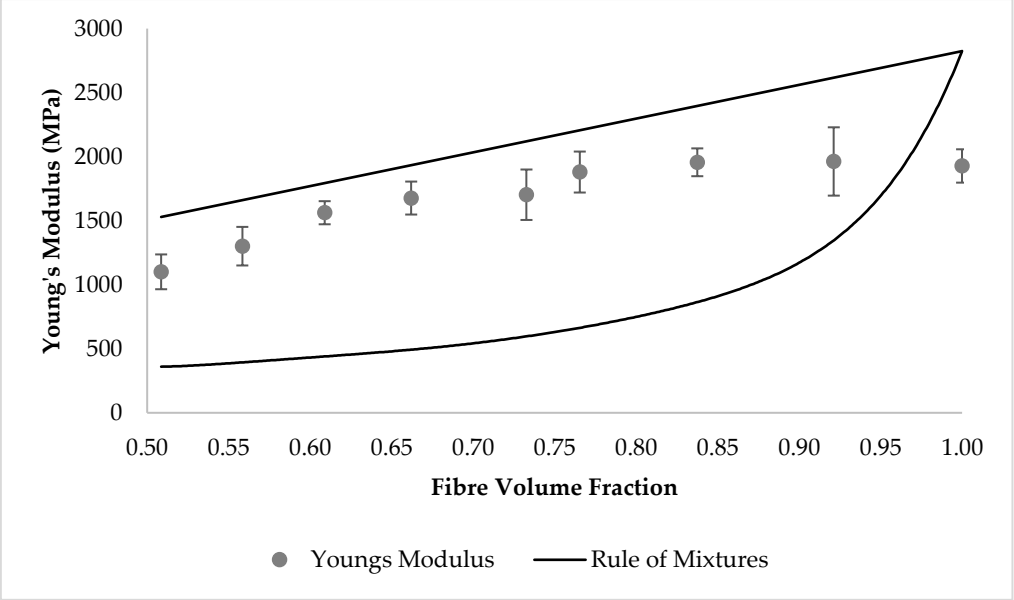

Figure 4.21: Measured Young's modulus of the electrospun composites compared to the upper and lower bound calculated by the rule of mixtures

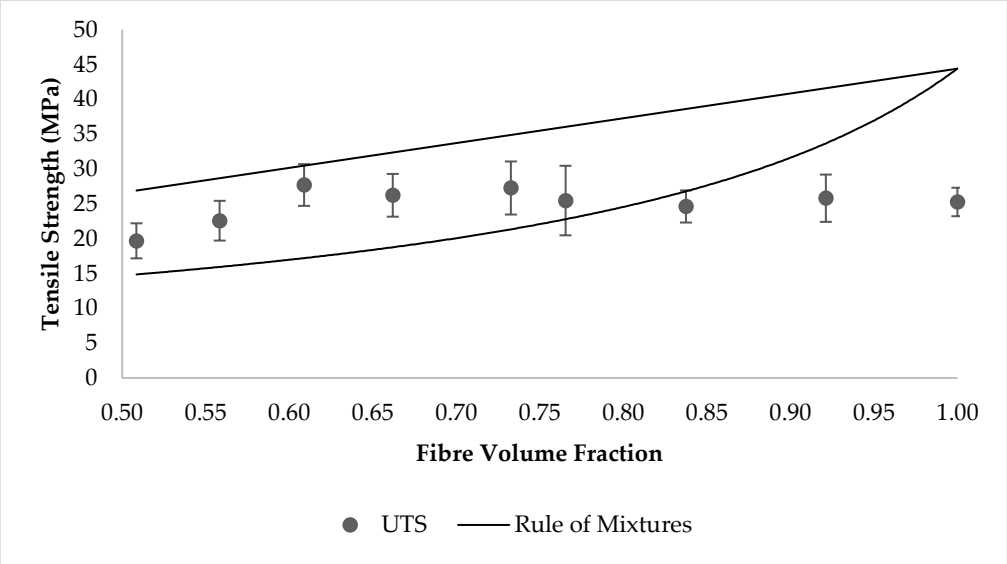

Figure 4.22: Measured tensile strength of the electrospun composites compared to the upper and lower bound calculated by the rule of mixtures

There are three main imperfections causing the disparity between the rule of mixtures and the measured values. In this experiment, the fibre volume ratio is being varied, which will affect the distribution of stain across the composite, while the other two mentioned will not have been affected between experiments. At high fibre

volume fractions there is less matrix to distribute the strain across the fibres, resulting in an uneven strain in the fibres and a cascade of fibre breakage. At low volume fractions, the fibres have a tendency to agglomerate creating areas of high fibre density and areas of high matrix density (Figure 4.23). This can cause a small variation in the strain distribution, and an increase of void in the matrix-rich sections.[2]

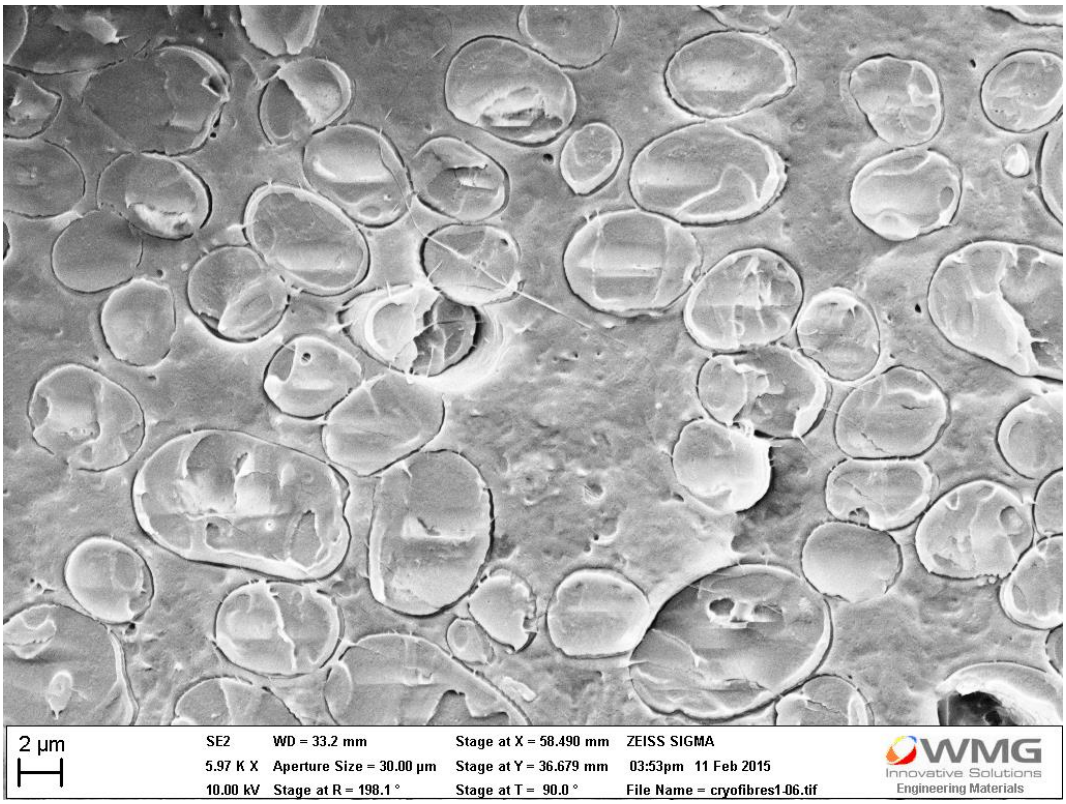

Figure 4.23: Cross section of a 0.56 fibre volume fraction composite showing uneven distribution of PLA fibres in the PCL matrix

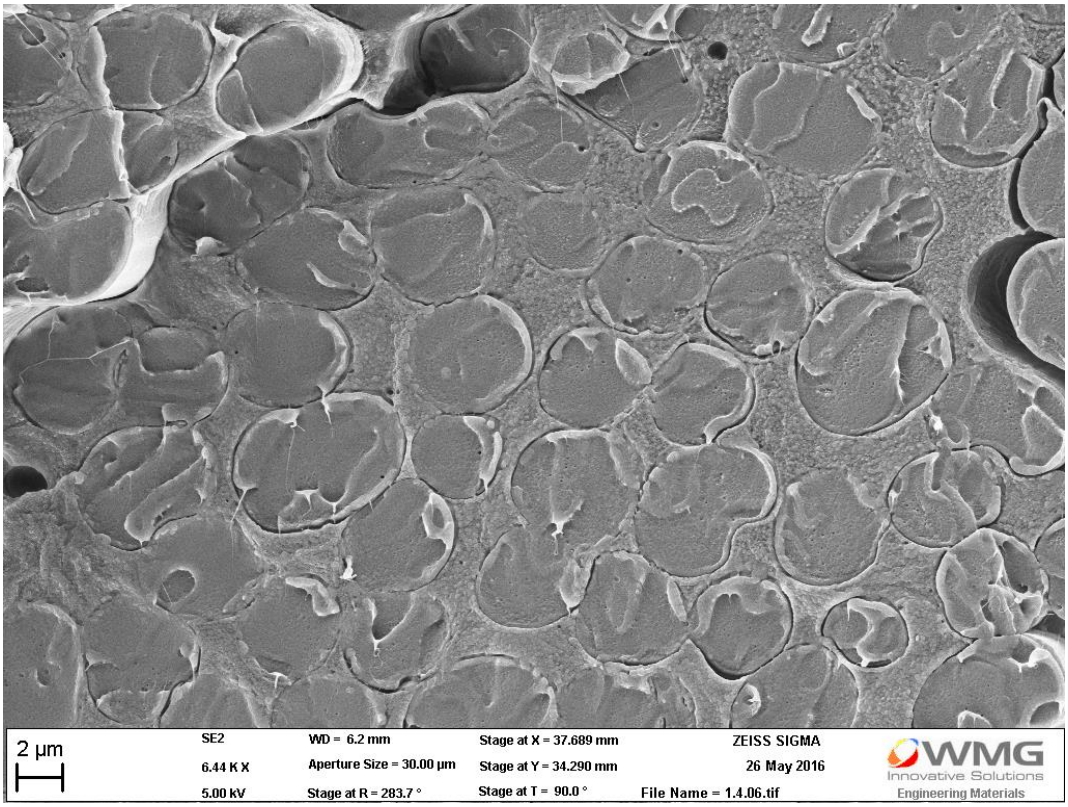

Figure 4.24: Cross section of a 0.73 fibre volume fraction composite showing even distribution of PLA fibres in the PCL matrix

Figure 4.24 shows a cross-section of a composite with a higher fibre volume ratio. As there is less space for the fibres, they have fewer opportunities to form agglomerations within the composite, resulting in a more even distribution. This allows for more uniform stress distribution, creating a composite with higher tensile strength, as stress concentrations will lead to failure in these areas first, and premature failure of the structure. This can be seen in Figure 4.15, as the tensile strength increases as the fibre volume fraction increases.

In both composite cross sections in Figure 4.23 and Figure 4.24, it is apparent that the fibres vary in shape. This may have been as a result of the electrospinning process, however, it is likely that the hot pressing process would have had some effect on the

shape of the PLA fibre with the temperature and pressure used, as the temperature of the press was higher that the glass transition temperature of PLA (56 °C). This will be explored in the next experimental chapter (5.0) which highlights variations in the hot pressing technique.

The results show that for this electrospun composite, the gap in the tensile properties calculated from the rule of mixtures and the test results varies over the different fibre volume fractions. The difference is lowest in the 0.61 fibre volume fraction sample, showing that these samples contained the best interactions and strain distribution between the fibres and the matrix. Whilst in the samples with higher volume ratio, the interaction may not have been as good, according to the rule of mixtures, there was still an increase in tensile strength and Young's modulus. This shows that the addition of fibres outweighs the loss in strength from the interactions and stress distribution.

4.5 Conclusions

The characterisation of the composite proved that coaxial electrospun fibres could be produced from PLA and PCL using the equipment, and the resulting fibre mat could be easily pressed to form a unidirectional composite. The ratio between the core and shell polymer proved easy to adjust by controlling the solution flow rate during electrospinning with little effect on the other parameters of the process. Although TGA provides degradation information of the composite as a whole, it can be considered unreliable as the PLA degrades before the PCL but is being encased by

the PCL. These results did, however show a pure composite with no residual solvent from electrospinning or moisture absorption. NMR was more accurate in characterising the polymer fractions in the composite. These results also demonstrated the high purity of the composite.

The SEM images of the composite cross-section show that cryo-breaking is an adequate method to image the formed composite. These images show the uneven distribution of fibres in low fibre volume composites, and more even distribution in the higher fibre volume composites, contributing to improved distribution of stress across the fibres in the composite.

From the tensile testing results it can be concluded that 0.73 fibre volume provided the best all round tensile properties, with the highest average tensile strength and comparable Young's modulus compared with higher volume fractions. The stress strain curves also show a good degree of plastic deformation of the composite, which is not present in the higher volume fractions, a result of better stress distribution across the fibres.

The experiment shows that coaxial electrospinning can be an easy way to produce thermoplastic fibre reinforced composites with accurate fibre volume ratios; with at least 0.03 higher fibre volume fractions than traditionally produced thermoset composite, and even higher than for a thermoplastic composite. This suggests that this method of producing composites will have improved tensile results over traditional methods. This is due to the matrix being prepositioned around the fibres

by the coaxial electrospinning, so that molten matrix does not require as much penetration through the fibres, leaving a composite with good distribution of fibres, and low void content.

5 Composite forming variation

5.1 Introduction

In preliminary testing the composites were formed using a vacuum bag technique. This consisted of layering sheets of electrospun polymer fibres onto a PTFE coated aluminium sheet, sticking a sheet of nylon release film over the top with black tack, and attaching a hose fitting. A foam mesh channel was placed from the hose attachment around the sample to evenly distribute the vacuum pressure. However, this limits the pressure being used to consolidate the composite to 1 bar, and cooling rate cannot be accurately controlled. By using a small heated hydraulic press, the composite can be formed under a variety of controlled pressures. Higher forming pressures can reduce the number of voids within the composite and improve the fibre-matrix interaction, thus improving the tensile properties. However, this also risks transverse deformation of the fibres, creating weak points in the composite and decreasing its tensile properties. This chapter is concerned with analysing the effects of variation in the temperature, cooling rate, and forming pressure of the process, in order to find the variables which will produce composite with higher tensile strength and stiffness.

In addition to physical microscopic variation, the differences in the heat and pressure can have an effect on the chemical structure of the polymers. The interactions and alignment of the polymer chains can be altered causing a transition

between an amorphous and a crystalline structure. Although it is not usual for a polymer be fully crystalline, a polymer with partial crystallinity is considered to be semi-crystalline. These differences in crystalline structure are known to effect the tensile properties of polymers, with high crystalline polymers having higher tensile strength and greater stiffness.[124] Polymer crystallinity is typically measured using differential scanning calorimetry (DSC) or X-ray diffraction (XRD).

5.2 Crystallinity

Differential scanning calorimetry (DSC) is used to characterise the glass transition temperature (T_g), melting temperature (T_m), and crystallinity of a polymer by measuring the heat flow required to raise the temperature of a sample at a set rate. T_g can be identified by an endothermic shift in the baseline of the curve, and the T_m can be identified at an endothermic peak, as more energy is required to break down any crystalline structure in the polymer to achieve the molten form. Both the onset of melting and peak melting temperatures are considered for different types of polymer. The crystallinity of the polymer can also be calculated from this melting peak. By taking the integral of the peak against the baseline, the energy per gram to melt the polymer can be found. Depending on processing conditions, some polymers, mostly polyesters, can undergo crystal formation during the heating process. This is identified on the DSC as an exothermic peak, as this crystalline state is energetically favourable. The integral of this peak must also be taken and subtracted from the melting peaking to calculate the total energy required prior to

the thermal analysis. This value can be compared against a known 100 % crystalline version of the polymer (usually found in literature), which is calculated by extrapolation, to find the crystallinity of the sample.

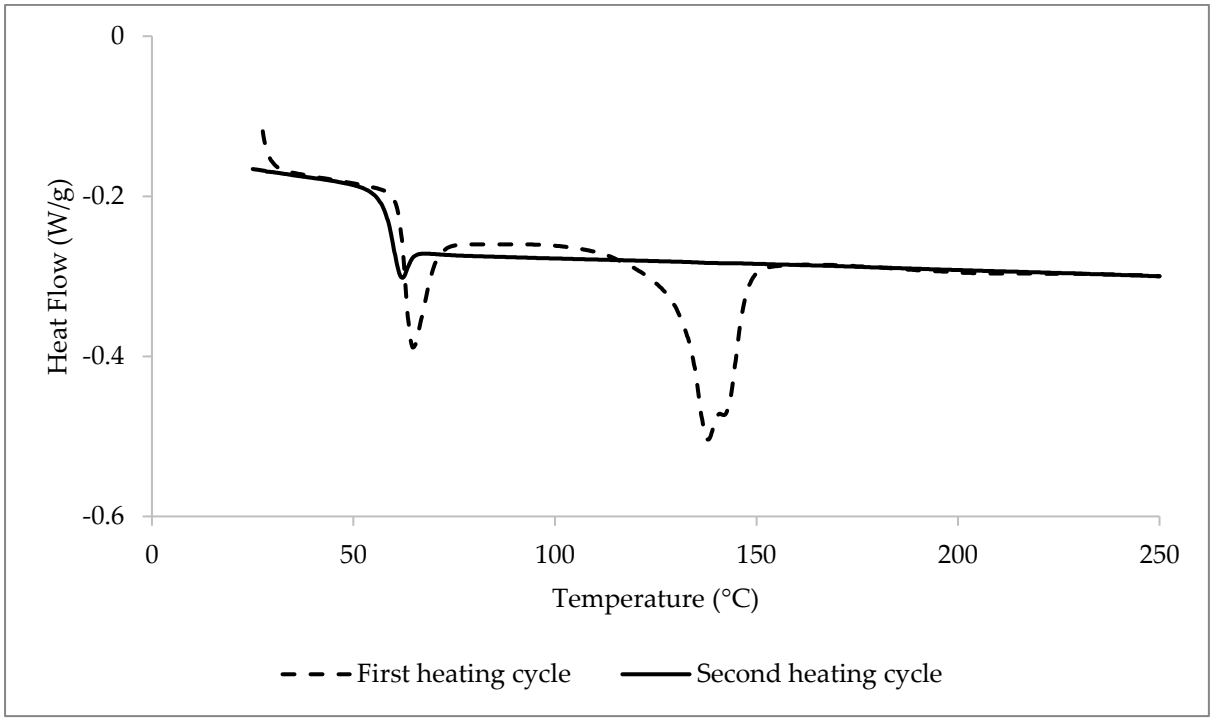

Figure 5.1: DSC curve of PLA as received, showing two cycles of heating

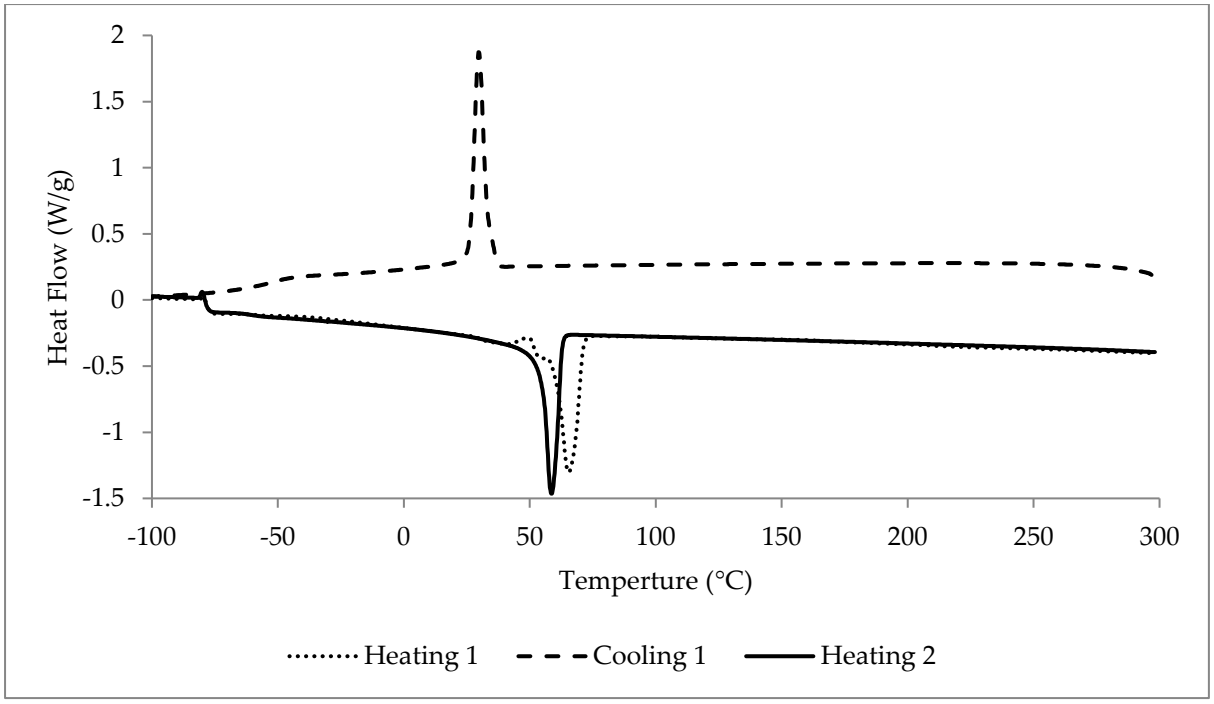

Figure 5.2: DSC curve of PCL as received, showing two heating cycles and the first cooling cycle.

The two polymers used in this study were first characterised as received using DSC. Figure 5.1 shows a DSC curve for a sample of as received PLA with two cycles of heating and cooling. The first heating curve includes the thermal history of the polymer, and integration of the melting peak reveals an area of 19.9 J g^{-1} which compared to the literature value of 100 % crystalline PLA of 93.6 J g^{-1},[125] equals crystallisation of 21 % from the manufacturing process. The second heating cycle, however show no peaks except for the glass transition between 50 – 60 °C. This show that it is an amorphous polymer, but some crystallisation can be introduced during manufacturing.

Figure 5.2 show a DSC curve for a pellet of PCL as received with two heating cycles and the first cooling cycle. Due to limitations of the equipment, the glass transition

temperature on the polymer is not shown on the curve, which is around -60 °C. However, this is not an important aspect of this study which is focusing on the tensile strength at room temperature, and the temperature of the composite forming process. The first and second heating cycles show melting peaks at 65.3 °C and 58.5 °C respectively, with each area equal to 59.2 J g^{-1} which, when compared to the literature value of 100 % crystalline PCL of 139.5 J g^{-1},[126] shows that the sample of PCL has a crystallinity of 42 %, which was unaffected by the manufacturing process despite a slight shift in the peak. This peak is also visible in the cooling cycle at 29.8 °C where the crystalline structure is formed upon cooling.

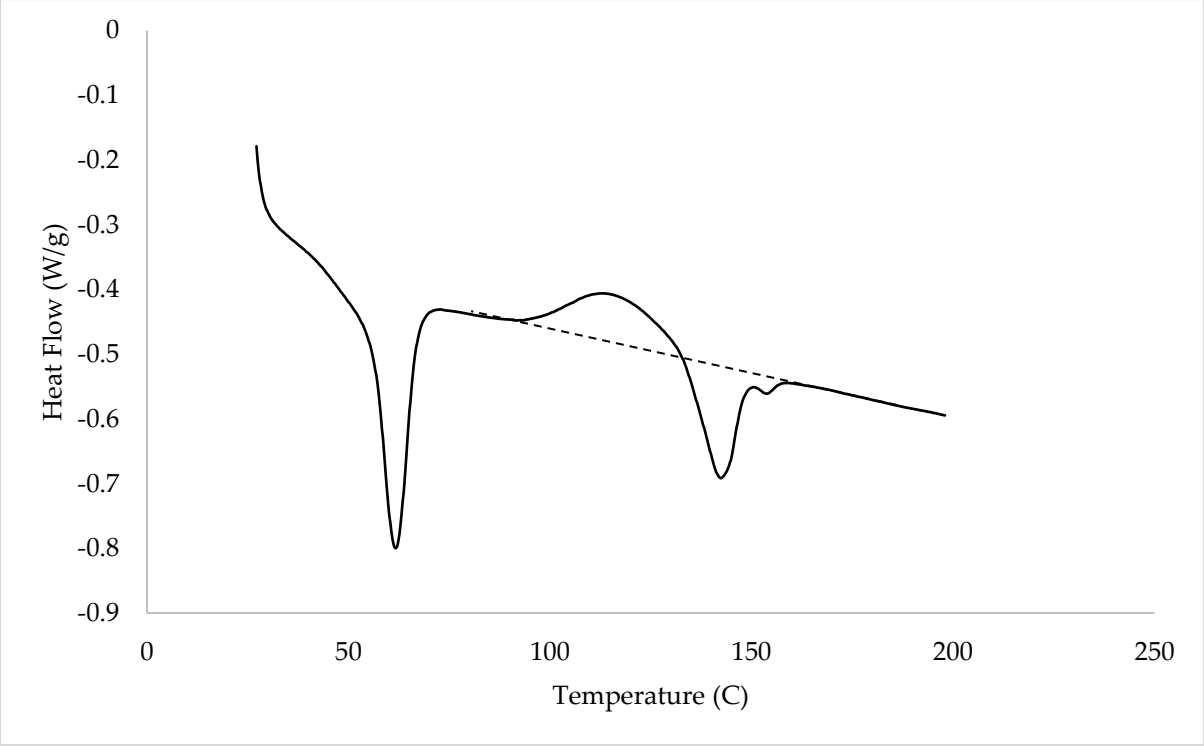

Figure 5.3: DSC curve for a sample of coaxial PCL/PLA as spun, before hot pressing.

Figure 5.3 shows a DSC curve of a sample of coaxial PCL/PLA as spun, before hot pressing. On heating (from left to right), the first peak shows a combination of the

melting peak from the PCL and is combined with the glass transition peak from the PLA. The onset melting point of the PCL is 54 °C and the glass transition temperature (T_g) of the PLA is 56 °C. Since these are so similar, they cannot be distinguished between one another on the DSC curve. As a results of this the crystallinity of the PCL cannot be accurately measured using this method. Despite this, the DSC curves did not differentiate in this area. After this point, as the PCL is beyond its melting point, the following peaks are the properties of the PLA. The next peak is in the opposite direction, indicating an exothermic process, with and onset temperature of 94.0 °C and an area of 9.95 J g^{-1} - this is where the PLA chains are moving into a more energetically favourable state. The PLA is past its T_g, and the molecular chains have some freedom to move and adjust to form a crystal structure. The forming of crystalline structures at this point in the heating cycle is a typical characteristic on polyesters which have solidified rapidly. Following this peak is an endothermic peak with an area of 9.92 J g^{-1} and a peak temperature of 142.3 °C, where more energy is absorbed by the system. This is the melting point of the polymer. More energy is required to break apart any crystal structure that formed in the previous event and any crystals that were present before the DSC analysis. The heat values can be processed taking into account the mass ratio of the PLA to PCL and the literature value for a 100 % crystalline sample of PLA, 93.6 J g^{-1}[125] to find the percentage crystallinity of the sample. In this case of the electrospun sample before hot pressing, 0 % crystallinity is observed.

Although no crystallinity has been introduced into the polymers from the stretching and drying of the electrospinning process, an exothermic peak in-between the glass transition temperature and the melting point of the polymer indicates that the polymer undergoes cold crystallisation when heated.[127–133] This phenomenon is common in polyesters which have solidified rapidly, as this annealing gives the polymer molecules more time while in a mobile state above the T_g to arrange into a more energetically favourable structure. Variables were chosen in the method to promote this crystallinity, as more crystalline polymers exhibit greater tensile strength and elastic modulus.[128]

The process to analyse the as-spun sample was also followed for the hot pressed samples and the results are displayed in Table 5.1.

Table 5.1: Raw crystallinity results for the hot pressed samples

Cooling Rate (K min^{-1})	**Pressure (bar)**	**Temp. (°C)**	**Crysta. H_C (J g^{-1})**	**Melt. H_M (J g^{-1})**	**Melting Temp. T_p (°C)**		**Crysta. of PLA (%)**
					Peak 1	**Peak 2**	
10	1	70	9.39	-9.83	-	141.3	0.61
1	5	70	7.88	-9.65	-	142.2	2.47
5	10	70	6.59	-12.10	-	141.3	7.69
5	1	90	1.35	-18.87	132.0	140.3	24.44
10	5	90	2.81	-18.31	136.0	142.8	21.62
1	10	90	1.37	-19.26	135.7	143.3	24.95
1	1	110	0.00	-19.60	-	141.8	27.34
5	5	110	2.55	-18.19	-	141.2	21.81
10	10	110	0.00	-19.82	-	140.8	27.64

It was noticed that in the heat of melting for the PLA, two different peaks were present. The temperature values for these peaks have been included in the results table. These results show that when all the crystalline structure in the polymer is introduced in the DSC, or from the hot pressing only one peak is present. However, when the polymer samples have only crystallised partially during hot pressing, allowing for further crystallisation during the heating process of the DSC, two melting peaks are present, representing the two different stages of the crystallisation.

The heat of crystallization and melting must be corrected for the composite material, as there is also PCL present in the sample and the section of the DSC curve is only relevant for PLA. Considering a 0.75 fibre volume fraction, the results should be divided by 0.766, the fibre mass fraction, to find H_T. This is then compared to the melting enthalpy of the fully crystalline PLA from the literature 93.6 J g^{-1},[125] from which the percentage crystallinity can be calculated.

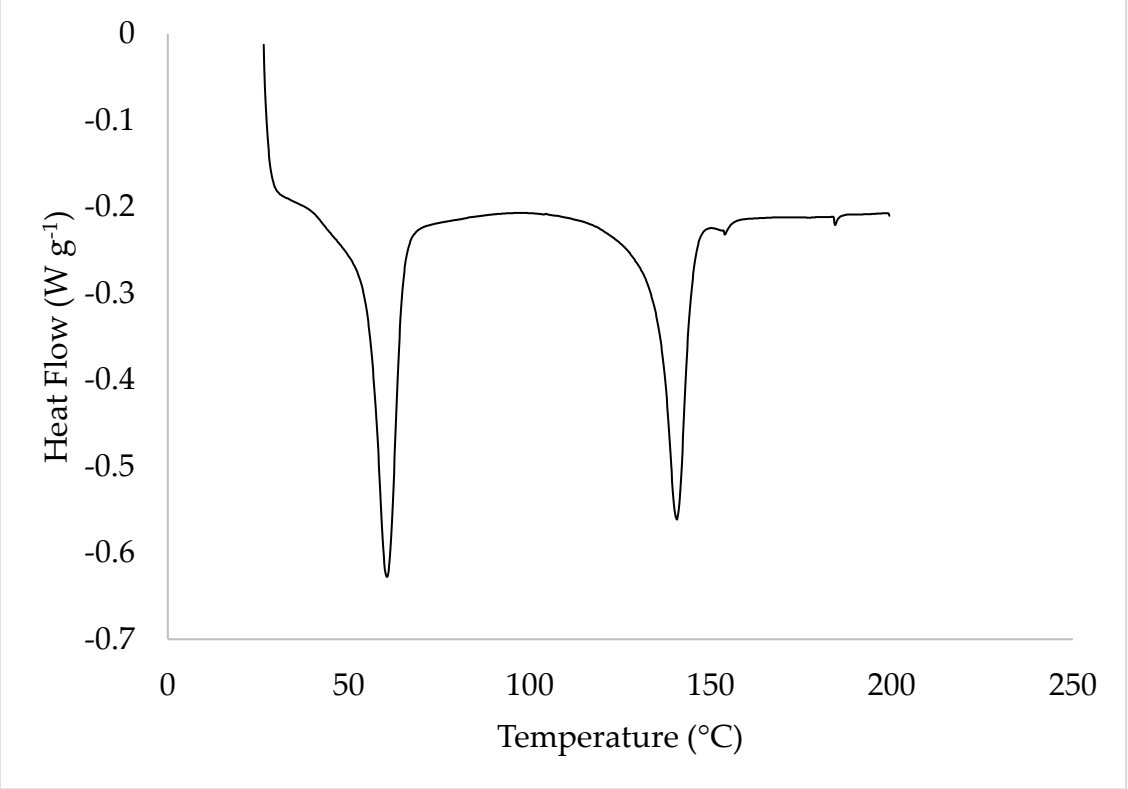

Figure 5.4: DSC curve for experiment 3, a composite pressed at 10 bar and 110 °C and cooled at 10 K/min, resulting in 27.64 % crystalline PLA.

Figure 5.4 shows another DSC curve for the most crystalline hot pressed sample. This sample was taken from a composite which was pressed at 10 bar and 110 °C, and cooled at 10 K min^{-1}, resulting in 27.64 % crystallinity. There is no heat of crystallisation peak between the T_g and the melting point, so it can be concluded that the sample could not be crystallised further by annealing.

It is clear from these results that the temperature to which the composite was heated while forming had the most significant effect on the crystal structure of the PLA fibres. The samples heated to 110 °C exhibited the most crystallinity, and the samples heated to 70 °C the least. The pressure also shows a slight trend with the higher pressure producing slightly more crystalline fibres. The cooling rate does not appear

to have any noticeable effect on the end result. A maximum crystallinity of 27.6 % was achieved during testing, and this is comparable to the results found in the literature, where up to 40 % crystallinity could be obtained by annealing PLA.[19,134]

These results can be explained by looking at the DSC curve for any of the less crystallised samples, or a raw sample of the coaxial electrospun fibres. The curves show that heat of crystallisation has an onset of 95 °C, so for the polymer to be annealed by the process, this temperature must be exceeded. The samples heated to 90 °C did not reach this threshold, however, so the polymer was able to partially crystallise.

The pressure would help to crystallise the polymer due to the mechanical deformation.[124] Although this effect was not pronounced in the results, some evidence of it can be seen. It was expected that a slower cooling rate of the polymer would give the crystals more time to form as they cooled, however, it appears that the range of cooling rates used did not affect the results as the crystallisation mechanism (cold crystallisation) is unaffected by the cooling.

5.3 Tensile Properties

It was expected that increasing the crystallinity of the polymers would increase the tensile strength and Young's Modulus of the composites.

Table 5.2: Experimental variables with crystallinity and average tensile testing results

Pressure (bar)	Temperature (°C)	Crystallinity (%)	Young's Modulus (MPa)	UTS (MPa)
1	70	0.61	1247	33.2
5	70	2.47	1154	32.3
10	70	7.69	1135	29.1
10	90	24.95	1313	27.7
1	90	24.44	1210	23.1
5	90	21.62	1281	22.9
1	110	27.34	1262	20.3
10	110	27.64	1166	18.8
5	110	21.81	1178	18.0

The results shown in Table 5.2 list the results in order of deceasing tensile strength. The trend shows that as the crystallinity of the polymer fibres increased, the ultimate tensile strength (UTS) decreased (Figure 5.5), however, there was no clear trend in the Young's modulus (Figure 5.6) as there was little change throughout the experiment.

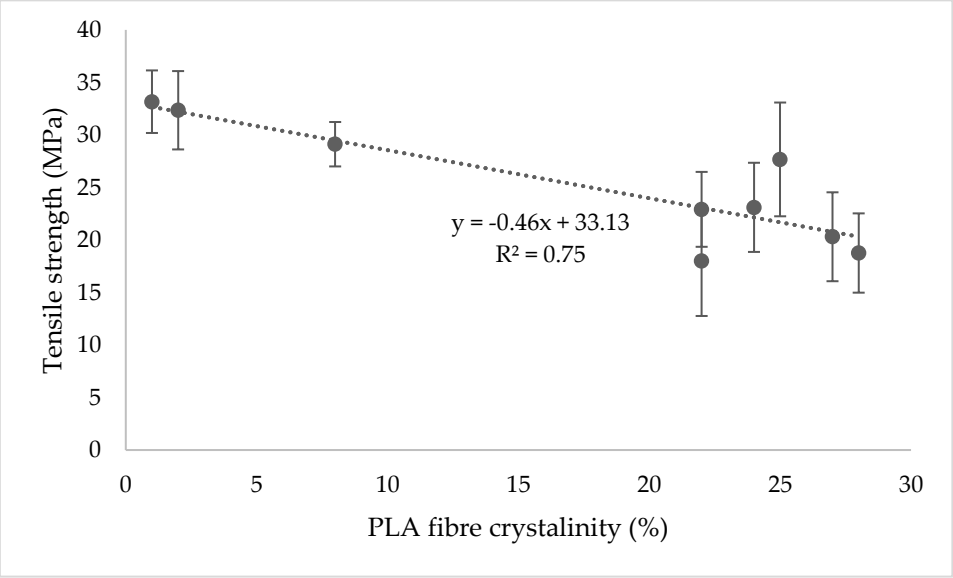

Figure 5.5: Effect of PLA fibre crystallinity on the tensile strength of the composites

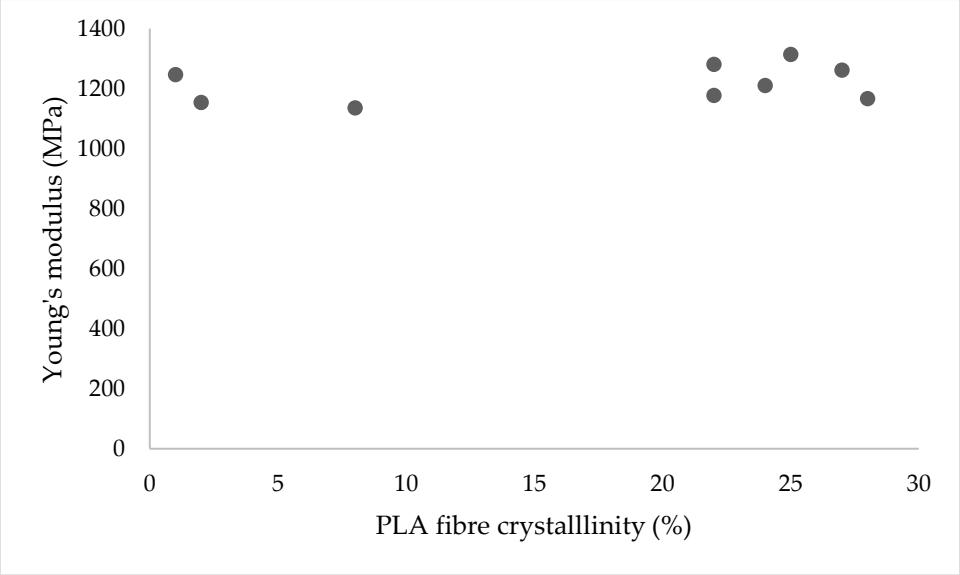

Figure 5.6: Effect of PLA fibre crystallinity on the Young's modulus of the composites

The trend of the results is clear in these two graphs. In Figure 5.5 the trendline displays an R squared value of 0.75, showing a moderate correlation. This was unexpected as an increase in the crystallinity of a polymer typically improves its tensile strength. In this case, the polymer is being heated beyond the T_g and being subjected to pressure, increases the crystallinity. However, it also leaves the fibres vulnerable to deformation. This deformation of the fibres decreases the homogeneity of the composite, and can introduce weakness and defects. In order to view this deformation of the fibres, the composites were immersed in liquid nitrogen and snapped perpendicular to the direction of the fibres. It is therefore considered that the advantages of forming the composite at higher temperature with regards to the crystallinity of the polymers are outweighed by the negatives of the deformation of the fibres from the heat and pressure. This resulted in a decrease in tensile strength as the temperature of the forming process increased (Figure 5.7). This graph displays an R squared value of 0.90, indicating a good correlation, higher than the correlation

against crystallinity. This show that the tensile strength is more affected by the temperature of the forming process rather than the crystallinity of the polymer fibres.

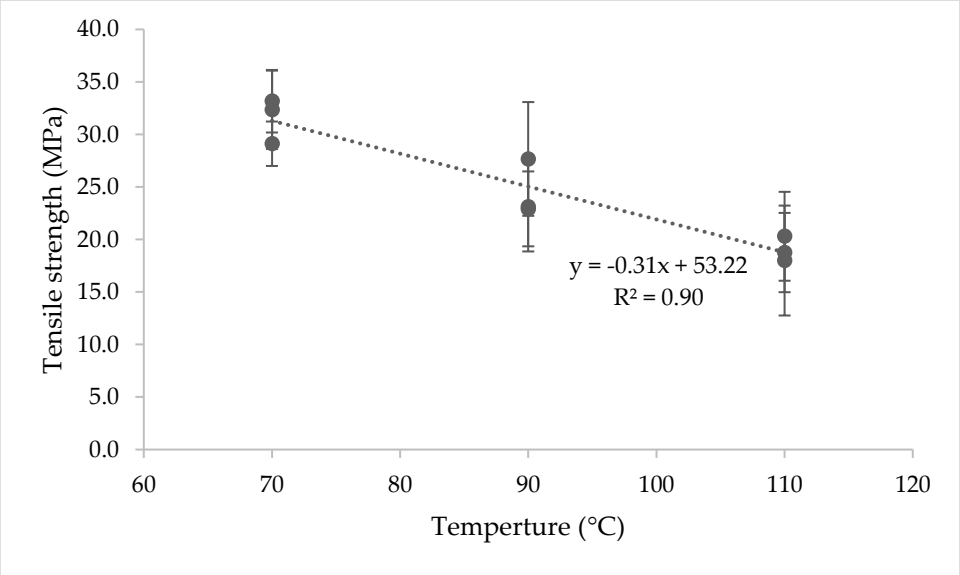

Figure 5.7: Effect of composite forming temperature on the tensile strength

5.4 Fibre Deformation

Deformation of the fibres within the composite in clearly visible in the images captured using SEM.

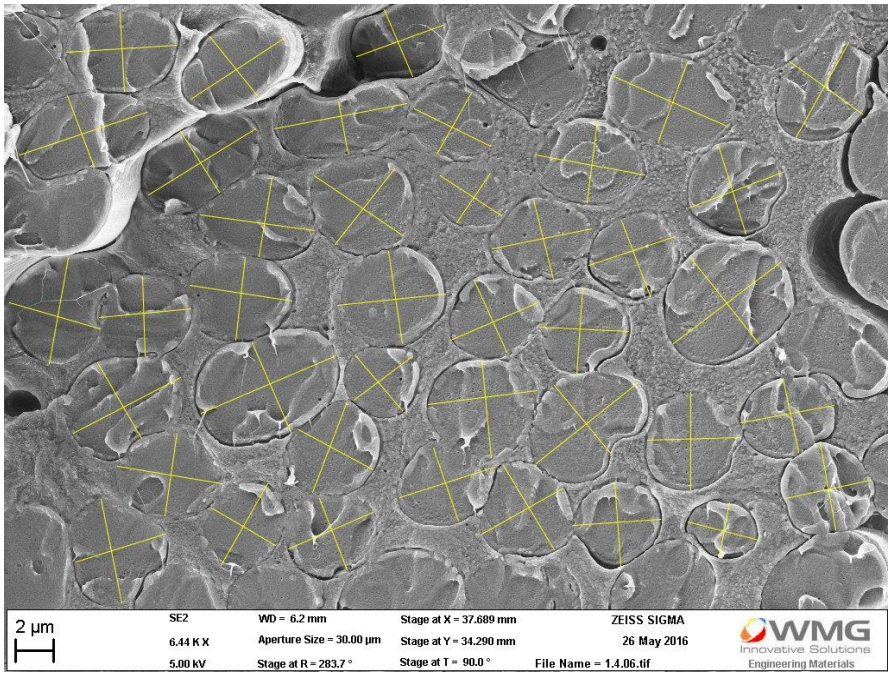

Figure 5.8: Cross-section of a composite pressed at 70 °C and 1 bar

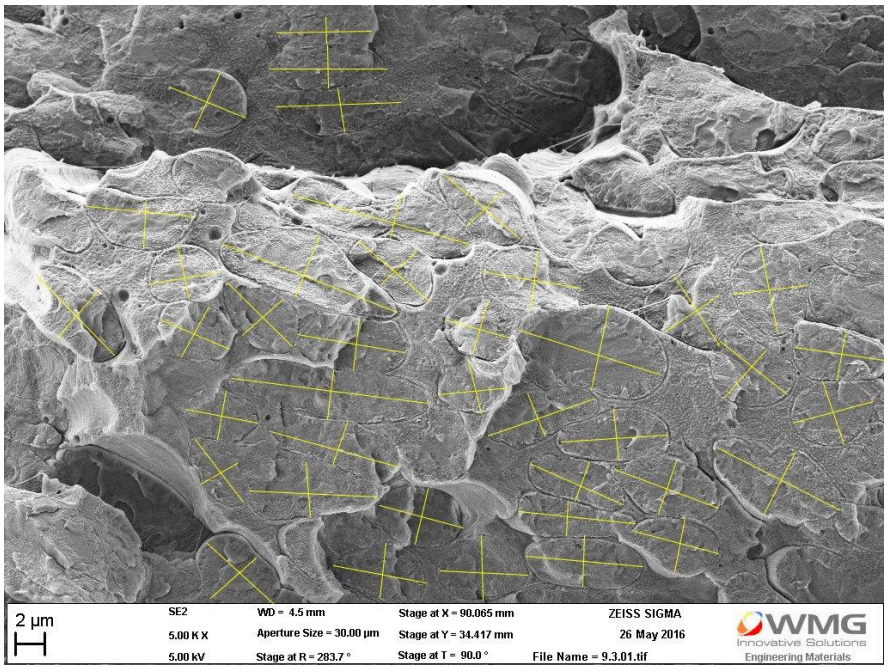

Figure 5.9: Cross-section of a composite pressed at 110 °C and 1 bar

In Figure 5.8 and Figure 5.9, yellow lines have been drawn to indicate the positions of the fibres and the measurements taken to calculate the deformation of the fibres by measuring the difference between the largest and shortest diameter of the fibres, henceforth this value with be referred to as the cross-section ratio. Although in

geometry, this measurement would be known as the "aspect ratio", this term will be avoided here to minimise confusion with the same term in composite materials which refers to ratio of the length and diameter of the reinforcing fibres.

Throughout the samples, the cross-section ratio of the fibres in the middle of the composite sheet remained mostly circular, and the fibres were increasingly deformed towards the sides of the composite. To provide a clear comparison between the different composites, the cross-section ratio measurements were taken from the sides of the composite. The average of these are in displayed in Table 5.3.

Table 5.3: Cross-section ratio of fibres compared to UTS of the composite

Pressure (bar)	**Temperature (°C)**	**Cross-Section Ratio**	**UTS (MPa)**
1	70	1.29	33.2
5	70	1.50	32.6
10	70	1.46	29.1
10	90	2.04	28.3
1	90	1.89	23.1
5	90	1.94	22.9
1	110	2.12	20.5
10	110	n/a	18.8
5	110	n/a	18.0

These results show that the increase in temperature and pressure show a general trend in the cross-section ratio of the fibres within the formed composite. The deformation of the fibres resulted in the weakening of the composite material, shown by the decrease in tensile strength as the fibre cross-section ratio increased.

There are no results for the cross-section ratio of the fibres in the composites produced with the highest temperature and pressures, because there were no clear fibres visible under the SEM in the region close to the sides of the composite.

5.5 Conclusions

The experimental data showed that the cooling rate of the procedure did not appear have any effect on the tensile properties, concurrent with the DSC results which showed no change in the crystalline structure of the PLA fibres during the cooling process. There was little change in the Young's modulus throughout the results, which no clear trend emerging. The temperature of the pressing process was the driving factor in the results, as temperature increased, there was an increase in crystallinity of the PLA fibres, and a decrease in the tensile strength. A similar, but lesser trend was apparent for the pressure. As the pressure increased, the crystallinity increased, and the tensile strength decreased. The composite pressed at lower temperature (70 °C) and lowest pressure (1 bar) exhibited the highest tensile strength, 33.2 MPa, while the lowest tensile strength was produced by the composite pressed at 110 °C at 10 and 5 bar which exhibited tensile strengths of 18.8 and 18.0 MPa, respectively.

It was expected that an increase in the crystallinity of the PLA fibres would increase the tensile strength and Young's modulus,[124] however, while the crystallinity could be encouraged during the forming process by increasing the temperature, this temperature increase is so far above the T_g of PLA that it is enough to cause

deformation of the fibres, even at low pressure. Although this did not appear to affect the fibres in the middle of the composite, the deformed fibres around the edges were enough to significantly reduce the tensile strength of the composite. This could mean that the effect of the deformation would be less apparent on a thicker composite if the size of the deformed section remained the same and was not relative to the thickness of the composite. Due to the speed of the electrospinning process, however, a significantly thicker composite would take a long time to produce unless the production method was scaled up.

It is possible that the polymers could be annealed at a high temperature to produce a crystalline structure in the PLA fibres, and in a separate step pressed into a composite at a lower temperature to lessen the deformation of the fibres. However, this adds an extra step to the process which is undesirable, and whichever way round these processes are conducted the high temperature step would disrupt the structure of the composite. If the high temperature step is conducted while in the co-axial fibre state, the flow of the matrix polymer would encourage an uneven distribution of matrix and fibres when pressed into a composite, lessening the advantage of the co-axial electrospinning process. If conducted after the composite has been formed, the heating without the presence of pressure would encourage delamination of the matrix from the fibres, reducing adhesion, resulting in uneven stress transfer across the composite and a weaker composite.

6 Coaxial and layering

6.1 Introduction

Coaxial electrospinning adds a degree of complexity into the simple process of electrospinning. While electrospinning can be conducted using a set-up of standard laboratory equipment with a high voltage power supply, coaxial electrospinning, on the other hand, requires a specialised nozzle to produce the fibres. These nozzles are not widely available, and often have to be custom made. In the context of creating fibre reinforced composites, coaxial electrospinning removes a step in the forming of the composites by providing the matrix material with the fibres, producing a fibre mat akin to pre-preg fibres used in industry. This experiment seeks to compare the tensile properties of the coaxial composite to that of composite formed without coaxial electrospinning. This composite was created by electrospinning the single polymer PLA reinforcing fibres, and combining with a sheet of PCL during the hot pressing. It was important to ensure that each of the materials were carefully measure before combining to ensure an accurate fibre volume ratio.

6.2 Electrospinning

The coaxial fibres were successfully electrospun using the same parameters used in the previous experiment in chapter 5, as these were discovered in chapter 4 to possess the highest tensile strength and a high Young's modulus compared with other fibre volume ratios. This was important to investigate how the single polymer

electrospun composite compared to the coaxial electrospun composite created using these conditions which where optimised for tensile strength and Young's modulus.

The PLA fibre mats, needed to be spun, aligned and characterised to ensure that they were comparable to the PLA fibre within the PCL sheath of the coaxial fibres. The diameter of the PLA fibres in the coaxial composite was measured from the cross section samples of the composite, which were produced by snapping the samples in liquid nitrogen. Over 250 fibres were measured using image processing software ImageJ, resulting in an average fibre diameter of 4.94 μm for the reinforcing PLA fibre diameter in the coaxial composites. The same was done for the single polymer PLA fibres electrospun using different concentrations of PLA; the results of these are displayed in Table 6.1.

Table 6.1: PLA fibre diameters from different methods of electrospinning

	Fibre Diameter (μm)
Coaxial PLA core	4.94
25 wt% PLA in THF	10.98
15 wt% PLA in THF:DMF (3:1)	0.76
20 wt% PLA in THF:DMF (3:1)	1.28
25 wt% PLA in THF:DMF (3:1)	2.81

The final diameter of the coaxial fibres was measured for cross-sections of the formed composite for accuracy, however, in some cases the diameter of the core fibre needs to be known before going through the pressing and breaking of the samples. An estimate of the core fibre diameter can be calculated by making some

assumptions about the geometric structure of the fibres, and measuring the diameter of the coaxial fibres under SEM, assuming the fibres are perfectly concentric as in Figure 6.1.

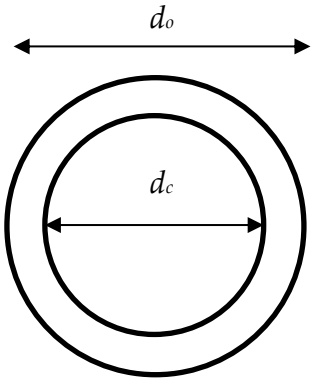

Figure 6.1: Assuming coaxial fibre geometry to calculate the diameter of the core fibre

With this assumption of the geometry, knowing the polymer volume ratio (fibre volume ratio in the composite) (f), and the total diameter of the coaxial fibre (d_o), the equation (6.1) can be derived to find the diameter of the core fibre (d_c).

$$d_c = d_o\sqrt{f} \tag{6.1}$$

Although the diameters of the PLA fibres electrospun are slightly smaller (2.81 μm) than the PLA fibres in the composite (4.94 μm), as discussed previously, due to the large size of the fibres, above 1 μm, this should not have a great effect on the tensile properties.[107] These single polymer fibres were successfully aligned using the maximum speed of the motor within the voltage range (Figure 6.2).

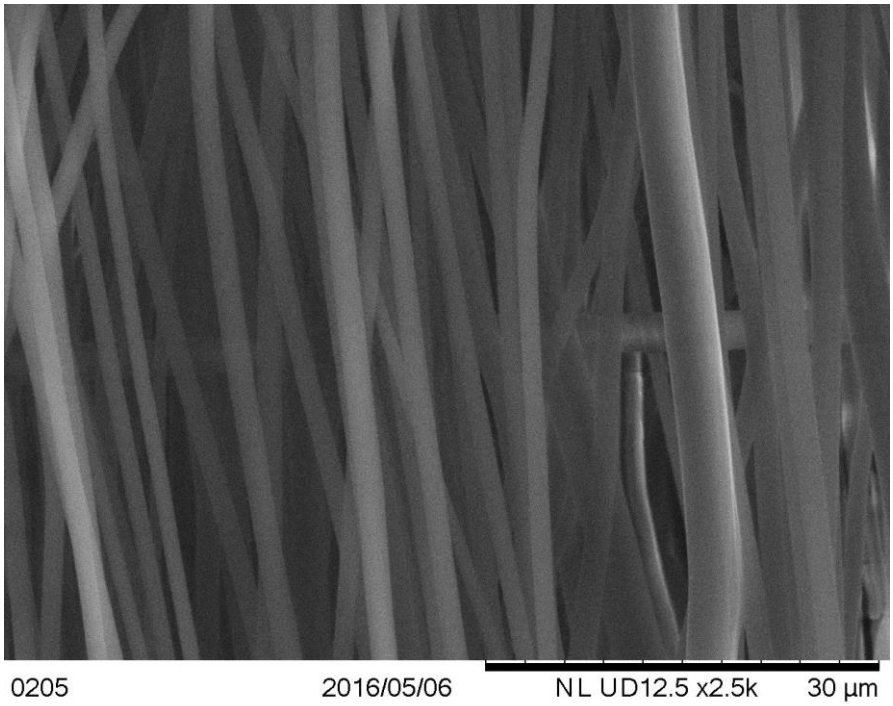

Figure 6.2: Aligned PLA fibres

6.3 Composite Forming

Composites from the coaxial electrospun fibres were successfully formed as in previous experimentation. The parameters chosen were those used to produce the composite with the highest tensile strength in the previous section, chapter 5. This was low temperature (70 °C) and pressure (1 bar) to minimise the deformation of the reinforcing PLA fibres.

The single polymer PLA fibre mats were formed into composite sheets by using a sheet of PCL to form the matrix around the fibres. Initial attempts to electrospin this sheet of PCL produced unsatisfactory results as the mass of the sheet could not be controlled sufficiently. As proved in previous experimentation in chapter 4, the volume ratio of fibres to matrix material can have a profound effect on the tensile properties of the composite. PCL sheets were attempted to be created from drying a

solution of PCL in a mould, however, the dried PCL was often uneven and difficult to remove from the substrate without breaking. A more successful method involved pressing granules of PCL in a hot press in an iterative process of cutting and weighing the sheet produced to obtain a sheet of the necessary dimensions and mass. The mass of the PCL sheet required was calculated by using the mass of the PLA fibre sheets to be pressed into the composite. Due to the varying weight of these fibre mats, each of the PCL sheets produced were made to match up with specific PLA fibre sheets. This was a very time consuming process, and restricted the composite forming to these specific sets of material sheets, rather than the coaxial process which allowed for more freedom of the layering of sheets to produce the composite. It was originally the intention to have the PCL films of the matrix cover each side of the electrospun PLA fibre mats evenly. Due to the light weight of the electrospun fibre mats, it proved difficult to create films of PCL thin enough to do this. Instead, only a thin film of PCL was included between two mats of PLA fibres. The mass and thickness of the sheets produced are listed in Table 6.2. These PLA fibre mats and PCL sheets were successfully pressed into composites in the same way as the composites produced from the coaxial electrospun fibres.

Table 6.2: Mass and thickness of polymer sheets used in creating composite material from single polymer electrospun PLA fibres

Total mass of PLA fibres (mg)	Total mass of PCL used (mg)	Average thickness of PCL sheet (μm)	Calculated fibre volume ratio
0.6391	0.1946	30.21	0.7505
0.6379	0.1986	30.84	0.7463
0.7119	0.2163	33.58	0.7509
0.7317	0.2248	34.90	0.7488

6.4 Tensile Properties

To increase the accuracy of the results in this final experimental section, a camera extensometer was use during tensile testing. The addition of the camera removes the effect of the deflection of the frame and grips of the testing rig, and the slipping of the sample, allowing for the use of tabbing to reduce breakage of the samples at the grips of the testing rig.

Tests were conducted to measure the effectiveness of different tabbing mediums to ensure it would not cause any inaccuracies in the data. Firstly, a stiff card reinforcing material was attached to the end of some sample using a Loctite super glue and a Bostik all-purpose adhesive, however due to the high solubility of the polymers used in the study, these adhesives partly dissolved the polymers causing weaknesses in the samples. Hot glue is often used as a tabbing adhesive, however, due to the low melting point of PCL (60 °C), this was not considered here as hot glue melts at higher temperatures than this. As adhesives were not successful, a series of tapes were tested. Scotch magic tap worked well, but did not provide much additional

strength to the ends of the composite strips. Gorilla branded cloth reinforced tape provided a lot of strength, but the thick adhesive layer did not hold under the sheer force of the tensile testing. The same was true for two Scotch banded industrial strength masking tapes. The best results were from an unbranded standard masking tape, which had a thin enough layer of adhesive not to sheer, and a good degree of thickness and roughness for grip on the surface. The composite samples in this study were successfully tabbed using this masking tape.

Figure 6.3: Samples tabbed with different grades of masking tape. Each square on the mat is 10 x 10 mm.

With the addition of the camera to measure the extension of the samples, positioned need to be marked on the samples of the camera to me

asure from. Initially this was done using a variety of marker pens, however, the little solvent present in these pens introduced a weak point in the composite sheet as the samples would break at the marks. Instead, stickers were used to mark these positions on the samples, which place no apparent detrimental effect on the integrity of the composite materials. However, these are not as stable as marks drawn onto the sample as they can move around or fall off as the sample stretches.

Tensile testing was conducted successfully, and an average of the test results are displayed in Figure 6.4.

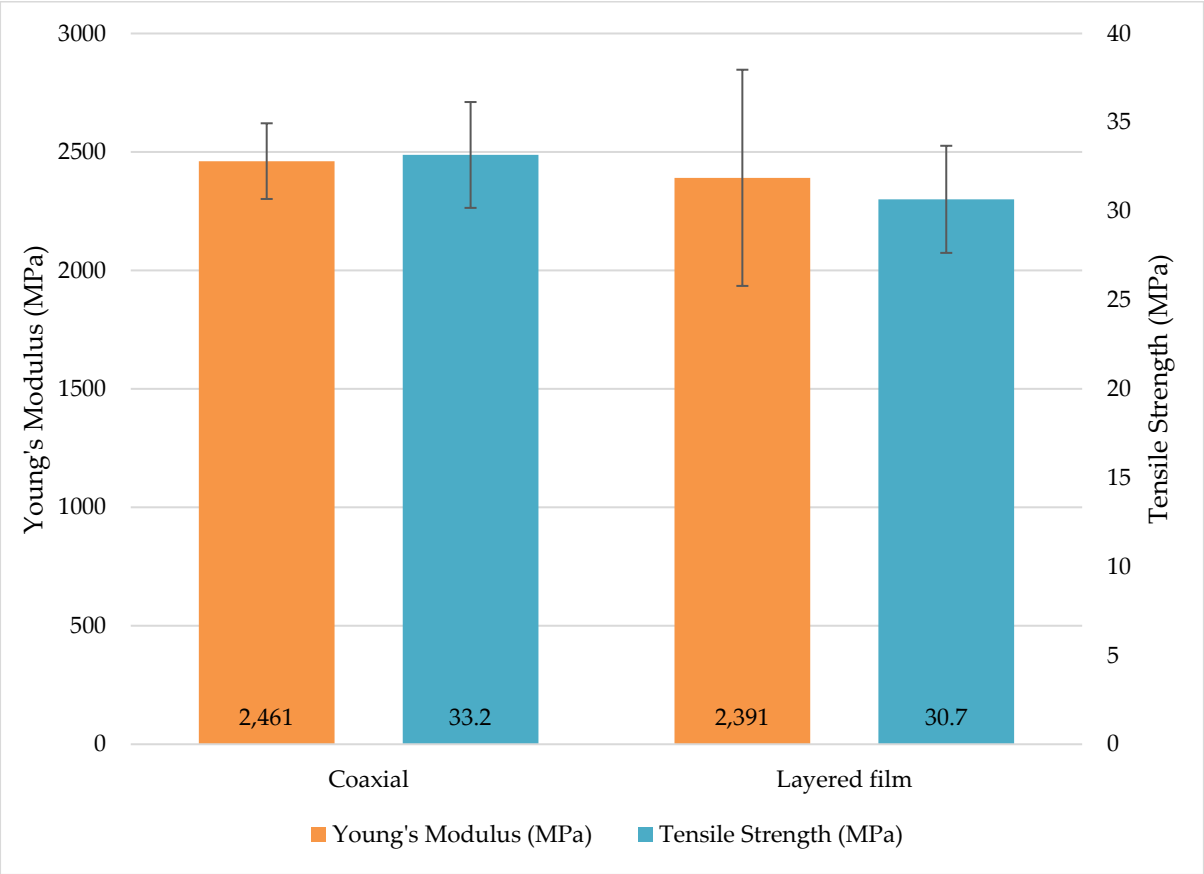

Figure 6.4: Comparison of tensile properties between the composite produced from coaxial electrospun fibres and a composite produced from electrospun PLA fibres and PCL sheet material

The average tensile strength and Young's modulus of the film layered composite is slightly lower than the coaxial composite, although, just within the experimental error of the results. There is a much larger error margin in the Young's Modulus of the layered film samples. This is due to the electrospun fibre mats being unevenly deposited on the collector drum resulting in the fibre mats being slightly thicker in the middle and thinner towards the sides. As the PCL matrix films were hot pressed to a comparatively even thickness, this resulted in an uneven fibre volume ratio

throughout the sample. This is consistent with the results shown in chapter 4, in which tensile strength varied little amongst higher volume fractions, whereas, the Young's modulus continued to increase.

6.5 Conclusions

This experiment showed that the coaxial electrospinning technique does result in an increase in tensile properties compared with electrospinning the reinforcing fibres separately from the matrix. Although the differences in the averages is small, within 10 %, the variation in the Young's modulus was significantly larger in the composite formed the layered films, which is undesirable for commercial applications. This was due to the differences in the thickness of the fibre sheets and the matrix film. The fibre sheets produced from electrospinning do not have an even thickness, as there are thicker towards the middle and thinner at the edges. By comparison, the matrix films were of even thickness from forming in the hot press. This created a slight variation in the fibre volume ratio of the composite formed with the PLA fibre mats and the PCL films. The thickness of the PLA fibre mats could be evened out with equipment to oscillate the collector perpendicular to the direction of the fibre collection. However, even with additional equipment, the electrospinning process can be unpredictable and is prone to these inaccuracies.

The drop in tensile strength will be for similar reasons as discussed in chapter 4 regarding fibre volume ratio, and the uneven distribution of matrix. Due to the matrix material all being in the same place, before the forming of the composite,

more penetration of the molten matrix around the reinforcing fibres is required. This is unlike the coaxial fibre, where the matrix material is already in place around the fibres, and does not need to pass around them. An increase in the pressing temperature and pressure would help the matrix material penetrate more through the fibres, however, this results in the deformation of the PLA fibres as discovered in chapter 5.

Aside from the end results of the tensile testing, the forming of the layered film composite was very time consuming. Due to the nature of the electrospinning process, the thickness and mass of the mat produced is not always consistent, so films of the matrix material must be made up specifically for the fibre mats produced, increasing processing time. The coaxial electrospinning equipment might be more difficult to produce compared to a single polymer set-up, but once the capability has been established, the fibre volume ratio can be controlled with ease through the volume flow rates of the polymer solutions.

Overall, the coaxial electrospun fibres produced composite with higher tensile strength, higher Young's modulus, and with greater consistency. The coaxial fibre method proved a lot easier to control, and produced faster results. The ease of producing composites from pre-preg fibre sheets has shown its worth in industry, and similar benefits are seen here with the coaxial fibres, with the ease of manufacture from fibre sheets to composites, and the prepositioned matrix material.

7 Conclusions

The overall objectives of this work were accomplished. A fibre reinforced composite was successfully produced using coaxial electrospinning. The product was comprised entirely of thermoplastic polymers, poly(lactic acid) (PLA) and polycaprolactone (PCL). These two polymers are biodegradable and biocompatible, allowing them to be used within the body as structural reinforcement. These composites were improved by finding processing conditions which produced higher tensile strength and modulus. These conditions were a 0.73 fibre volume ratio, and consolidating the composite at 70 °C and at 1 bar of pressure. The fibre volume ratio proved to be reliably controlled by the coaxial electrospinning process, and the lower pressure requirement makes the composite suitable for vacuum forming. The composite produced in this way proved to have increased tensile strength and less variation in Young's modulus compared to a composite produced without coaxial electrospinning.

Biomedical applications such as tendon reinforcement were thought to be a potential application for the composites produced in this research. In section 1.4, it was stated that tendons have a wide range of tensile properties throughout the body with Young's modulus from 0.6 – 2 GPa , ultimate tensile strength from 4 – 100 MPa, and elongation at break from 3 – 10 %. The finalised composite produced in this research exhibited an average Young's Modulus of 2.5 GPa, ultimate tensile strength of 33.2 MPa, and elongation at break of 3.8 %. The ultimate tensile strength and

elongation at break fit within the range, but applications would need to be chosen carefully to ensure adequate strength. The Young's Modulus of the composite exceeds the range, which would allow the composite to take the strain off the biological tendon, however, if this was needed to be lower, the fibre volume fraction of the composite could be reduced if the subsequent reduction of tensile strength would not be an issue.

This work could be built upon to further enhance and tailor the properties of the composites produced. Minor changes could be made to the process to improve consistency and reliability, such as improving on the coaxial concentric structure of the fibres or the uniform thickness of the fibre mats produced by electrospinning. Major changes could alter the chemical structure of the composite, increasing fibre-matrix adhesion, or to introduce more functionality into the composite. These changes are discussed further in section 7.4.

The following sub-chapters summarise the conclusions made in the previous chapters 4, 5, and 6.

7.1 Fibre volume ratio

The experimentation in this section concluded, firstly, that coaxial fibres could be electrospun using the two polymers chosen, and these coaxial fibre mats could be successfully formed into a fibre reinforced polymer material. Secondly, NMR analysis showed that variation of the solution flow rates could accurately control the

fibre volume of the composite produced. Finally, the tensile testing revealed results echoing theoretical calculations at medium volume fractions, and deviation from this at higher volume fractions as predicted in the literature.

The results showed that the interaction between the fibres and matrix started to decrease after a fibre volume ratio of 0.66, however, tensile properties continued to increase until a ratio of 0.73. This was because although the interactions were weaker overall, the addition of fibres was continuing to strengthen and stiffen the composite. Past a ratio of 0.77, tensile strength began to drop, and the Young's modulus began to level off. It was also noticed at this point that the elongation at break dropped sharply as there was no longer any plastic deformation in the samples. Due to these reasons, the 0.73 fibre volume ratio composite was considered to be the maximum that this process could produce. Thermoplastic, such as the polymers used here, are higher viscosity when molten than uncured thermosets, and typically results in composites with lower fibre volume ratios. Even considering this, the thermoplastic composite produced here from coaxial electrospinning is at least 0.03 higher than that found for other thermoset polymer matrix composites which are usually from 0.60 – 0.70. The same conditions to produce the 0.73 ratio composite were used in the remaining chapters.

7.2 Composite forming variation

The composite forming process in the previous experiment was designed with arbitrary values which were able to melt the sheath polymer of the coaxial fibres and

be successful at pressing them into a composite material. This experiment seeks to improve on this by controlling and varying the parameters during the composite pressing to investigate how they affect the tensile properties of the composite.

The parameters varied were the temperature, pressure, and cooling rate. The cooling did not appear to have any effect on the composites, however, the temperature and pressure variations did affect the crystalline structure and geometry of the reinforcing fibres, and the tensile properties of the composite. The change in temperature had the greatest effect on the results, with the pressure trailing. As the temperature of the forming process increased, the crystalline structure of the PLA fibres increased as expected due to the annealing effect resulting in crystal growth. Although this was expected to increase the tensile strength and Young's modulus of the composite, this also caused increasing deformation of the reinforcing PLA fibres around the outer edges of the composite. The overall result of this was a decrease in tensile strength of the composite, from its maximum of 33.2 MPa at 70 °C and 1 bar, to 18.0 MPa at 110 °C at 5 bar. There was little change in the Young's modulus throughout the experimentation.

Since lower pressure forming resulting in a composite with higher tensile strength due to less deformation of the fibres, vacuum forming of the composite could be considered. This allows for three-dimensional shapes to be moulded out of the electrospun fibre mats without the need for expensive moulds to be created for compression moulding.

7.3 Coaxial and layering

This experimentation sought to investigate a comparison between the composite produced by coaxial electrospinning, and a composite produced by single polymer electrospinning and layering up of the matrix material during the pressing process.

The experiment showed that control of the fibre volume ratio in the composite made from the single polymer electrospinning was difficult and time consuming compared with the method used for the coaxial electrospun fibres. Despite simplifying the process by removing the aspect of coaxial electrospinning, the addition of this extra step to control the fibre volume ratio added another degree of complexity to the process. Even by controlling the average fibre volume ratio across the composite sheet, the variation of thickness of the electrospun fibre mat created an unevenly distribute material once pressed, with higher matrix content towards the sides of the sheet where the fibre mat was thinnest, and higher fibre content in the middle, where it was thickest. This caused more variation in the tensile testing results, and a greater error margin in the Young's modulus.

The single polymer electrospun composite exhibited lower tensile strength (30.7 MPa) than the composite created by coaxial electrospinning (33.2 MPa). This was due to the need for the thermoplastic matrix to penetrate through the mat of the fibres to adequately distribute the load across the fibres. However, the molten thermoplastic is too viscous, and cannot distribute itself adequately through the fibre mat. The coaxial fibre's advantage here is that the matrix material is already in place

and only needs to bind together during the pressing rather than pass between the fibres in the mat.

7.4 Recommendations for Future Work

If the project were to continue the tensile properties of the composite could be further improve upon, and to the composite could be reworked for different end uses.

Thinner fibres

As mentioned within the report (chapter 4), although controlled, the diameter of the reinforcing fibres was not investigated due to equipment limitations, to reduce the effects of fibre variation throughout the experiments. By using fibres with a large diameter, the experiments were less affected by small changes in the fibre dimensions caused due to variation in the other electrospinning parameters, or even the environment. Thinner fibres would increase the alignment of the polymer chains within the fibre and reduce the number of defects in the structure of the fibres. This would increase the tensile strength and the Young's modulus of the fibre, and therefore the composite. Thinner fibres could be created by altering the polymer solutions. A less volatile solvent, such as DMF, would increase the time taken for the fibres to solidify, and allow them to stretch more, reducing the diameter. This, however, is limited by the solvents available for the polymers being used. An alternative is to use polymer with a high molecular mass. Longer polymer chains result in a more viscous solution, so the concentration of the solutions can be

decreased. As with using less volatile solvent, this slows down the solidification of the fibres. Using higher molecular weight polymers would also increase the tensile properties of the composite without any changes to the dimensions of the fibres, since as molecular weight increases as does the stiffness and strength of the polymer.

Fibre-matrix adhesion

The adhesion between the matrix and the fibres is an important aspect of the composite structure as it greatly affects how the stress is distributed.[135–137] Increased adhesion typically results in increased tensile strength, however, sometimes excessive bond strength can result in a brittle material.[135] It is typical within the composites industry to use additives in the form of surface treatment and coatings to increase the adhesion between the two materials to improve the composite.[135] The fibre-matrix adhesion could be investigated in the coaxial electrospun composite to improve further improve the tensile properties. Although the solutions being used contain the same solvent, the polymers themselves are immiscible.[122] While this results in smooth fibres and definition between the core and shell of the coaxial fibre, adhesion could be increased by introducing some diffusion between the polymers. This diffusion could be promoted between the polymers during the electrospinning process with the addition of a small concentration of a block co-polymer blend of poly(ethylene glycol) and poly(propylene glycol),[138] or the isocyanate, lysine triisocyanate.[139] This could introduce a degree of chain entanglement and mechanical locking between the polymers, increasing adhesion and tensile strength.

Hollow fibre

The prospect of adding an additional layer of polymer to the coaxial fibre structure can allow for the production of a hollow fibre composite. This would be done by electrospinning the core and outer sheath with the matrix material and the intermediate layer with the reinforcing fibre material. A hollow fibre composite increases the surface are of the contact between the fibre and the matrix, allowing for increased adhesion without additives.

The channel in the centre of the fibre could be used to contain a repair medium to allow for self-healing of the composite,[140] or as a drug delivery system.[71]

Drug delivery

The electrospinning process used to produce the composites is extremely versatile, and as shown in the literature review, various additives can be included in the solutions to affect the final product. Drugs and medicine can be added into the fibres (section 2.5.4), or into another layer in the structure which will slowly diffuse though the polymers into the body. Combining this with the composite could produce material for reinforcement and drug delivery to increase healing time, or to reduce pain and inflammation.

8 References

1. *BS ISO 8672. Air quality. Determination of the number concentration of airborne inorganic fibres by phase contrast optical microscopy. Membrane filter method*. **44,** (BSI, 1993).
2. Hull, D. & Clyne, T. W. *An Introduction to Composite Materials*. (Cambridge University Press, 1996).
3. Barbero, E. J. *Introduction to Composite Materials Design*. (CRC Press, 2010).
4. Mohanty, A. K., Misra, M. & Drzal, L. T. Sustainable Bio-Composites from Renewable Resources: Opportunities and Challenges in the Green Materials World. *J. Polym. Environ.* **10,** 19–26 (2002).
5. Lee, K. *et al.* Stress-strain behavior of the electrospun thermoplastic polyurethane elastomer fiber mats. *Macromol. Res.* **13,** 441–445 (2005).
6. Shin, Y. M., Hohman, M. M., Brenner, M. P. & Rutledge, G. C. Experimental characterization of electrospinning: the electrically forced jet and instabilities. *Polymer (Guildf).* **42,** 09955–09967 (2001).
7. Fridrikh, S., Yu, J., Brenner, M. & Rutledge, G. Controlling the Fiber Diameter during Electrospinning. *Phys. Rev. Lett.* **90,** 144502 (2003).
8. Huang, Z.-M., Zhang, Y.-Z., Kotaki, M. & Ramakrishna, S. A review on polymer nanofibers by electrospinning and their applications in nanocomposites. *Compos. Sci. Technol.* **63,** 2223–2253 (2003).
9. Sundaray, B. *et al.* Electrospinning of continuous aligned polymer fibers. *Appl. Phys. Lett.* **84,** 1222 (2004).
10. Fennessey, S. F. & Farris, R. J. Fabrication of aligned and molecularly oriented electrospun polyacrylonitrile nanofibers and the mechanical behavior of their twisted yarns. *Polymer (Guildf).* **45,** 4217–4225 (2004).
11. Gatford, J. A diagram of the electrospinning process showing the onset of instability. *New Zeal. Inst. Plant Food Res. Ltd* (2008).
12. Xu, H. *et al.* Host Response to Human Acellular Dermal Matrix Transplantation in a Primate Model of Abdominal Wall Repair. *Tissue Eng. Part A* **14,** 2009–2019 (2008).
13. Smart, N., Bryan, N., Hunt, J. & Daniels, I. Porcine dermis implants in soft-tissue reconstruction: current status. *Biol. Targets Ther.* **8,** 83 (2014).
14. Nilsson, A. *et al.* Results from a degradable TMC joint Spacer (Artelon) compared with tendon arthroplasty. *J. Hand Surg. Am.* **30,** 380–389 (2005).
15. Maganaris, C. N. & Narici, M. V. in *Tendon Inj.* 14–21 (Springer-Verlag, 2005). doi:10.1007/1-84628-050-8_2
16. Louis-Ugbo, J., Leeson, B. & Hutton, W. C. Tensile properties of fresh human calcaneal (achilles) tendons. *Clin. Anat.* **17,** 30–35 (2004).
17. Maganaris, C. N. & Paul, J. P. Tensile properties of the in vivo human

gastrocnemius tendon. *J. Biomech.* **35,** 1639–1646 (2002).

18. Maganaris, C. N. & Paul, J. P. In vivo human tendon mechanical properties. *J. Physiol.* **521 Pt 1,** 307–13 (1999).
19. Tabi, T., Sajo, I. E., Szabo, F., Luyt, A. S. & Kovacs, J. G. Crystalline structure of annealed polylactic acid and its relation to processing. *Express Polym. Lett.* **4,** 659–668 (2010).
20. Ramakrishna, S., Fujihara, K., Teo, W.-E., Lim, T.-C. & Ma, Z. *An Introduction to Electrospinning and Nanofibers*. (World Scientific Publishing Co. Pte. Ltd., 2005).
21. Boys, C. V. On the Production, Properties, and some suggested Uses of the Finest Threads. *Proc. Phys. Soc. London* **9,** 8–19 (1887).
22. Cooley, J. F. Improved Methods of and Apparatus for Electrically Separating the Relatively Volatile Liquid Component from the Component of Relatively Fixed Substances of Composite Fluids. (19 May 1900). Patent GB190006385
23. Cooley, J. F. Apparatus for Electrically Dispersing Fluids. (4 February 1902). Patent US692,631
24. Morton, W. J. Method of dispersing fluids. (29 July 1902). Patent US0705691
25. Zeleny, J. The Discharge of Electricity from Pointed Conductors Differing in Size. *Phys. Rev. (Series I)* **25,** 305–333 (1907).
26. Zeleny, J. The Electrical Discharge from Liquid Points, and a Hydrostatic Method of Measuring the Electric Intensity at Their Surfaces. *Phys. Rev.* **3,** 69–91 (1914).
27. Zeleny, J. The Influence of Humidity upon the Electrical Discharge from Points in Air. *Phys. Rev. (Series I)* **26,** 448–453 (1908).
28. Zeleny, J. Instability of Electrified Liquid Surfaces. *Phys. Rev.* **10,** 1–6 (1917).
29. Zeleny., J. Electrical Discharges from Pointed Conductors. *Phys. Rev.* **16,** 102–125 (1920).
30. Tucker, N., Stanger, J. J., Staiger, M. P. & Hofman, K. The History of the Science and Technology of Electrospinning from 1600 to 1995. in *Int. Istanbul Text. Congr.* (2013).
31. Formhals, A. Process and Apparatus for Preparing Artificial Threads. (2 October 1934). Patent US1,975,504
32. Formhals, A. Artificial Fiber Construction. (22 February 1938). Patent US2,109,333
33. Formhals, A. Method and Apparatus for the Production of Fibers. (10 May 1938). Patent US2,116,942
34. Formhals, A. Method and Apparatus for the Production of Fibers. (19 July 1938). Patent US2,123,992
35. Formhals, A. Method and Apparatus for Spinning. (6 June 1939). Patent US2,160,962
36. Formhals, A. Method of Producing Artificial Fibers. (16 May 1939). Patent

US2,158,415

37. Formhals, A. Artificial Thread and Method of Producing Same. (16 January 1940). Patent US2,187,306

38. Formhals, A. Production of Artificial Fibers from Fiber Forming Liquids. (29 June 1943). Patent US2,323,025

39. Formhals, A. Method and Apparatus for Spinning. (30 May 1944). Patent US2,349,950

40. Taylor, G. Disintegration of Water Drops in an Electric Field. *Proc. R. Soc. A Math. Phys. Eng. Sci.* **280,** 383–397 (1964).

41. Lamberts, R. Photograph of a meniscus of Polyvinyl Alcohol in aqueous solution showing a fibre drawn from a Taylor Cone by the process of electrospinning. *New Zeal. Inst. Plant Food Res. Ltd* (2008).

42. Doshi, J. & Reneker, D. H. Electrospinning process and applications of electrospun fibers. *J. Electrostat.* **35,** 151–160 (1995).

43. Hu, C. *et al.* Long-term drug release from electrospun fibers for in vivo inflammation prevention in the prevention of peritendinous adhesions. *Acta Biomater.* **9,** 7381–8 (2013).

44. Khil, M., Cha, D., Kim, H.-Y., Kim, I. & Bhattarai, N. Electrospun nanofibrous polyurethane membrane as wound dressing. *J. Biomed. Mater. Res. B. Appl. Biomater.* **67,** 675–9 (2003).

45. Maleki, H., Gharehaghaji, a. a. & Dijkstra, P. J. A novel honey-based nanofibrous scaffold for wound dressing application. *J. Appl. Polym. Sci.* **127,** 4086–4092 (2013).

46. Zahedi, P., Rezaeian, I., Ranaei-Siadat, S.-O., Jafari, S.-H. & Supaphol, P. A review on wound dressings with an emphasis on electrospun nanofibrous polymeric bandages. *Polym. Adv. Technol.* n/a-n/a (2009). doi:10.1002/pat.1625

47. Yoshimoto, H., Shin, Y. M., Terai, H. & Vacanti, J. P. A biodegradable nanofiber scaffold by electrospinning and its potential for bone tissue engineering. *Biomaterials* **24,** 2077–2082 (2003).

48. Bose, S., Roy, M. & Bandyopadhyay, A. Recent advances in bone tissue engineering scaffolds. *Trends Biotechnol.* **30,** 546–54 (2012).

49. Ghasemi, M., Shahgaldi, S., Ismail, M., Yaakob, Z. & Daud, W. R. W. New generation of carbon nanocomposite proton exchange membranes in microbial fuel cell systems. *Chem. Eng. J.* **184,** 82–89 (2012).

50. Hwang, T. H., Lee, Y. M., Kong, B.-S., Seo, J.-S. & Choi, J. W. Electrospun core-shell fibers for robust silicon nanoparticle-based lithium ion battery anodes. *Nano Lett.* **12,** 802–7 (2012).

51. Coles, S. R. *et al.* A design of experiments (DoE) approach to material properties optimization of electrospun nanofibers. *J. Appl. Polym. Sci.* **117,** 2251–2257 (2010).

52. Coles, S. R. & Wooldridge, A. in *Electrospinning Princ. Pract. Possibilities* (Mitchell, G. R.) 57–70 (The Royal Society of Chemistry, 2015). doi:10.1039/9781849735575-00057

53. Eda, G. & Shivkumar, S. Bead-to-fiber transition in electrospun polystyrene. *J. Appl. Polym. Sci.* **106,** 475–487 (2007).

54. Yang, Q. *et al.* Influence of solvents on the formation of ultrathin uniform poly(vinyl pyrrolidone) nanofibers with electrospinning. *J. Polym. Sci. Part B Polym. Phys.* **42,** 3721–3726 (2004).

55. Rayleigh, J. W. S. B. in *Sci. Pap. 1887-1892* 585–593 (University Press, 1902).

56. Druesedow, C. J., Batur, C., Cakmak, M. & Yalcin, B. Pressure control system for electrospinning process. *Polym. Eng. Sci.* **50,** 800–810 (2010).

57. Casper, C. L., Stephens, J. S., Tassi, N. G., Chase, D. B. & Rabolt, J. F. Controlling Surface Morphology of Electrospun Polystyrene Fibers: Effect of Humidity and Molecular Weight in the Electrospinning Process. *Macromolecules* **37,** 573–578 (2004).

58. Huang, L., Bui, N.-N., Manickam, S. S. & McCutcheon, J. R. Controlling electrospun nanofiber morphology and mechanical properties using humidity. *J. Polym. Sci. Part B Polym. Phys.* **49,** 1734–1744 (2011).

59. Sun, D., Chang, C., Li, S. & Lin, L. Near-field electrospinning. *Nano Lett.* **6,** 839–42 (2006).

60. Xin, Y. & Reneker, D. H. Hierarchical polystyrene patterns produced by electrospinning. *Polymer (Guildf).* **53,** 4254–4261 (2012).

61. Brown, T. D., Dalton, P. D. & Hutmacher, D. W. Direct writing by way of melt electrospinning. *Adv. Mater.* **23,** 5651–7 (2011).

62. Han, D. & Steckl, A. J. Superhydrophobic and oleophobic fibers by coaxial electrospinning. *Langmuir* **25,** 9454–62 (2009).

63. Sun, Z., Zussman, E., Yarin, A. L., Wendorff, J. H. & Greiner, A. Compound Core-Shell Polymer Nanofibers by Co-Electrospinning. *Adv. Mater.* **15,** 1929–1932 (2003).

64. Bazilevsky, A. V, Yarin, A. L. & Megaridis, C. M. Co-electrospinning of core-shell fibers using a single-nozzle technique. *Langmuir* **23,** 2311–4 (2007).

65. Hu, Q. Rubber composite fibers containing silver nanoparticles prepared by electrospinning and in-situ chemical crosslinking. *Express Polym. Lett.* **6,** 258–265 (2012).

66. Chen, S. *et al.* Effect of Different Bicomponent Electrospinning Techniques on the Formation of Polymeric Nanosprings. *Macromol. Mater. Eng.* **294,** 781–786 (2009).

67. Zhao, Y., Cao, X. & Jiang, L. Bio-mimic multichannel microtubes by a facile method. *J. Am. Chem. Soc.* **129,** 764–5 (2007).

68. Grojean, R. E., Sousa, J. a & Henry, M. C. Utilization of solar radiation by polar animals: an optical model for pelts. *Appl. Opt.* **19,** 339–46 (1980).

69. Lallave, M. *et al.* Filled and Hollow Carbon Nanofibers by Coaxial Electrospinning of Alcell Lignin without Binder Polymers. *Adv. Mater.* **19,** 4292–4296 (2007).

70. Liu, W., Ni, C., Chase, D. B. & Rabolt, J. F. Preparation of Multilayer Biodegradable Nanofibers by Triaxial Electrospinning. *ACS Macro Lett.* **2,** 466–468 (2013).

71. Han, D. & Steckl, A. J. Triaxial electrospun nanofiber membranes for controlled dual release of functional molecules. *ACS Appl. Mater. Interfaces* **5,** 8241–5 (2013).

72. Jirsak, O. *et al.* A method of nanofibres production from a polymer solution using electrostatic spinning and a device for carrying out the method. (17 March 2005). Patent WO/2005/024101

73. Yan, X. *et al.* High-Throughput Needleless Electrospinning of Core-Sheath Fibers. in *Fiber Soc.* (2012).

74. Liu, Y. & He, J.-H. Bubble Electrospinning for Mass Production of Nanofibers. *Int. J. Nonlinear Sci. Numer. Simul.* **8,** 393–396 (2007).

75. Kong, C. S., Yoo, W. S., Lee, K. Y. & Kim, H. S. Nanofiber deposition by electroblowing of PVA (polyvinyl alcohol). *J. Mater. Sci.* **44,** 1107–1112 (2009).

76. Um, I. C., Fang, D., Hsiao, B. S., Okamoto, A. & Chu, B. Electro-spinning and electro-blowing of hyaluronic acid. *Biomacromolecules* **5,** 1428–36 (2004).

77. Forward, K. M., Flores, A. & Rutledge, G. C. Coaxial-Free Surface Electrospinning. in *Fiber Soc.* (2012).

78. Griffith, A. A. The Phenomena of Rupture and Flow in Solids. *Philos. Trans. R. Soc. London. Ser. A, Contain. Pap. a Math. or Phys. Character* **221,** 163–198 (1921).

79. De Rosa, C. & Auriemma, F. *Crystals and crystallinity in polymers : diffraction analysis of ordered and disordered crystals*.

80. Takano, M. & Nielsen, L. E. Effects of orientation and chemical structure on the strength properties of some polymers. *Polym. Eng. Sci.* **17,** 229–233 (1977).

81. Elmar Witten, Thomas Kraus & Michael Kühnel. *Composites Market Report 2015*. (2015). at <http://www.eucia.eu/userfiles/files/Composites_Market Report_2015.pdf>

82. Zussman, E. *et al.* Mechanical and structural characterization of electrospun PAN-derived carbon nanofibers. *Carbon N. Y.* **43,** 2175–2185 (2005).

83. Zhang, L., Aboagye, A., Kelkar, A., Lai, C. & Fong, H. A review: carbon nanofibers from electrospun polyacrylonitrile and their applications. *J. Mater. Sci.* **49,** 463–480 (2014).

84. Wu, H. *et al.* Electrospun metal nanofiber webs as high-performance transparent electrode. *Nano Lett.* **10,** 4242–8 (2010).

85. Bergshoef, M. M. & Vancso, G. J. Transparent Nanocomposites with Ultrathin, Electrospun Nylon-4,6 Fiber Reinforcement. *Adv. Mater.* **11,** 1362–1365 (1999).

86. Kim, J. & Reneker, D. H. Mechanical properties of composites using ultrafine electrospun fibers. *Polym. Compos.* **20,** 124–131 (1999).

87. Li, G. *et al.* Inhomogeneous toughening of carbon fiber/epoxy composite using electrospun polysulfone nanofibrous membranes by in situ phase separation.

Compos. Sci. Technol. **68,** 987–994 (2008).

88. Zhang, J., Lin, T. & Wang, X. Electrospun nanofibre toughened carbon/epoxy composites: Effects of polyetherketone cardo (PEK-C) nanofibre diameter and interlayer thickness. *Compos. Sci. Technol.* **70,** 1660–1666 (2010).
89. Magniez, K., Chaffraix, T. & Fox, B. Toughening of a Carbon-Fibre Composite Using Electrospun Poly(Hydroxyether of Bisphenol A) Nanofibrous Membranes Through Inverse Phase Separation and Inter-Domain Etherification. *Materials (Basel).* **4,** 1967–1984 (2011).
90. Revolution Fibres. Xantu.Layr Product Catalog. (2012).
91. Hayes, T. An Introduction to Revolution Fibres. in *Nanofibres to Nanocomposites III* (Nottingham Trent University, 2014).
92. Gao, C., Yu, L., Liu, H. & Chen, L. Development of self-reinforced polymer composites. *Prog. Polym. Sci.* **37,** 767–780 (2012).
93. Nakamura, H., Tanaka, Y., Nakai, A., Kobayashi, S. & Ikuta, N. Interfacial properties of carbon fiber reinforced thermoplastic composites. in *10th Int. Conf. Flow Process. Compos. Mater.* (2010). at <https://www.fose1.plymouth.ac.uk/sme/fpcm/fpcm10/fpcm10_submission_11.pdf>
94. DIT. Pure Composites. at <http://www.ditweaving.com/about_pure.php?page=pure_technology>
95. Milliken. Milliken & Company: A Global Innovation Leader. at <http://www.milliken.com/en-us/Pages/default.aspx>
96. Milliken. Tegris - Thermoplastic Composites. at <http://tegris.milliken.com/en-us/technology/Documents/Tegris Overview 2015.pdf>
97. DIT. PURE® - sheets: Technical Data Sheet. at <http://www.ditweaving.com/pdf/datasheet pure sheet.pdf>
98. Kabeel, M. A., Bassett, D. C., Olley, R. H., Hine, P. J. & Ward, I. M. Compaction of high-modulus melt-spun polyethylene fibres at temperatures above and below the optimum. *J. Mater. Sci.* **29,** 4694–4699 (1994).
99. Olley, R. H., Bassett, D. C., Hine, P. J. & Ward, I. M. Morphology of compacted polyethylene fibres. *J. Mater. Sci.* **28,** 1107–1112 (1993).
100. Hine, P. J., Ward, I. M., Olley, R. H. & Bassett, D. C. The hot compaction of high modulus melt-spun polyethylene fibres. *J. Mater. Sci.* **28,** 316–324 (1993).
101. Hine, P. ., Ward, I. ., Jordan, N. ., Olley, R. & Bassett, D. . The hot compaction behaviour of woven oriented polypropylene fibres and tapes. I. Mechanical properties. *Polymer (Guildf).* **44,** 1117–1131 (2003).
102. Romhány, G., Bárány, T., Czigány, T. & Karger-Kocsis, J. Fracture and failure behavior of fabric-reinforced all-poly(propylene) composite (Curv®). *Polym. Adv. Technol.* **18,** 90–96 (2007).
103. Ward, I. M. & Hine, P. J. The science and technology of hot compaction. *Polymer (Guildf).* **45,** 1413–1427 (2004).

104. *Plastics - Determination of tensile properties. Part 5: Test conditions for unidirectional fibre-reinforced plastic composites*. (BS EN ISO 527-5, 2009).

105. Gramlich, W. M. *et al.* Copolymerization of isoprene and hydroxyl containing monomers by controlled radical and emulsion methods. *Polym. Chem.* **3,** 1510 (2012).

106. Chachaty, C., Forchioni, A. & Ban, B. NMR study of the solid-state polymerization of γ-irradiated vinyl monomers. *J. Polym. Sci. Part B Polym. Lett.* **9,** 483–490 (1971).

107. Pai, C.-L., Boyce, M. C. & Rutledge, G. C. Mechanical properties of individual electrospun PA 6(3)T fibers and their variation with fiber diameter. *Polymer (Guildf).* **52,** 2295–2301 (2011).

108. Liu, W., Huang, C. & Jin, X. Electrospinning of Grooved Polystyrene Fibers: Effect of Solvent Systems. *Nanoscale Res. Lett.* **10,** 237 (2015).

109. Shawon, J. & Sung, C. Electrospinning of polycarbonate nanofibers with solvent mixtures THF and DMF. *J. Mater. Sci.* **39,** 4605–4613 (2004).

110. Lee, K. H., Kim, H. Y., La, Y. M., Lee, D. R. & Sung, N. H. Influence of a mixing solvent with tetrahydrofuran andN,N-dimethylformamide on electrospun poly(vinyl chloride) nonwoven mats. *J. Polym. Sci. Part B Polym. Phys.* **40,** 2259–2268 (2002).

111. Mccullen, S. D. *et al.* Development, Optimization, and Characterization of Electrospun Poly(lactic acid) Nanofibers Containing Multi-Walled Carbon Nanotubes. *J Appl Polym Sci* **105,** 1668–1678 (2007).

112. Jones, R. M. *Mechanics Of Composite Materials*. (Taylor & Francis, 1998).

113. Gibson, R. F. *Principles of Composite Materials Mechanics*. (CRC Press, 2007).

114. Balasubramanian, M. *Composite Materials and Processing*. (CRC Press, 2013). doi:10.1201/b15551

115. Jones, F. R. *Handbook of Polymer-Fibre Composites*. (Longman Scientific & Technical, 1994).

116. Brahim, S. Ben & Cheikh, R. Ben. Influence of fibre orientation and volume fraction on the tensile properties of unidirectional Alfa-polyester composite. *Compos. Sci. Technol.* **67,** 140–147 (2007).

117. Ku, H., Wang, H., Pattarachaiyakoop, N. & Trada, M. A review on the tensile properties of natural fiber reinforced polymer composites. *Compos. Part B Eng.* **42,** 856–873 (2011).

118. Shah, D. U. Characterisation and optimisation of the mechanical performance of plant fibre composites for structural applications. (2013).

119. Peijs, T., Garkhail, S., Heijenrath, R., Van Den Oever, M. & Bos, H. Thermoplastic composites based on flax fibres and polypropylene: Influence of fibre length and fibre volume fraction on mechanical properties. *Macromol. Symp.* **127,** 193–203 (1998).

120. Shah, D. U., Schubel, P. J., Licence, P. & Clifford, M. J. Determining the minimum, critical and maximum fibre content for twisted yarn reinforced plant

fibre composites. *Compos. Sci. Technol.* **72,** 1909–1917 (2012).

121. Adams, D. F. Engineering composite materials. *Composites* **18,** 261 (1987).
122. Todo, M. & Takayama, T. in *Biomater. - Phys. Chem.* (Pignatello, R.) 375–394 (InTech, 2011).
123. Mallick, P. K. *Composite Engineering Handbook*. (Marcel Dekker, Inc., 1997). at <https://books.google.co.uk/books?id=e1id9bKG100C&printsec=frontcover&source=gbs_ge_summary_r&cad=0#v=onepage&q&f=false>
124. Carraher, C. E. J. *Introduction to Polymer Chemistry*. (CRC Press, 2010). at <https://www.crcpress.com/textbooks/evaluation/9781439809532>
125. Fischer, E. W., Sterzel, H. J. & Wegner, G. Investigation of the structure of solution grown crystals of lactide copolymers by means of chemical reactions. *Kolloid-Zeitschrift Zeitschrift f??r Polym.* **251,** 980–990 (1973).
126. Wang, Y., Rodriguez-Perez, M. a., Reis, R. L. & Mano, J. F. Thermal and thermomechanical behaviour of polycaprolactone and starch/polycaprolactone blends for biomedical applications. *Macromol. Mater. Eng.* **290,** 792–801 (2005).
127. Hartmann, M. H. in *Biopolym. from Renew. Resour.* (Kaplan, D. L.) 367–411 (Springer-Verlag, 1998).
128. Stevens, M. P. *Polymer Chemistry: An Introduction*. (Oxford University Press, 1999).
129. Young, R. J. & Lovell, P. A. *Introduction to Polymers*. (Chapman & Hall, 1991).
130. Salmerón Sánchez, M., Mathot, V. B. F., Vanden Poel, G. & Gómez Ribelles, J. L. Effect of the Cooling Rate on the Nucleation Kinetics of Poly(L-Lactic Acid) and Its Influence on Morphology. *Macromolecules* **40,** 7989–7997 (2007).
131. Sarasua, J.-R., Prud'homme, R. E., Wisniewski, M., Le Borgne, A. & Spassky, N. Crystallization and Melting Behavior of Polylactides. *Macromolecules* **31,** 3895–3905 (1998).
132. Magoń, A. & Pyda, M. Study of crystalline and amorphous phases of biodegradable poly(lactic acid) by advanced thermal analysis. *Polymer (Guildf).* **50,** 3967–3973 (2009).
133. Yu, L., Liu, H., Dean, K. & Chen, L. Cold crystallization and postmelting crystallization of PLA plasticized by compressed carbon dioxide. *J. Polym. Sci. Part B Polym. Phys.* **46,** 2630–2636 (2008).
134. Naga, N., Yoshida, Y., Noguchi, K. & Murase, S. Crystallization of Amorphous Poly (Lactic Acid) Induced by Vapor of Acetone to Form High Crystallinity and Transparency Specimen. **2013,** 29–33 (2013).
135. Drzal, L. T. & Madhukar, M. Fibre-matrix adhesion and its relationship to composite mechanical properties. *J. Mater. Sci.* **28,** 569–610 (1993).
136. Herrera-Franco, P. J. & Drzal, L. T. Comparison of methods for the measurement of fibre/matrix adhesion in composites. *Composites* **23,** 2–27 (1992).
137. Zhou, X.-F., Nairn, J. . & Wagner, H. . Fiber–matrix adhesion from the single-fiber composite test: nucleation of interfacial debonding. *Compos. Part A Appl.*

Sci. Manuf. **30,** 1387–1400 (1999).

138. Chavalitpanya, K. & Phattanarudee, S. Poly(Lactic Acid)/Polycaprolactone Blends Compatibilized with Block Copolymer. *Energy Procedia* **34,** 542–548 (2013).

139. Todo, M. & Takayama, T. Improvement of mechanical properties of Poly (l-lactic acid) by blending of lysine triisocyanate. *J. Mater. Sci.* **42,** 4712–4715 (2007).

140. Pang, J. W. C. & Bond, I. P. A hollow fibre reinforced polymer composite encompassing self-healing and enhanced damage visibility. *Compos. Sci. Technol.* **65,** 1791–1799 (2005).

9 Appendix

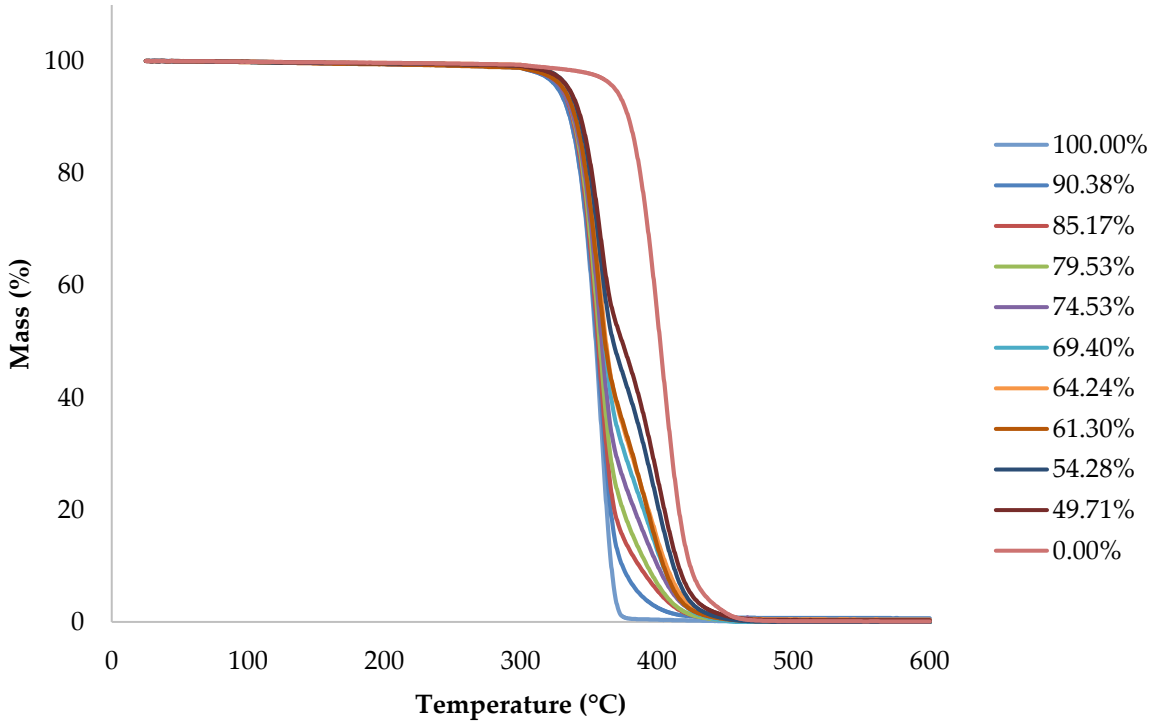

Figure 9.1: TGA results for known volume fractions of PLA in a mixture of PLA and PCL

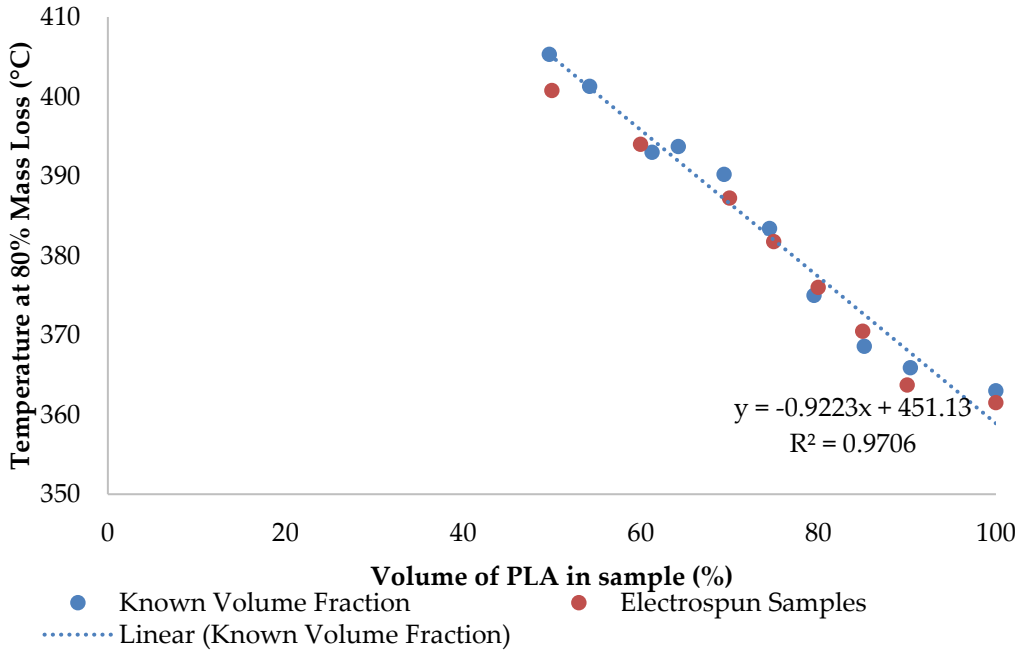

Figure 9.2: Temperature at 80% mass loss for known volume fractions of PLA in a mixture of PLA and PCL compared with results from electrospun samples.